

---

Masters Theses

Student Theses and Dissertations

---

1968

## Transient response of a class of distributed systems

Jaw-Shyong Tzeng

Follow this and additional works at: [https://scholarsmine.mst.edu/masters\\_theses](https://scholarsmine.mst.edu/masters_theses)



Part of the [Electrical and Computer Engineering Commons](#)

Department:

---

### Recommended Citation

Tzeng, Jaw-Shyong, "Transient response of a class of distributed systems" (1968). *Masters Theses*. 5195.  
[https://scholarsmine.mst.edu/masters\\_theses/5195](https://scholarsmine.mst.edu/masters_theses/5195)

This thesis is brought to you by Scholars' Mine, a service of the Missouri S&T Library and Learning Resources. This work is protected by U. S. Copyright Law. Unauthorized use including reproduction for redistribution requires the permission of the copyright holder. For more information, please contact [scholarsmine@mst.edu](mailto:scholarsmine@mst.edu).

TRANSIENT RESPONSE OF A CLASS OF DISTRIBUTED SYSTEMS

BY

JAW-SHYONG TZENG, 1968

---

A

THESIS

submitted to the faculty of

THE UNIVERSITY OF MISSOURI - ROLLA

in partial fulfillment of the requirements for the

Degree of

MASTER OF SCIENCE IN ELECTRICAL ENGINEERING

Rolla, Missouri

1968

---

approved by

Thomas Baril

Jack A. Kousguy  
(advisor)

E. C. Bertinelli

147522

## ABSTRACT

The transient response of uniform distributed systems with any transfer function that is rational in  $w = e^{\sqrt{T}s}$  can be analyzed with the basic form of the transfer function  $\frac{1}{w-a}$  after partial fraction expansion, where the pole  $a$  can be real or complex in the  $w$  plane.

With the complex pole within the stable region in the  $w$  plane, there are only two possible combinations of the basic transfer function  $\frac{1}{w-a}$ , i.e.  $\frac{1}{w-a} + \frac{1}{w-a^*}$ , for physical realizability.

The imaginary part of the transient response of the basic transfer function  $\frac{1}{w-a}$  can describe the response of the transfer function  $\frac{1}{w-a} - \frac{1}{w-a^*}$ ; while the transient response of the transfer function  $\frac{1}{w-a} + \frac{1}{w-a^*}$  can be observed from the real part of the response of  $\frac{1}{w-a}$ .

Therefore, for the basic transfer function  $\frac{1}{w-a}$ , impulse and step responses are computer plotted for various real and complex-conjugate pole locations both within and outside the  $w$ -plane region of bounded input-bounded output stability.

Some characteristics of the impulse and step responses of this basic transfer function are investigated, by which the relation between the transient response and the stability as a function of pole location is discussed.

## ACKNOWLEDGEMENTS

The author wishes to acknowledge the guidance and the assistance of his advisor Dr. Jack J. Bourquin, Associate Professor of Electrical Engineering, throughout the course of his thesis.

The author expresses his sincere appreciation to his wife, M. Y. Hsueh, for typing the original copy.



TABLE OF CONTENTS	page
ABSTRACT .....	ii
ACKNOWLEDGEMENTS .....	iii
LIST OF FIGURES .....	v
LIST OF TABLES .....	x
LIST OF SYMBOLS .....	xi
I. INTRODUCTION	
(A) Purpose of Thesis .....	1
(B) Review of the Literature .....	4
II. IMPULSE RESPONSE	
(A) A System having a Single Pole on the Real Axis in the w Plane .....	8
(B) A System having Conjugated Poles in the w Plane	
(1) With the Transfer Function $\frac{1}{w-a} - \frac{1}{w-a^*}$ .....	12
(2) With the Transfer Function $\frac{1}{w-a} + \frac{1}{w-a^*}$ .....	35
III. STEP RESPONSE	
(A) A System having a Single Pole on the Real Axis in the w Plane .....	60
(B) A System having Conjugated Poles in the w Plane .	67
IV. CONCLUSION	
(A) Results .....	89
(B) Suggestions for Further Investigation .....	90
APPENDIX	
(I) The Fortran Program for Impulse Response .....	93
(II) The Fortran Program for Step Response .....	95
BIBLIOGRAPHY .....	97
VITA .....	98

## LIST OF FIGURES

Figure		page
1-1 :	Various regions and two points defined in the w plane and how they map into the $\sqrt{s}$ plane; the unstable regions are shown in shaded area .....	3
1-2 :	The region of stability for functions rational in w. (stable inside the curve) .....	7
2-1 :	Impulse response with a single pole on the positive real axis in the w plane .....	10
2-2 :	Impulse response with a single pole on the negative real axis in the w plane .....	11
2-3 :	Imaginary-part impulse response with pole magnitude $ a =0.2$ in the w plane .....	17
2-4 :	Imaginary-part impulse response with pole magnitude $ a =0.4$ in the w plane .....	18
2-5 :	Imaginary-part impulse response with pole magnitude $ a =0.6$ in the w plane .....	19
2-6 :	Imaginary-part impulse response with pole magnitude $ a =0.8$ in the w plane .....	20
2-7 :	Imaginary-part impulse response with pole magnitude $ a =1.0$ in the w plane .....	21
2-8 :	Imaginary-part impulse response with pole angle $\phi=15^\circ$ in the w plane .....	22
2-9 :	Imaginary-part impulse response with pole angle $\phi=30^\circ$ in the w plane .....	23
2-10 :	Imaginary-part impulse response with pole angle $\phi=45^\circ$ in the w plane .....	24

Figure	Page
2-11: Imaginary-part impulse response with pole angle $\phi = 60^\circ$ in the w plane .....	25
2-12: Imaginary-part impulse response with pole angle $\phi = 75^\circ$ in the w plane .....	26
2-13: Imaginary-part impulse response with pole angle $\phi = 90^\circ$ in the w plane .....	27
2-14: Imaginary-part impulse response with pole angle $\phi = 105^\circ$ in the w plane .....	28
2-15: imaginary-part impulse response with pole angle $\phi = 120^\circ$ in the w plane .....	29
2-16: Imaginary-part impulse response with pole angle $\phi = 135^\circ$ in the w plane .....	30
2-17: Imaginary-part impulse response with pole angle $\phi = 150^\circ$ in the w plane .....	31
2-18: Imaginary-part impulse response with pole angle $\phi = 165^\circ$ in the w plane .....	32
2-19: Real-part impulse response with pole magnitude $ a  = 0.2$ in the w plane .....	37
2-20: Real-part impulse response with pole magnitude $ a  = 0.4$ in the w plane .....	38
2-21: Real-part impulse response with pole magnitude $ a  = 0.6$ in the w plane .....	39
2-22: Real-part impulse response with pole magnitude $ a  = 0.8$ in the w plane .....	40
2-23: Real-part impulse response with pole magnitude $ a  = 1.0$ in the w plane .....	41

Figure	page
2-24: Real-part impulse response with pole angle $\phi=15^\circ$ in the w plane .....	43
2-25: Real-part impulse response with pole angle $\phi=30^\circ$ in the w plane .....	44
2-26: Real-part impulse response with pole angle $\phi=45^\circ$ in the w plane .....	45
2-27: Real-part impulse response with pole angle $\phi=60^\circ$ in the w plane .....	46
2-28: Real-part impulse response with pole angle $\phi=75^\circ$ in the w plane .....	47
2-29: Real-part impulse response with pole angle $\phi=90^\circ$ in the w plane .....	48
2-30: Real-part impulse response with pole angle $\phi=105^\circ$ in the w plane .....	49
2-31: Real-part impulse response with pole angle $\phi=120^\circ$ in the w plane .....	50
2-32: Real-part impulse response with pole angle $\phi=135^\circ$ in the w plane .....	51
2-33: Real-part impulse response with pole angle $\phi=150^\circ$ in the w plane .....	52
2-34: Real-part impulse response with pole angle $\phi=165^\circ$ in the w plane .....	53
2-35: The system with the lumped and distributed amplifiers.....	57
2-36: The response of the system with the transfer function in eq.(2-12) .....	59

Figure	page
3-1 : Unnormalized unit step response with a single pole on the positive real axis in the $w$ plane ..	63
3-2 : Normalized unit step response with a single pole on the positive real axis in the $w$ plane ..	64
3-3 : Step response with a single pole and with a double pole of magnitude $a = 0$ .....	65
3-4 : Unit step response with a single pole on the negative real axis in the $w$ plane .....	66
3-5 : Unit step response with pole magnitude $ a  = 0.2$ in the $w$ plane .....	69
3-6 : Unit step response with pole magnitude $ a  = 0.4$ in the $w$ plane .....	70
3-7 : Unit step response with pole magnitude $ a  = 0.6$ in the $w$ plane .....	71
3-8 : Unit step response with pole magnitude $ a  = 0.8$ in the $w$ plane .....	72
3-9 : Unit step response with pole magnitude $ a  = 1.0$ in the $w$ plane .....	73
3-10: Unit step response with pole angle $\phi = 15^\circ$ in the $w$ plane .....	78
3-11: Unit step response with pole angle $\phi = 30^\circ$ in the $w$ plane , .....	79
3-12: Unit step response with pole angle $\phi = 45^\circ$ in the $w$ plane .....	80
3-13: Unit step response with pole angle $\phi = 60^\circ$ in the $w$ plane .....	81

Figure	page
3-14: Unit step response with pole angle $\phi=75^\circ$ in the w plane .....	82
3-15: Unit step response with pole angle $\phi=90^\circ$ in the w plane .....	83
3-16: Unit step response with pole angle $\phi=105^\circ$ in the w plane .....	84
3-17: Unit step response with pole angle $\phi=120^\circ$ in the w plane .....	85
3-18: Unit step response with pole angle $\phi=135^\circ$ in the w plane .....	86
3-19: Unit step response with pole angle $\phi=150^\circ$ in the w plane .....	87
3-20: Unit step response with pole angle $\phi=165^\circ$ in the w plane .....	88

## LIST OF TABLES

Table	page
2-1: List of pole magnitude being plotted for impulse response .....	33
2-2: Oscillation period of impulse response with pole on the boundary of the region of stability .....	34
2-3: Calculation of the impulse response in eq.(2-12)	58
3-1: List of pole magnitude being plotted for step response .....	76
3-2: Some data of the characteristics of step response .....	77

## LIST OF SYMBOLS

$s$ : Complex frequency variable;  $s = \sigma + j\omega$

$w$ : Variable of  $e^{\sqrt{Ts}}$

$T$ : Time constant of the uniform distributed RC network, and  
normalized to unity throughout this thesis.

$\phi$ : The pole angle in the  $w$  plane.

$a$ : The pole in the  $w$  plane.

$t$ : The time of the response.

$h(t)$ : Impulse response, Laplace inverse transformation of

$$H(e^{\sqrt{Ts}}).$$

$v(t)$ : Step response, Laplace inverse transformation of

$$V(e^{\sqrt{Ts}}).$$



## I. INTRODUCTION

### (A) The Purpose of Thesis

Interest in the properties of distributed RC networks has recently increased with the advent of micro-electronic circuits. In the literature, it can be found that the immittance parameters and transfer function of a network consisting of uniform distributed RC sections are generally expressed as functions of  $\sqrt{s}$  and  $e^{\sqrt{Ts}}$ , in which  $s$  is the complex frequency variable [1]. Physical examples of this class of uniform distributed system include the uniform distributed RC network with either open circuit, short circuit, or matched termination and the distributed lag element, any of which can be combined in either passive or active systems. In Bourquin's paper [2], the analysis of this class of systems in the  $\sqrt{s}$  and  $w = e^{\sqrt{Ts}}$  planes has been developed, in which the impulse and step time function in the  $w$  plane are derived for the transfer function  $\frac{1}{w-a}$ . However, it is difficult to discuss these transient responses in the  $w$  plane directly from the time functions without any illustration. Hence, it is the first purpose of this thesis to illustrate graphically the transient response of this type of system in the  $w$  plane.

Secondly, by the relation between various regions of the  $w$  plane mapped onto the  $\sqrt{s}$  plane as shown in figure 1-1, the response for a pole in the  $w$  plane can be represented as the response of an infinite number of poles on a vertical line in the  $\sqrt{s}$  plane. Thus, the responses for various  $w$ -plane

pole locations provide a check on the concept of  $\sqrt{s}$  plane dominate poles [3].

Moreover, as described in Bourquin's paper, the transfer function  $\frac{1}{(w-a)^q}$ , where  $a = |a|e^{j\theta}$  in the  $w$  plane, is realizable if  $\frac{1}{w-a}$  is realizable, and it is bounded input-bounded output stable if, and only if,  $\frac{1}{w-a}$  is bounded input-bounded output stable. If the transfer function is of the form  $\frac{N(w)}{D(w)}$  where  $N(w)$  is a polynomial of degree  $n$ ,  $D(w)$  is one of degree  $m$ , and  $n \leq m$ , then by partial fraction expansion this transfer function can be rewritten as a linear combination of terms of the form  $\frac{1}{w-a}$ . In other words, the transfer function  $\frac{1}{w-a}$  can be considered as the basic one to realize any other type of  $w$ -plane transfer function in this class of systems. Whenever the response of the transfer function  $\frac{1}{w-a}$  is given, the resultant response of any other transfer function can then be predicted by various real or complex-conjugate poles of the form  $\frac{1}{w-a}$  with only algebraic manipulation.

Therefore, in this thesis, impulse and step responses for  $\frac{1}{w-a}$  are computer plotted for various real and complex-conjugate pole locations both within and outside the  $w$  plane region of bounded input-bounded output stability, which is defined in the next section. By this simplest form of the transfer function, the results of impulse and step responses are investigated, by which the relation between the transient response and the stability as a function of pole location is discussed.

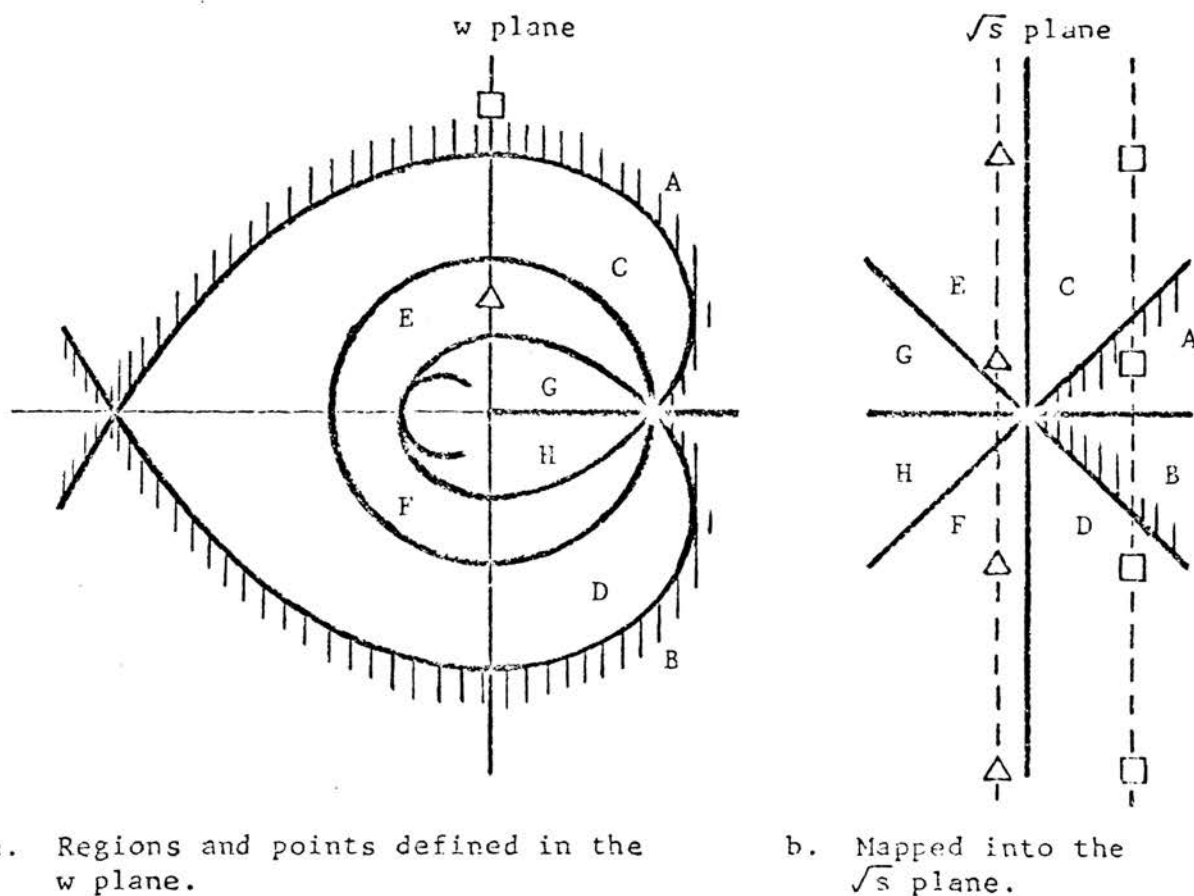


Figure 1-1: Various regions and two points defined in the  $w$  plane and how they map into the  $\sqrt{s}$  plane; the unstable regions are shown in shaded area.

## (B) Review of the Literature

As stated in Bourquin's paper [2], for bounded input-bounded output stability of a system with a transfer function rational in  $w = e^{\sqrt{T}s}$  with  $n \leq m$ , where  $n$  is the degree of the numerator of the transfer function and  $m$  is the denominator's, it is necessary and sufficient that all poles of the transfer function occur within the region in the  $w$  plane bounded by  $e^{|\phi| + j\phi}$ , where  $-\pi \leq \phi = \arg. w \leq \pi$ . The region of stability described above is shown in figure 1-2.

Now consider the impulse response  $h(t)$  of the transfer function  $\frac{1}{w-a}$ ,

$$h(t) = \mathcal{L}^{-1}\left[\frac{1}{w-a}\right] = \mathcal{L}^{-1}\left[\frac{1}{e^{\sqrt{s}} - a}\right] \dots\dots\dots (1-1a)$$

Let  $f(t) = \mathcal{L}^{-1}[F(s)]$ ,  $g(t) = \mathcal{L}^{-1}[G(s)]$ .

By applying the following relationship [4], if

$$G(s) = 2^{\frac{m}{2}} \prod_{s=1}^m s^{\frac{1}{2}} F(\sqrt{s}), \dots\dots\dots (1-1)$$

then,

$$g(t) = t^{\frac{m+1}{2}} \int_0^\infty e^{-\frac{y^2}{4t}} \text{He}_m\left(2^{\frac{1}{2}} y t^{-\frac{1}{2}}\right) f(y) dy \dots\dots\dots (1-2)$$

in which  $\text{He}_m(x)$  is Hermite polynomial and

$$\text{He}_m(x) = (-1)^m e^{\frac{x^2}{2}} \frac{d^m}{dx^m} \left( e^{-\frac{x^2}{2}} \right) \dots\dots\dots (1-3)$$

$$\text{If } F(\sqrt{s}) = (e^{\sqrt{s}} - a)^{-1}, \dots\dots\dots (1-4)$$

$m=1$ , then

$$\text{He}_1(x) = -e^{\frac{x^2}{2}} \frac{d}{dx} \left( e^{-\frac{x^2}{2}} \right) = x \dots\dots\dots (1-5)$$

$$\text{and } G(s) = \sqrt{2\pi} (e^{\sqrt{s}} - a)^{-1} \dots\dots\dots (1-5a)$$

which has the same form as the function in eq.(1-1a) with

$m=1$  and  $F(\sqrt{s})$  in eq.(1-4). From the tables [4],

$$\mathcal{L}^{-1}\left[s^{-1}(e^s - a)^{-1}\right] = \sum_{k=1}^n a^{k-1} u(t-k) \dots\dots\dots (1-6a)$$

where  $u(t)$  is the unit step function and  $t-1 < n < t$ . By applying the real differentiation theorem, then

$$\mathcal{L}^{-1}[(e^s - a)^{-1}] = f(t) = \sum_{k=1}^n a^{k-1} \delta(t-k) \quad \dots (1-6)$$

where  $\delta(t)$  is the unit impulse function, the time derivative of the unit step function. Hence, by letting  $x = \frac{y}{2t}$  in eq.(1-5) and substitution of (1-6) into eq.(1-2),

$$\begin{aligned} g(t) &= 2^{-\frac{1}{2}} t^{-\frac{3}{2}} \int_0^\infty \sum_{k=1}^n a^{k-1} y e^{-y^2/4t} \delta(y-k) dy \\ &= 2^{-\frac{1}{2}} t^{-\frac{3}{2}} \sum_{k=1}^\infty k a^{k-1} e^{-k^2/4t} \quad \dots (1-7) \end{aligned}$$

The last step is a result of the "sifting property" of the impulse function; i.e.  $\int_0^\infty f(t) \delta(t-\tau) dt = f(\tau)$ .

From eq.(1-5a) and eq.(1-7),

$$\begin{aligned} h(t) &= (2\pi)^{-\frac{1}{2}} T^{-1} g\left(\frac{t}{T}\right) \\ &= \frac{1}{2} \sqrt{\frac{T}{\pi t^3}} \left[ \sum_{n=1}^\infty n a^{n-1} e^{-n^2 T/4t} \right] \quad \dots (1-8) \end{aligned}$$

The series above (absolutely) convergences for all finite  $|a|$  and any finite  $t$  as can be seen by taking the ratio test:

$$\lim_{n \rightarrow \infty} \frac{|U_{n+1}|}{|U_n|} = \lim_{n \rightarrow \infty} \left(1 + \frac{1}{n}\right) a e^{-\frac{(2n+1)T}{4t}} = 0 \quad \dots (1-9)$$

The impulse response  $h(t)$  is evaluated numerically using eq.(1-8); eq.(1-9) serves as the error criterion for the summation of the series in the computer program [see appendix (I)].

In a similar way, the step response of the transfer function  $\frac{1}{w-a}$  can be found by letting  $F(\sqrt{s}) = s^{-\frac{1}{2}} (e^{\sqrt{s}-a})^{-1}$  and  $m = 0$  in eq.(1-1). From eq.(1-2),

$$g(t) = t^{-\frac{1}{2}} \int_0^{\infty} \sum_{k=1}^n a^{k-1} e^{-y^2/4t} u(y-k) dy \quad \dots\dots\dots (1-10)$$

Uniform convergence on  $y$  can be verified by the Weierstrass M-test, then

$$\begin{aligned} g(t) &= t^{-\frac{1}{2}} \sum_{n=1}^{\infty} a^{n-1} \int_0^{\infty} e^{-y^2/4t} u(y-n) dy \\ &= \sqrt{\pi} \sum_{n=1}^{\infty} a^{n-1} \operatorname{erfc}\left(\frac{n}{2\sqrt{t}}\right) \dots\dots\dots (1-11) \end{aligned}$$

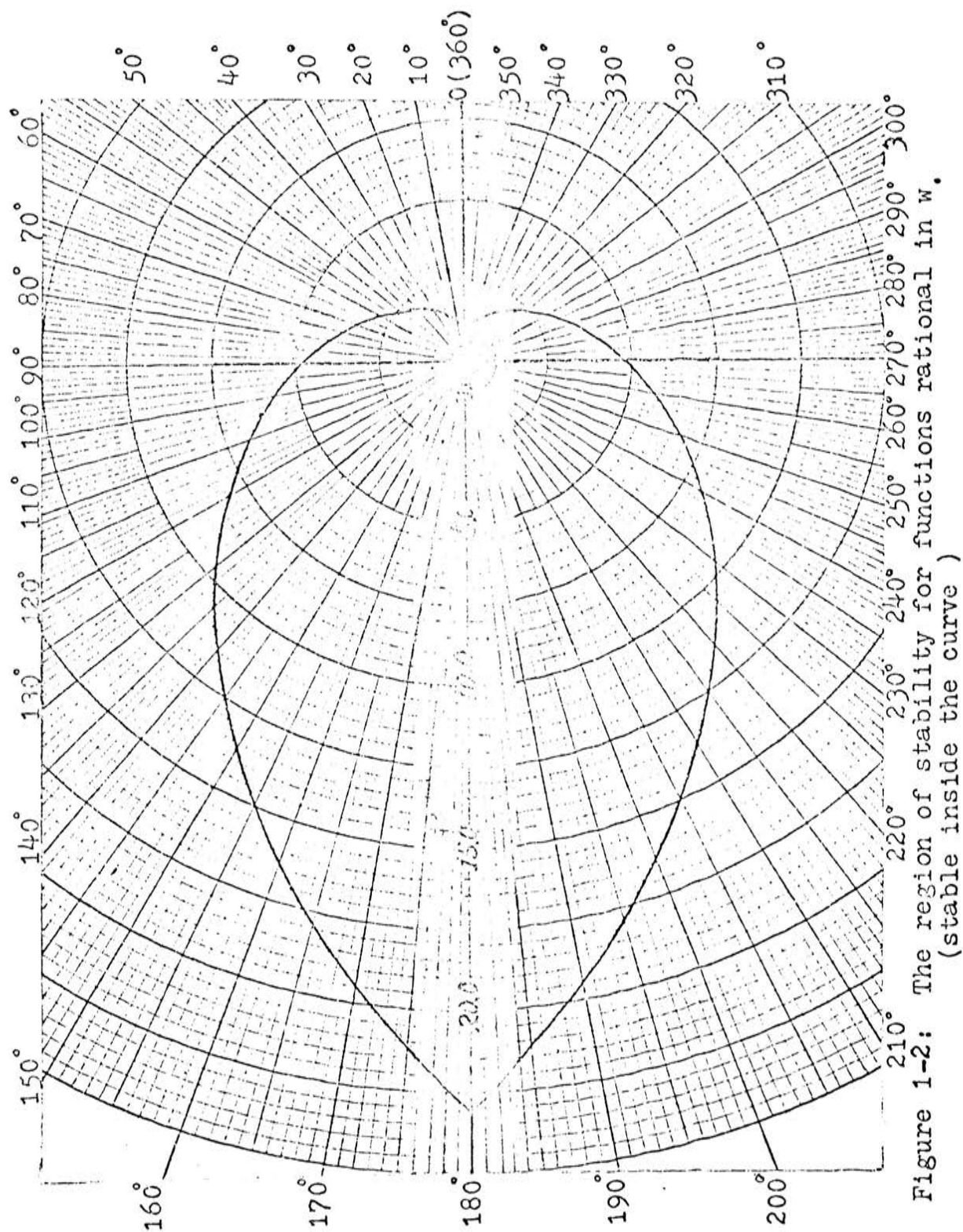
The last step of eq.(1-11) is derived by changing the variable  $x^2 = y^2/4t$ . Hence,

$$\begin{aligned} v(t) &= \mathcal{L}^{-1}[V(s)] = \mathcal{L}^{-1}\left[\pi^{-\frac{1}{2}} T G(Ts)\right] = \pi^{-\frac{1}{2}} g\left(\frac{t}{T}\right) \\ &= \sum_{n=1}^{\infty} a^{n-1} \operatorname{erfc}\left(\frac{n}{2}\sqrt{\frac{T}{t}}\right) \dots\dots\dots (1-12) \end{aligned}$$

The error criterion applied for evaluating the series in eq.(1-12) on the computer program [see appendix (II)] is established from the ratio test of eq.(1-12); i.e. for all finite  $|a|$  and finite  $t$ , the ratio

$$\lim_{n \rightarrow \infty} \frac{|a|^{n+1} \int_{\frac{n+1}{2}\sqrt{\frac{T}{t}}}^{\infty} e^{-x^2} dx}{|a|^n \int_{\frac{n}{2}\sqrt{\frac{T}{t}}}^{\infty} e^{-x^2} dx} = \lim_{k \rightarrow \infty} |a| e^{-\left(\frac{2k+1}{4}\right)\frac{T}{t}} = 0 \quad (1-13)$$

where  $k$  is a continuous variable substituted for  $n$ ; and the second limit follows the first after application of L'Hospital's rule and Leibnitz's rule for the differentiation of an integral.





## II. IMPULSE RESPONSE

### (A) A System having a Single Pole on the Real Axis in the $w$ Plane

As shown in figure 1-2, the stable values of pole magnitude on the positive real axis are smaller than unity.

As observed on figure 2-1, the response with pole magnitude  $a < 1$  decreases rapidly and becomes negligible within several seconds. But for  $a=1$ , the slope of the curve remains nearly constant after  $t=3$  seconds. By eq.(2-6) in the following section, it can be found that the oscillation period of this wave,  $a=1.0$ , becomes infinite. It means that the transient response with unity pole magnitude on the positive real axis does not oscillate at all, while those are oscillating with poles located on any other boundary of bounded input-bounded output stability, as shown in table 2-2 in the next section. Moreover, when pole magnitude is greater than unity, the larger the value of the pole on the positive real axis, the more rapidly the response becomes unbounded.

On the negative real axis in the  $w$  plane, the unstable response will occur when  $a \geq e^\pi = 23.1$ . Observing the graphs in figure 2-2, the impulse response for  $|a| < 10$  dampens rapidly and becomes less dampened for  $|a| = 15.0$ . For  $|a| = 23.0$ , the curve oscillates nearly without damping; and the magnitude of the impulse response, for  $|a| > 23.1$ , increases with time.

The curve for  $a = 0$  is also plotted on the figure for comparison. The function of this curve can be derived from



eq.(1-8), by letting  $a = 0$ ,

$$h(t) = \frac{\sqrt{T}}{2\sqrt{\pi}} t^{-3/2} e^{-T/4t} \dots\dots\dots(2-1)$$

All the initial portions of the transient response with a single pole on the positive real axis lie above the curve of eq.(2-1), but those, with a single pole on the negative real axis, lie below it. Therefore, as compared with the same pole magnitude, the system, for a single pole on the negative real axis, is more stable and the peak of the transient response is more narrower than that on the positive real axis in the  $w$  plane.

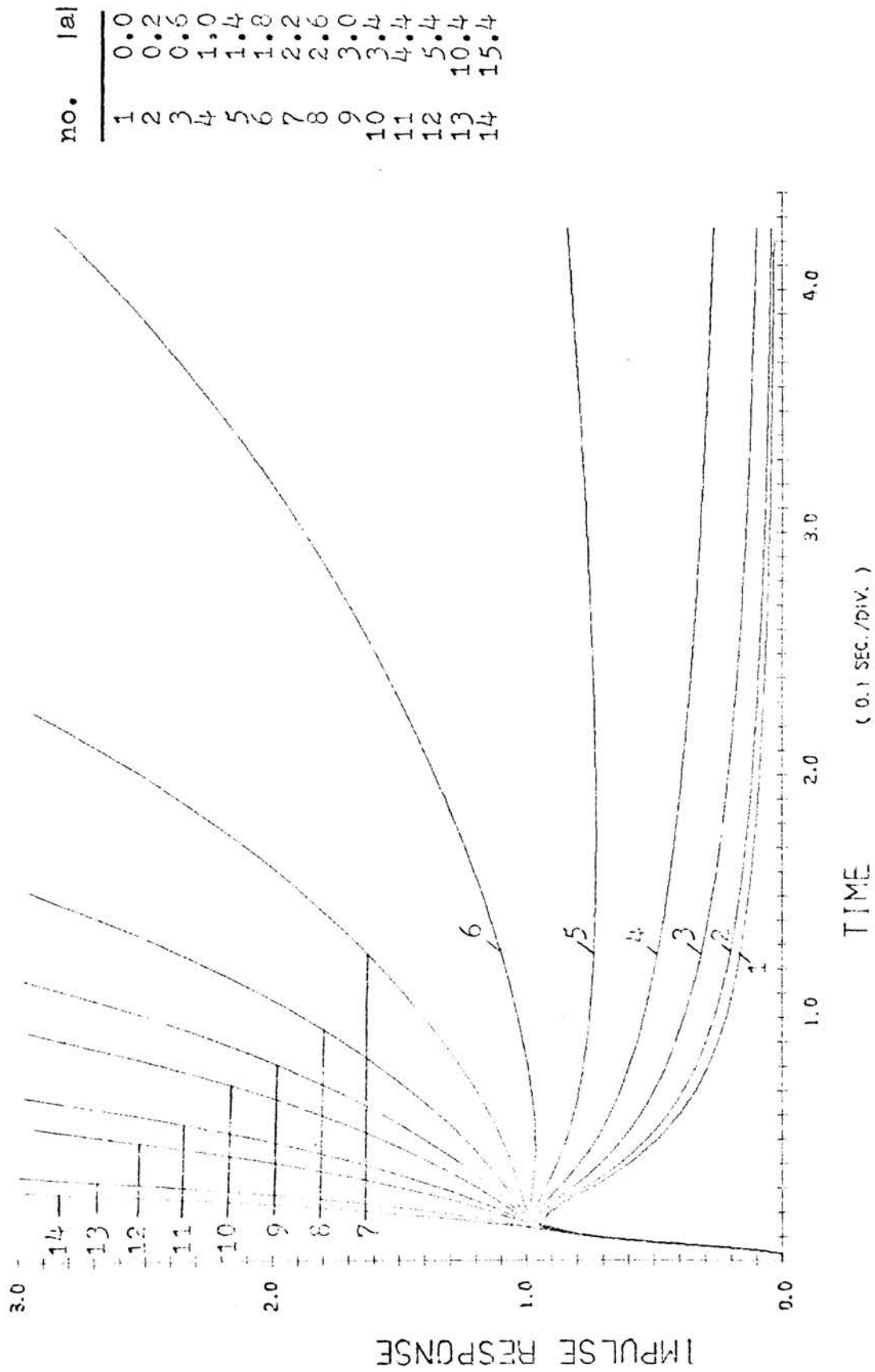


Figure 2-1: Impulse response with a single pole on the positive real axis in the  $w$  plane.

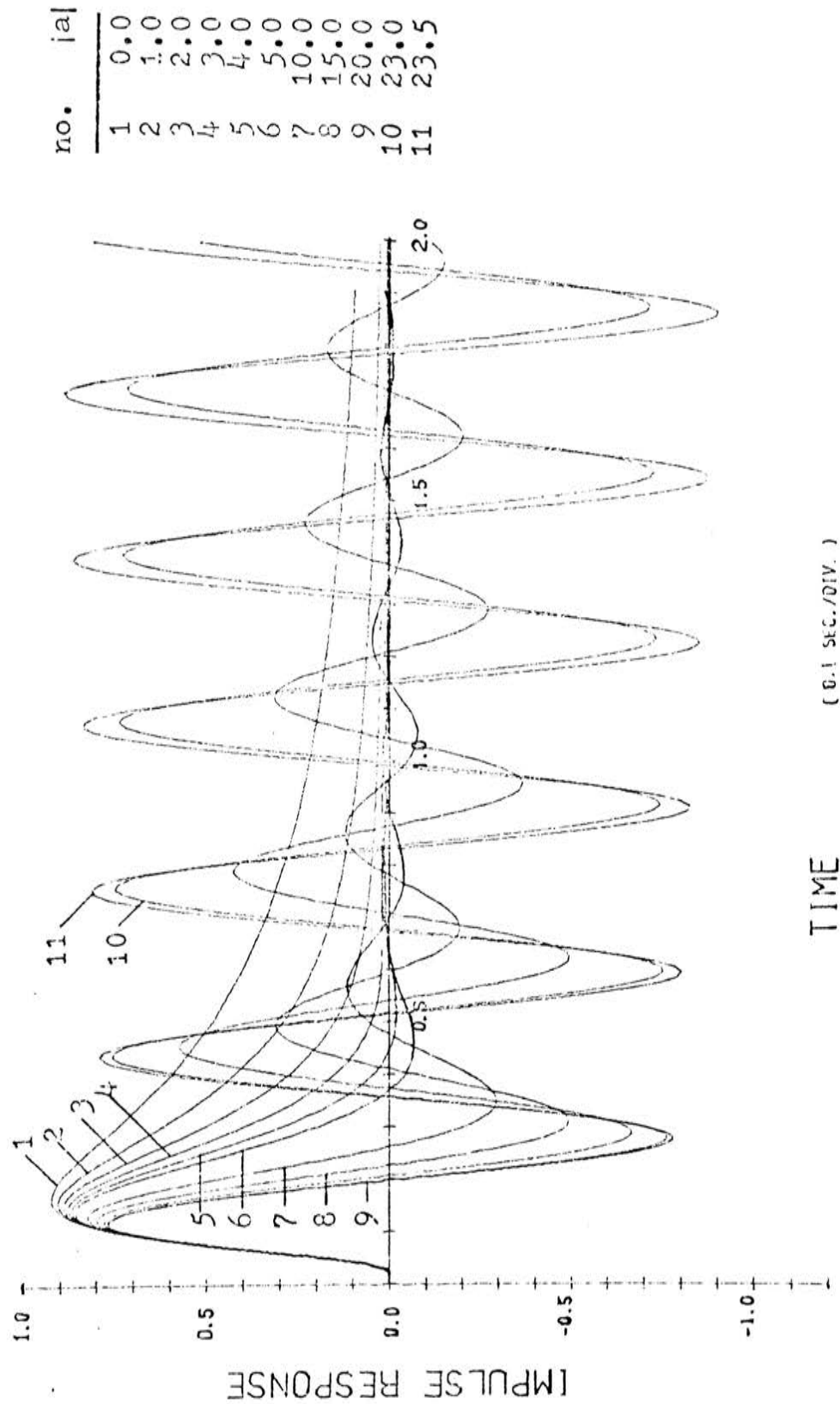


Figure 2-2: Impulse response with a single pole on the negative real axis in the w plane.

## (E) A System having Conjugated Poles in the w Plane

(1) With the transfer function  $\frac{1}{w-a} - \frac{1}{w-a^*}$

Whenever a w-plane pole occurs at any location other than on the real axis in w plane, i.e.  $a = \text{Re}[a] + j\text{Im}[a] = |a|e^{j\phi}$ , the impulse response has a complex form,  $h(t) = \text{Re}[h(t)] + j\text{Im}[h(t)]$ .

In order to meet the requirement of physical realizability, real coefficients in the impulse response, there must also exist a conjugate pole, i.e.  $\frac{1}{w-a^*}$ , where  $a^* = \text{Re}[a] - j\text{Im}[a] = |a|e^{-j\phi}$ . The response of  $\frac{1}{w-a^*}$  can be found from the conjugated response of  $\frac{1}{w-a}$ .

In other words, if the transient response of  $\frac{1}{w-a}$  has been established for  $0 < \phi < \pi$ , the response of  $\frac{1}{w-a^*}$  can be correspondingly predicted by taking its conjugate.

Now consider the transfer function,

$$T_1(w) = \frac{1}{w-a} - \frac{1}{w-a^*} = \frac{2\text{Im}[a]}{(w-a)(w-a^*)} \dots\dots\dots (2-2)$$

$$\text{Let } F_1(w) = \frac{1}{(w-a)(w-a^*)} \dots\dots\dots (2-3)$$

$$\text{then } F_1(w) = \frac{1}{2\text{Im}[a]} \left[ \frac{1}{w-a} - \frac{1}{w-a^*} \right] \dots\dots\dots (2-4)$$

By the inverse Laplace transformation of eq.(2-4), the time function for  $F_1(w)$  is

$$\begin{aligned}
f_1(t) &= \mathcal{L}^{-1}[F_1(w)] = \frac{1}{2\text{Im}[a]} \mathcal{L}^{-1}\left[\frac{1}{w-a} - \frac{1}{w-a^*}\right] \\
&= \frac{1}{2\text{Im}[a]} \left\{ \mathcal{L}^{-1}\left[\left(\frac{1}{w-a}\right)\right] - \mathcal{L}^{-1}\left[\left(\frac{1}{w-a^*}\right)\right] \right\} \\
&= \frac{1}{2\text{Im}[a]} [h(t) - h^*(t)] \\
&= \frac{\text{Im}[h(t)]}{\text{Im}[a]} \dots\dots\dots (2-5)
\end{aligned}$$

Therefore, if the transfer function is of the form of  $F_1(w)$ , as in eq.(2-3), with one pair of conjugated poles, the transient response of  $F_1(w)$  can be investigated from the imaginary part of the response for  $H(w) = \frac{1}{w-a}$  multiplied by a factor  $\frac{1}{\text{Im}[a]}$ . Thus, the imaginary part of the impulse response becomes important and informative for the response of  $F_1(w)$ , and has been plotted in figures 2-3 through 2-18. The first five figures are plotted for comparing the effects on the response of varying the pole angle,  $15^\circ$  each step, with fixed pole magnitude  $|a| \leq 1.0$ .

As shown in figures 2-3 through 2-7, the changing rate of the slope at the peak is faster in the  $\phi \geq 90^\circ$  case than that in the  $\phi < 90^\circ$  case.

The effect of pole angle on the response can be observed; with constant pole magnitude, the peak value becomes smaller as the pole get closer to either the real axis in the  $w$  plane.

Note that from figures 2-3 through 2-7 the curves of  $\phi=15^\circ$  in each graph remain nearly constant in slope after  $t=2$  seconds. Since this pole is located near the positive real axis and is close to the boundary of the region of instability, it is difficult to observe its stability on the curve within the first few seconds. Those responses, with the corresponding pole magnitude, are actually still stable as shown in figure 2-8. Thus, it is true that with smaller pole angles the system results in more slowly changing slopes of the response curves.

The transient response with constant pole angle and varying pole magnitude is plotted by choosing several locations within and outside the w-plane region of bounded input-bounded output stability, as listed in table 2-1. Observing the graphs in figures 2-8 through 2-18, constant angle with varying pole magnitude, the transient response dampens to zero as time approaches infinity and exhibits oscillation when the pole magnitude approaches the value on the boundary of the instability region; when the pole falls outside the stable region, the response becomes unstable with its magnitude increasing with time. The oscillation period of the response on the boundary of the stable region is evaluated to check the accuracy of the curves as follows.

Let  $w = a = e^{\phi + j\phi} = e^{\sqrt{s}}$  and solve for  $s$ ; since  $\sqrt{s} = \phi + j\phi$ , and  $s = \sigma + j\omega = \phi^2 - \phi^2 + j2\phi^2$ , i.e.  $\omega = 2\phi^2$ ,

Then the period of the oscillation  $T_p$  is

$$T_p = \frac{1}{f} = \frac{2\pi}{\omega} = \frac{\pi}{\phi^2}, \dots\dots\dots(2-6)$$

where  $T_p$  is in second.

The corresponding values of  $T_p$  have been checked in table 2-2 with the period  $T'_p$  measured from the curves; and it shows that those plotted curves possess high accuracy. Therefore, after multiplying by the factor  $\frac{1}{\ln[a]}$ , those responses can be considered as the transient responses for the transfer function  $F_1(w)$  in eq.(2-3).

The behaviors of the response with transfer function  $T_1(w)$  in eq.(2-2) are summarized as follows:

- (a) With fixed pole magnitude, the impulse response of the system with the  $T_1(w)$  transfer function has a broader peak in  $\phi < 90^\circ$  region.
- (b) The delay time of the output impulse response is about 0.12 second.
- (c) During the first 0.3 second, the positive slopes are the same between the curve pairs for which the sums of pole angles are  $180^\circ$ ; but for the smaller  $\phi$  case, the response remains at its peak longer.
- (d) When the pole magnitude approaches the boundary of the region of stability with constant pole angle, the response becomes less dampened but larger magnitude; and the frequency of oscillation of the response increases;

then the system with transfer function  $T_1(w)$  becomes less stable.



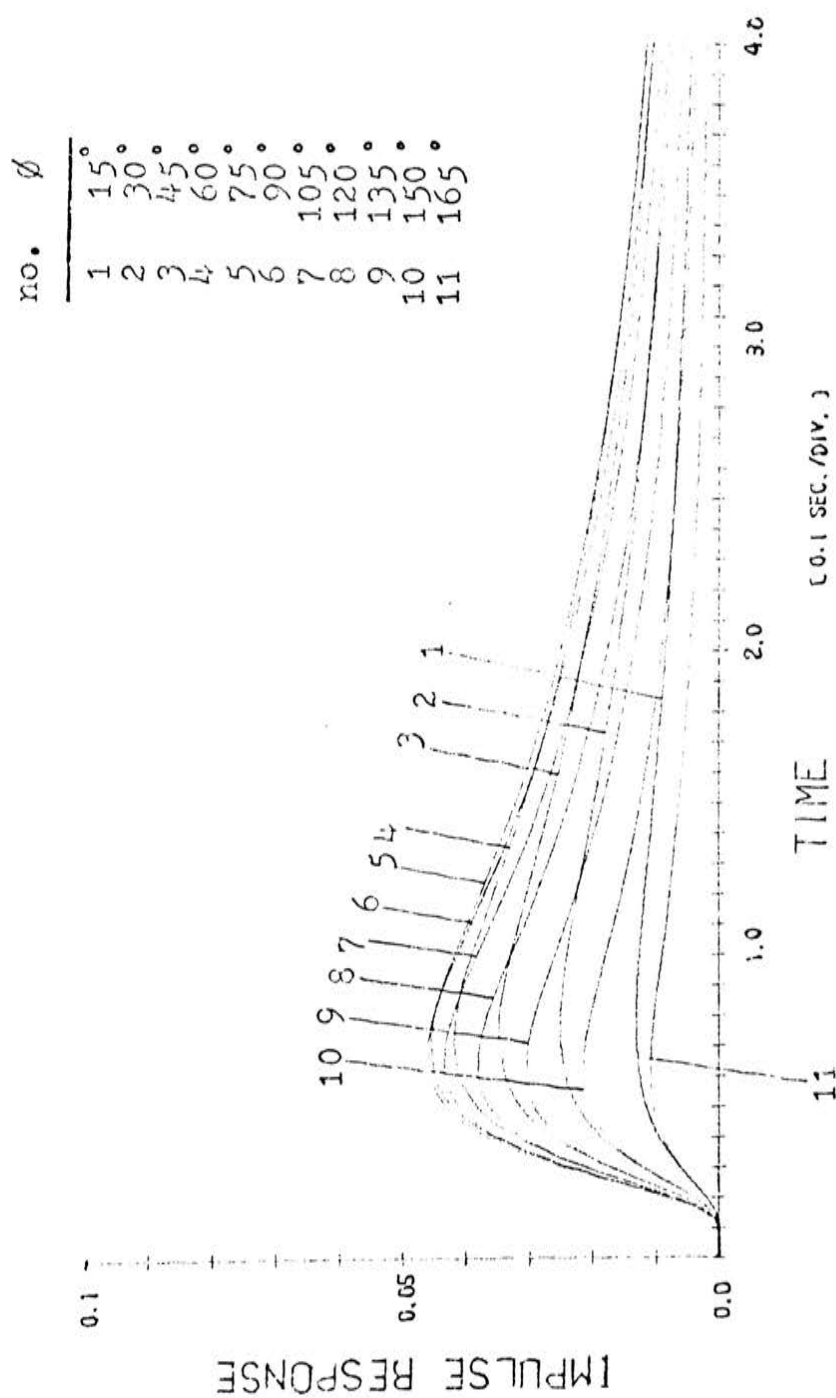


Figure 2-3: Imaginary-part impulse response with pole magnitude  $|a|=0.2$  in the  $w$  plane.

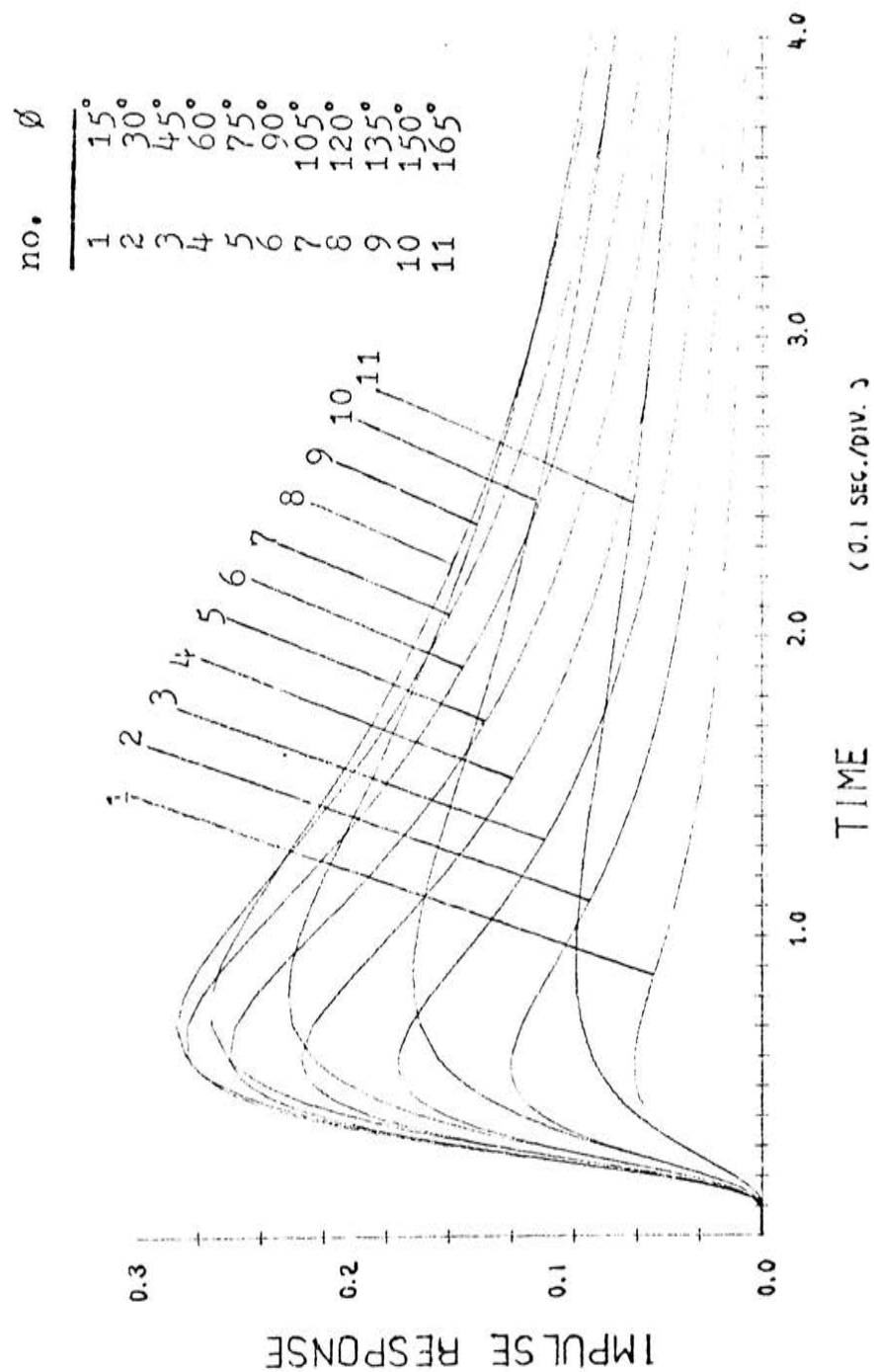


Figure 2-4: Imaginary-part impulse response with pole magnitude  $|a|=0.4$  in the w plane.

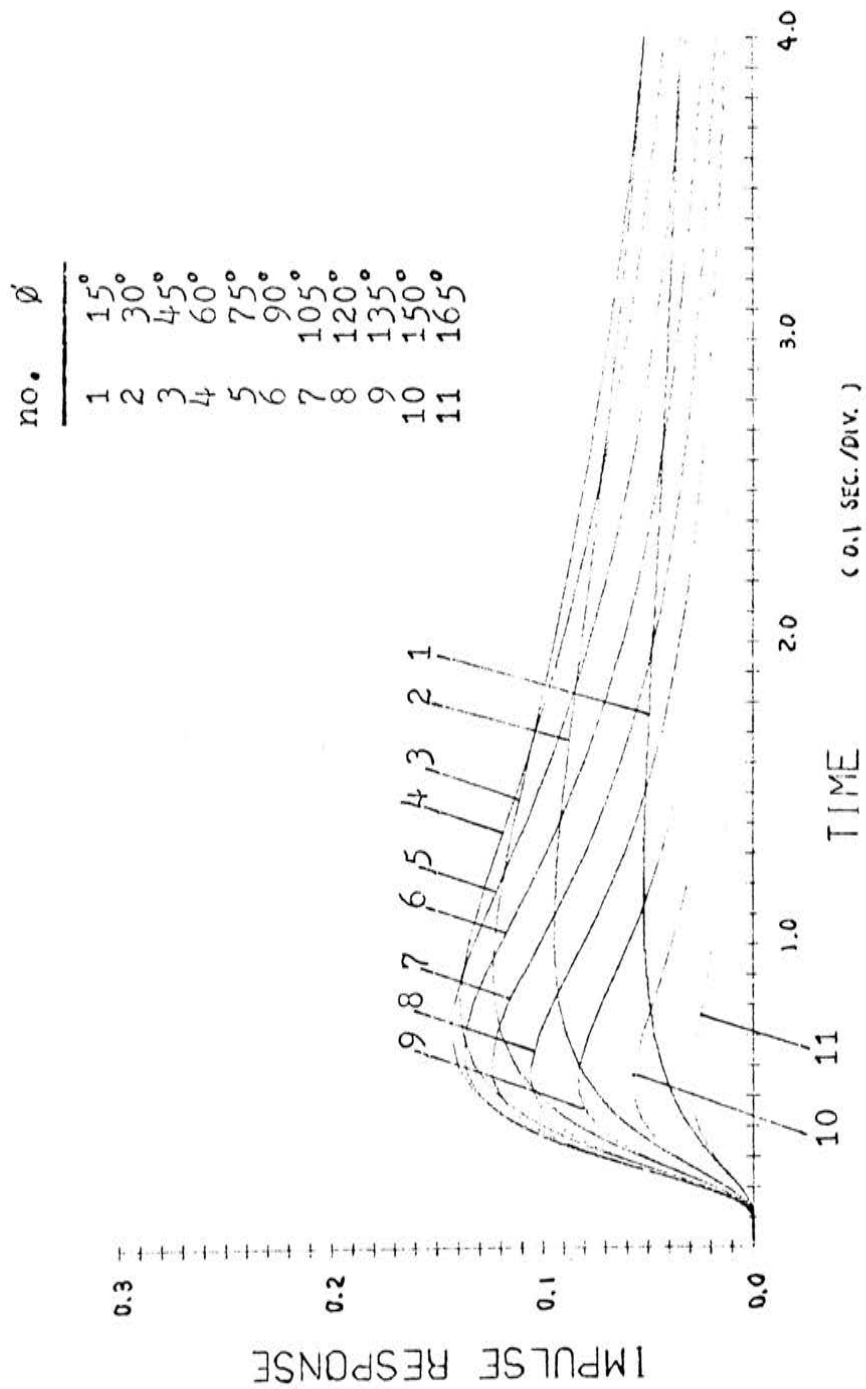


Figure 2-5: Imaginary-part impulse response with pole magnitude  $|a|=0.6$  in the  $w$  plane.

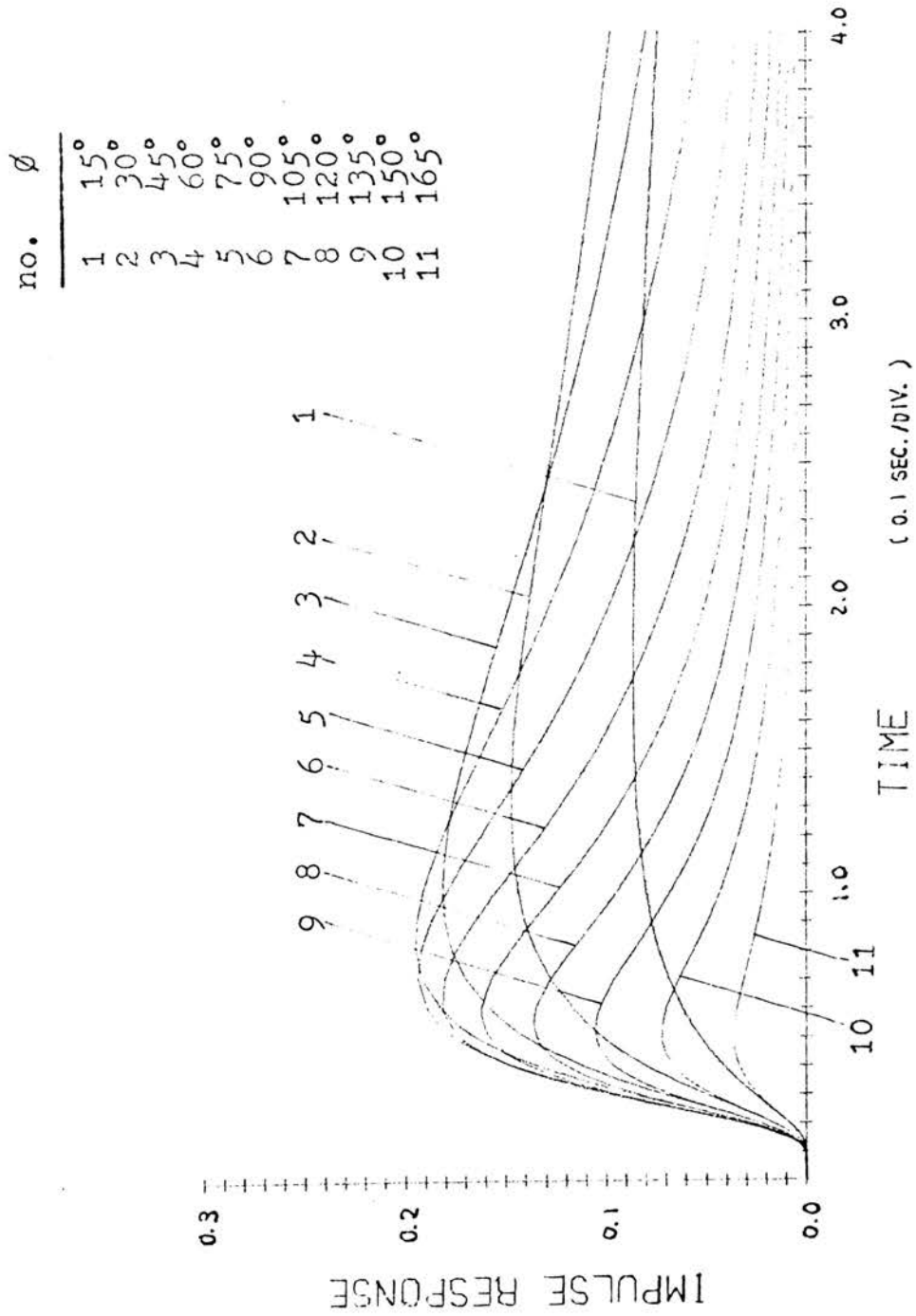


Figure 2-6: Imaginary-part impulse response with pole magnitude  $|a|=0.8$  in the  $w$  plane.

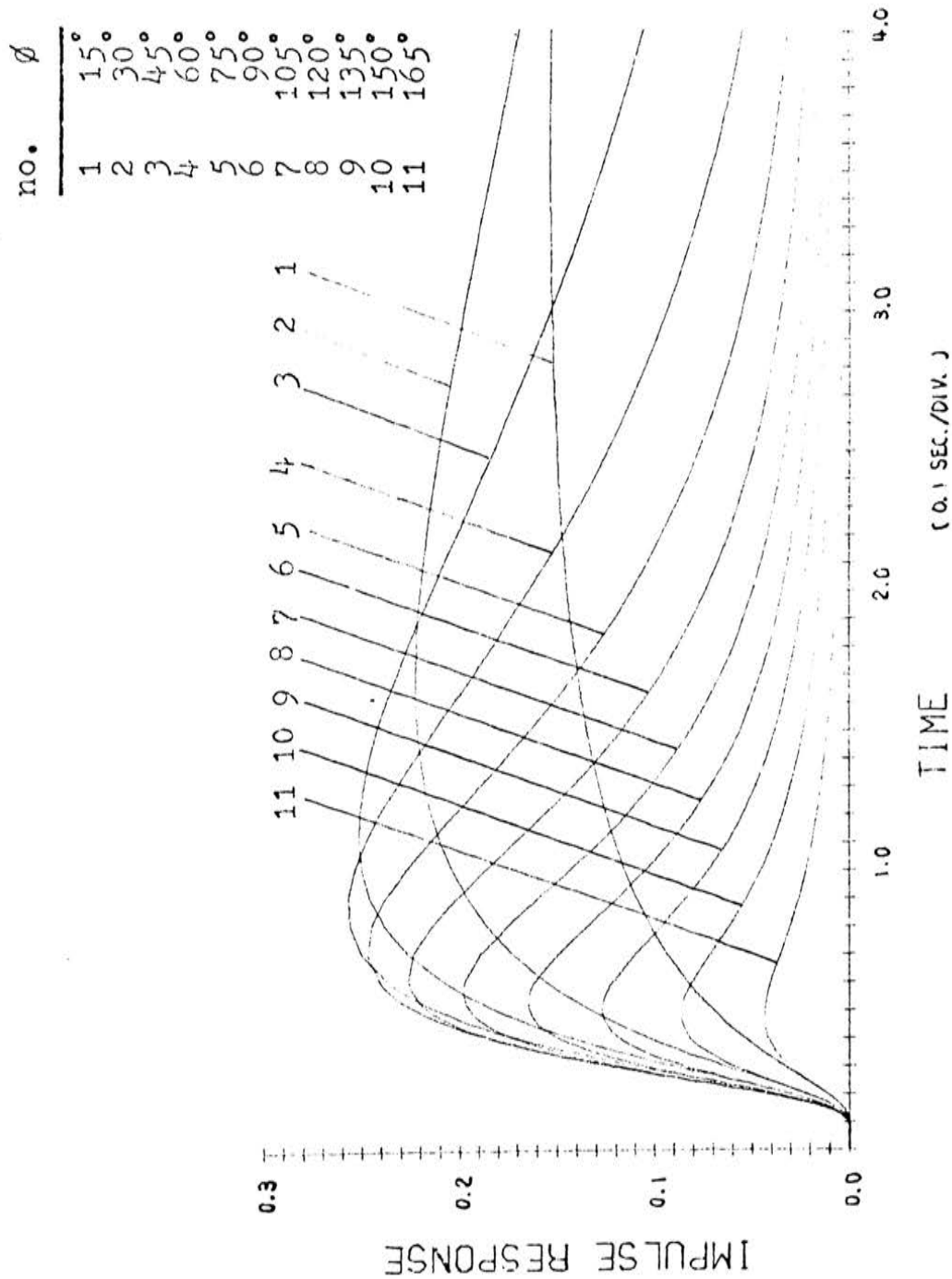


Figure 2-7: Imaginary-part impulse response with pole magnitude  $|a|=1.0$  in the  $w$  plane.

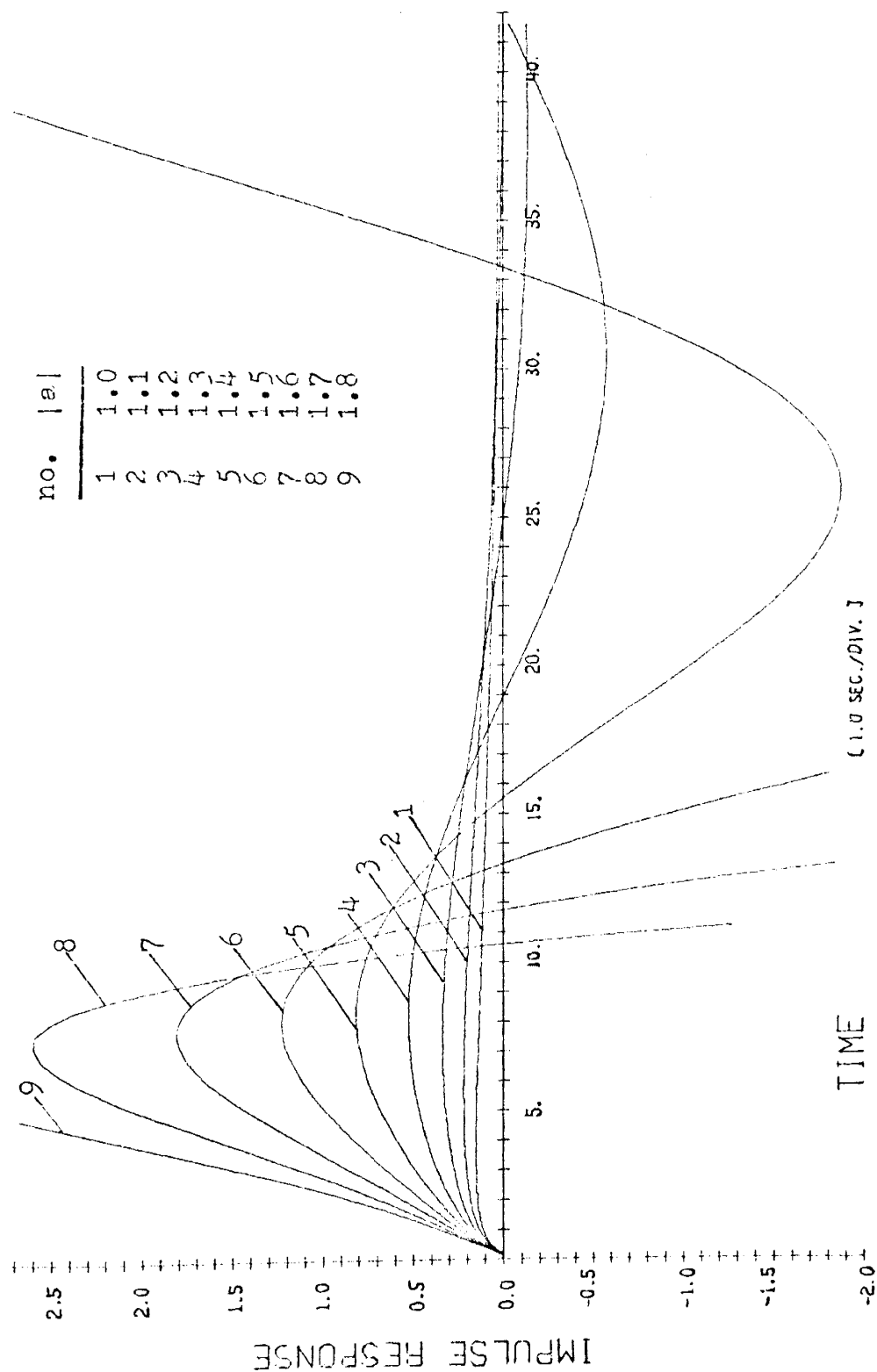


Figure 2-8: Imaginary-part impulse response with pole angle  $\phi = 15^\circ$  in the  $w$  plane.

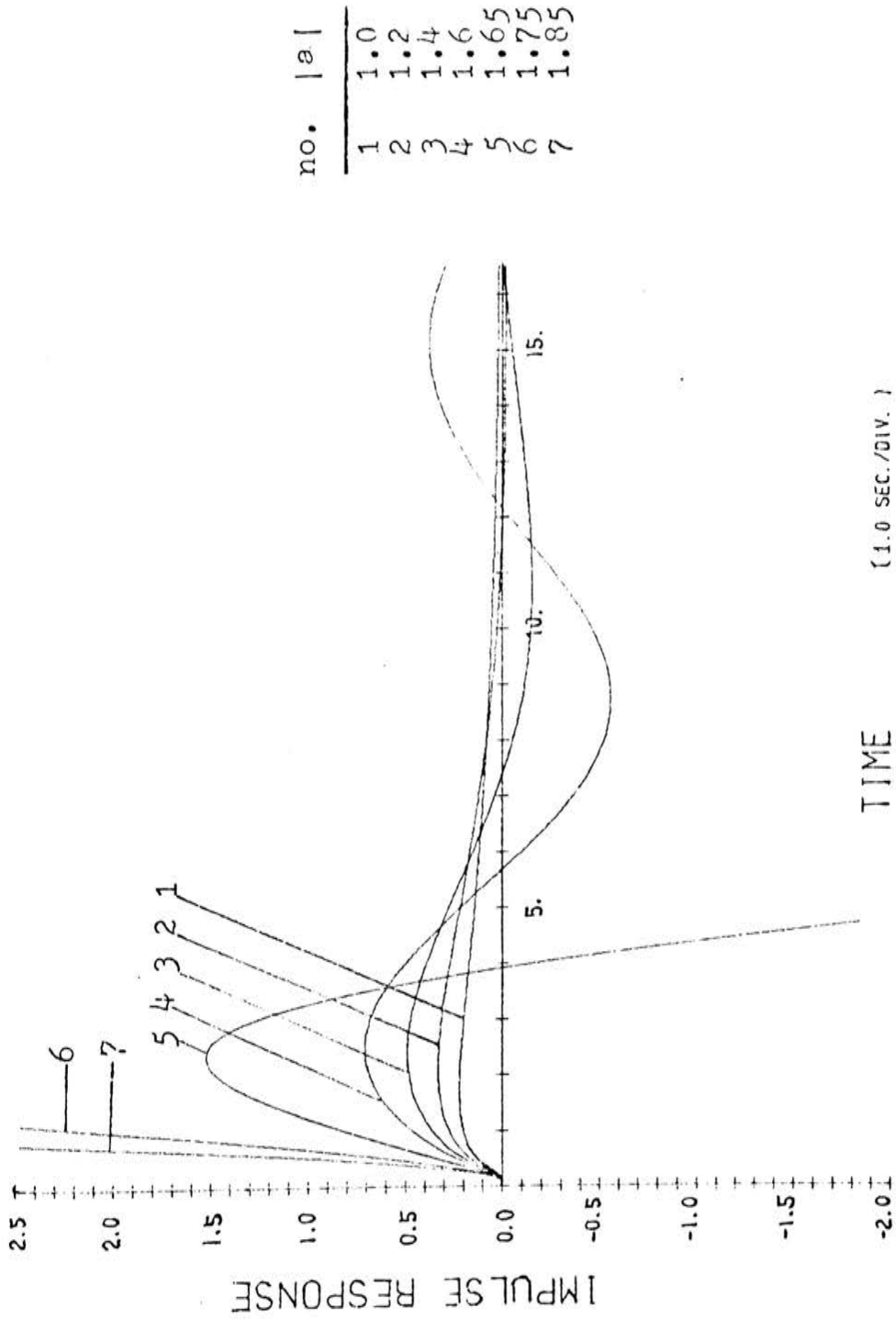


Figure 2-9: Imaginary-part impulse response with pole angle  $\phi=30^\circ$  in the  $w$  plane.

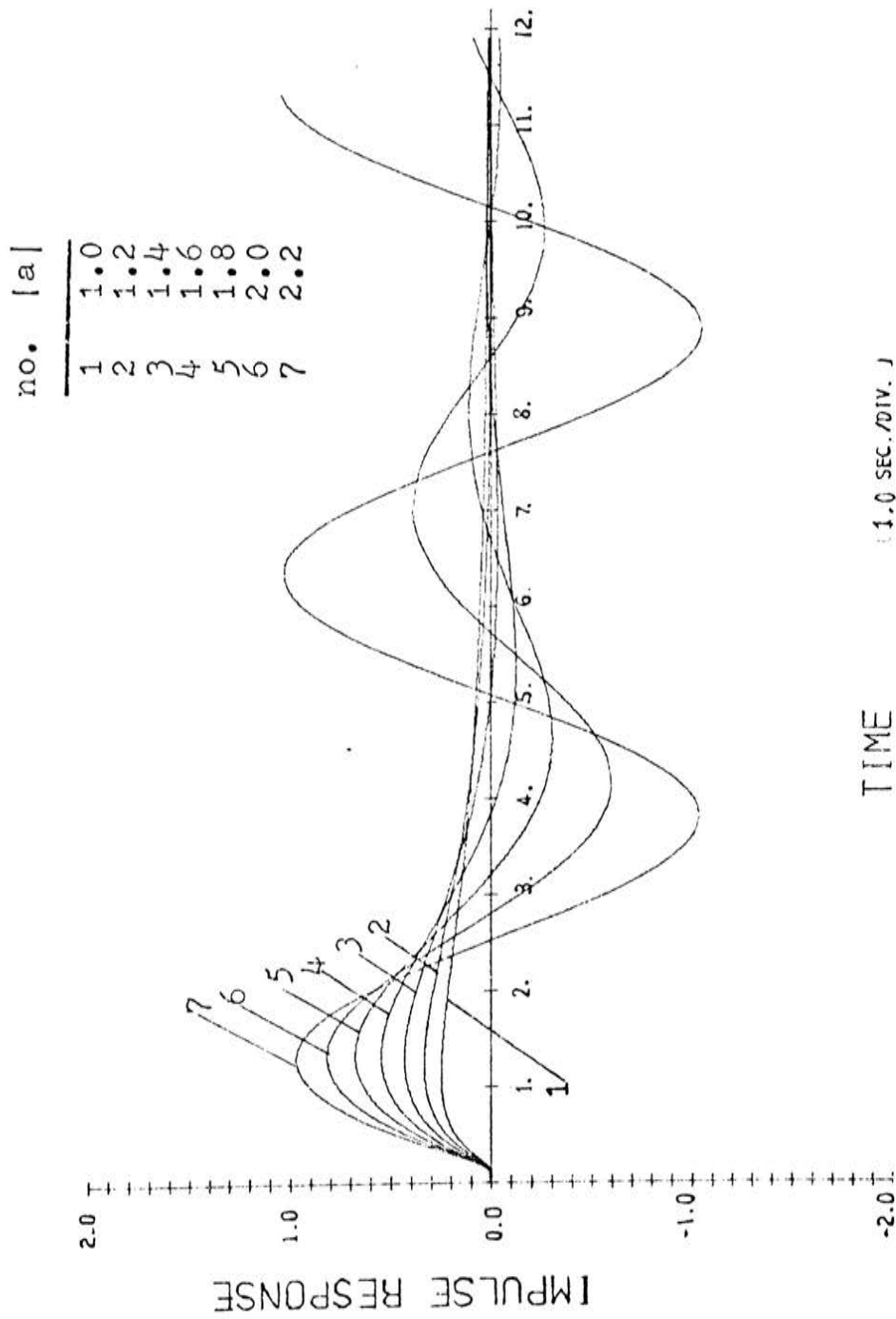


Figure 2-10: Imaginary-part impulse response with pole angle  $\phi=45^\circ$  in the  $w$  plane.



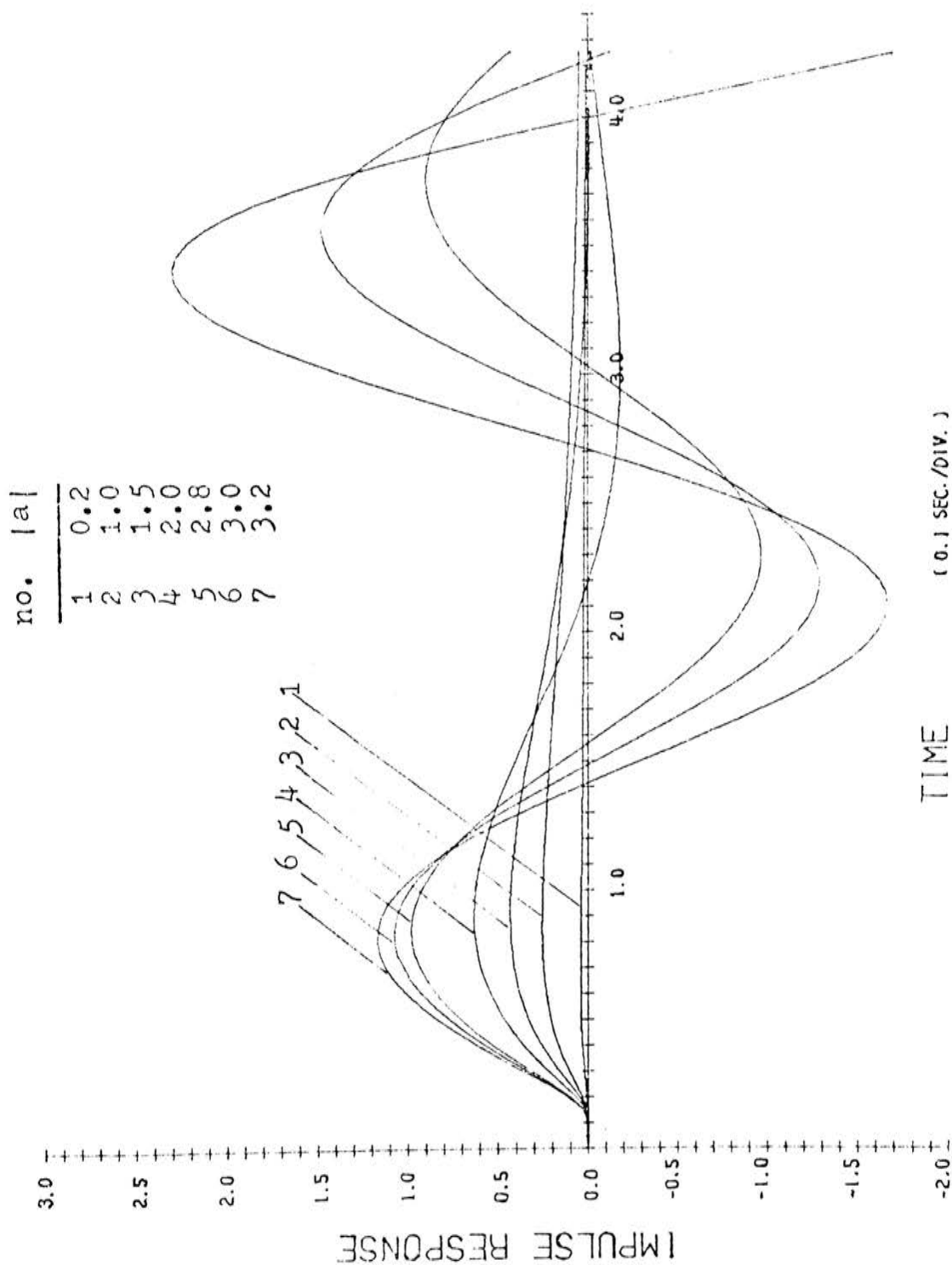


Figure 2-11: Imaginary-part impulse response with pole angle  $\phi=60^\circ$  in the  $w$  plane.

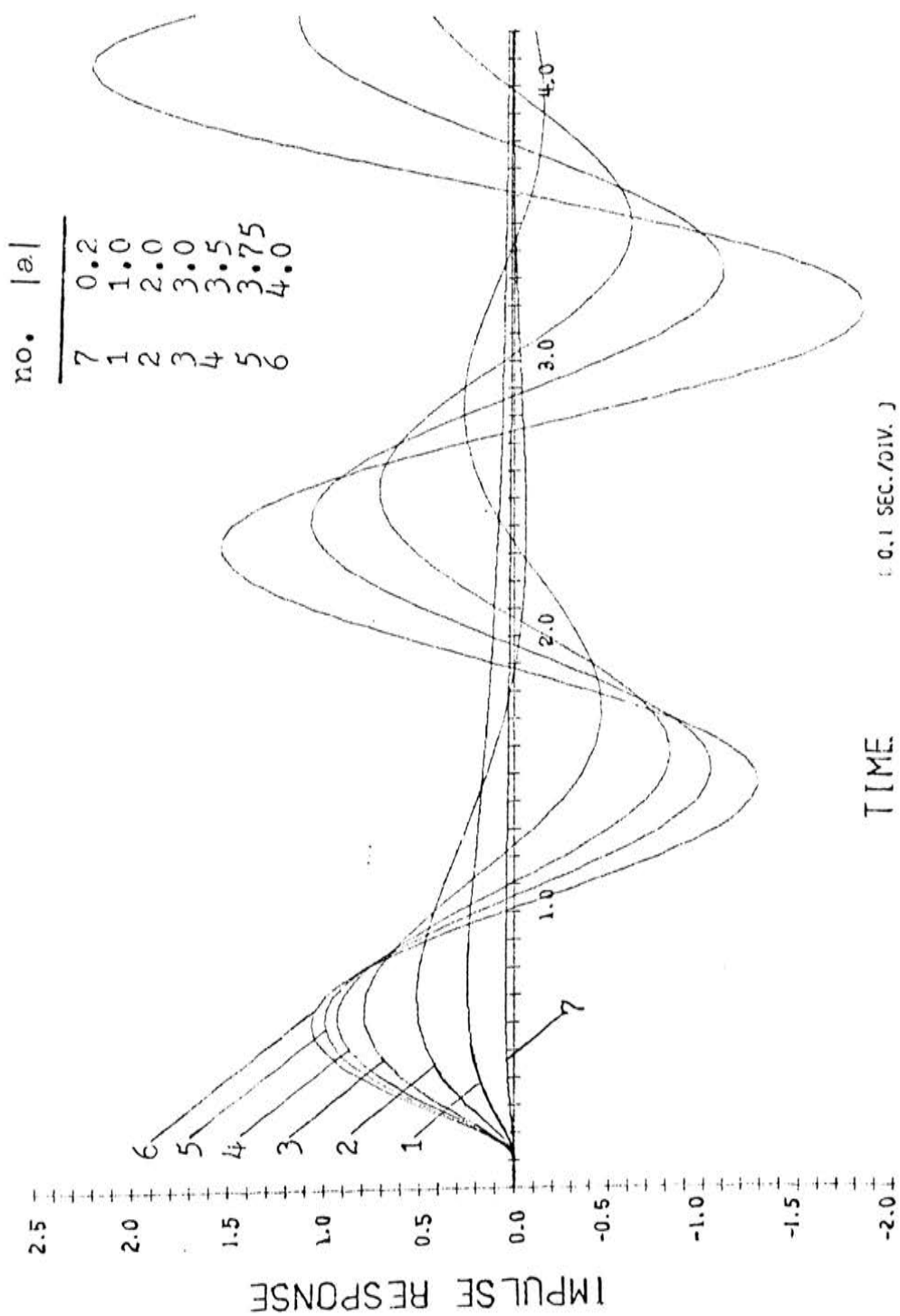


Figure 2-12: Imaginary-part impulse response with pole angle  $\phi=75^\circ$  in the  $w$  plane.

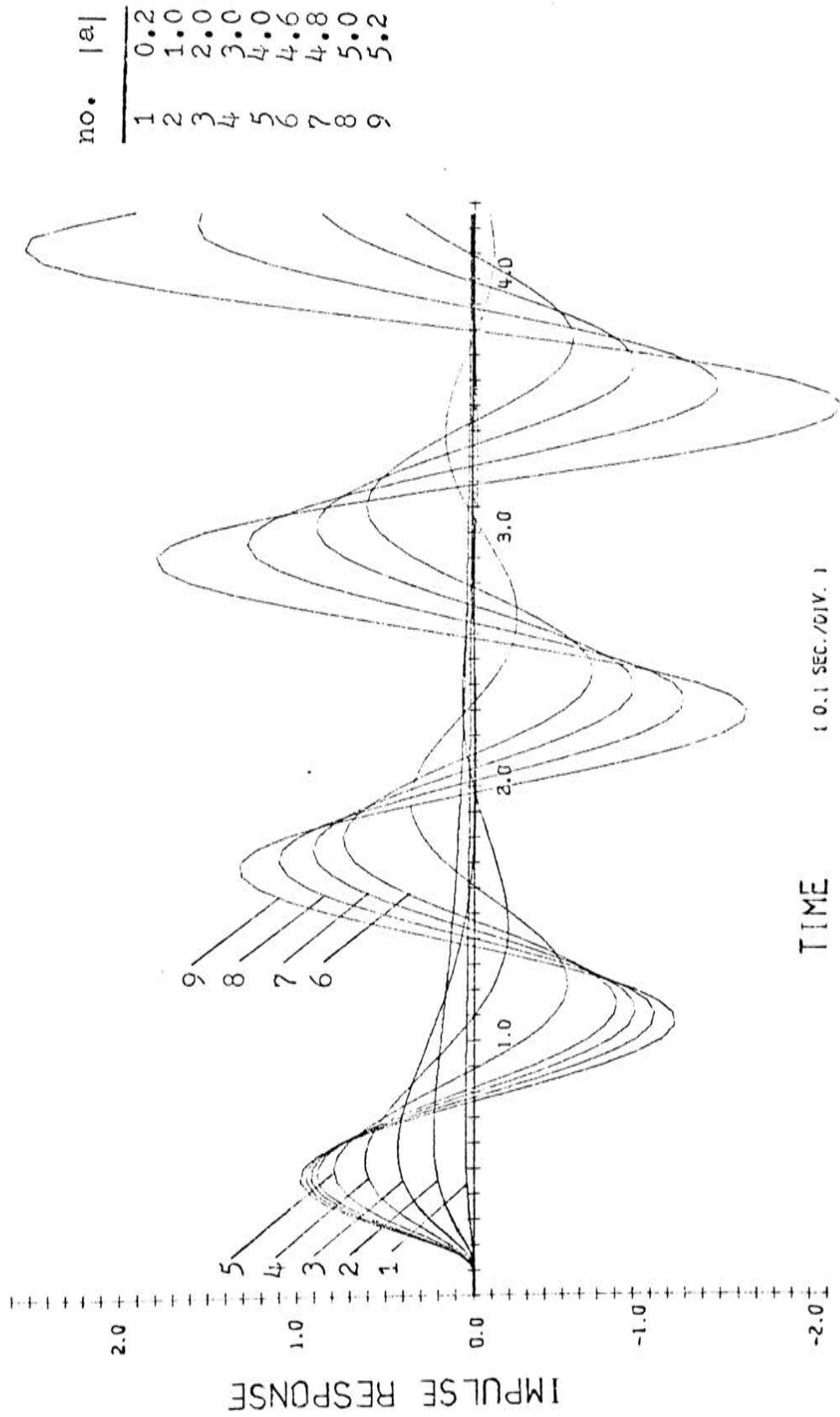


Figure 2-13: Imaginary-part impulse response with pole angle  $\phi=90^\circ$  in the  $w$  plane.

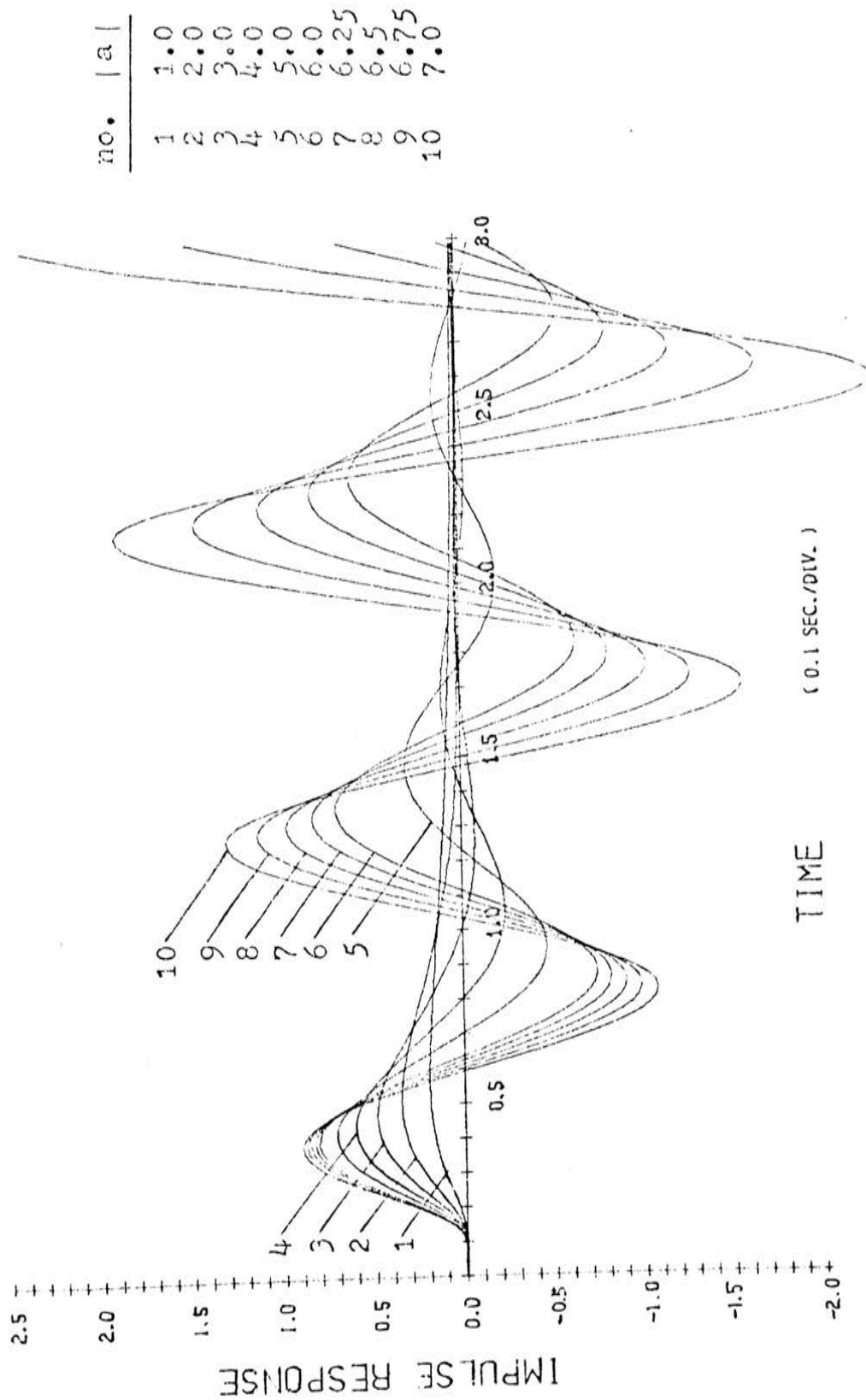


Figure 2-14: Imaginary-part impulse response with pole angle  $\phi=105^\circ$  in the  $w$  plane.

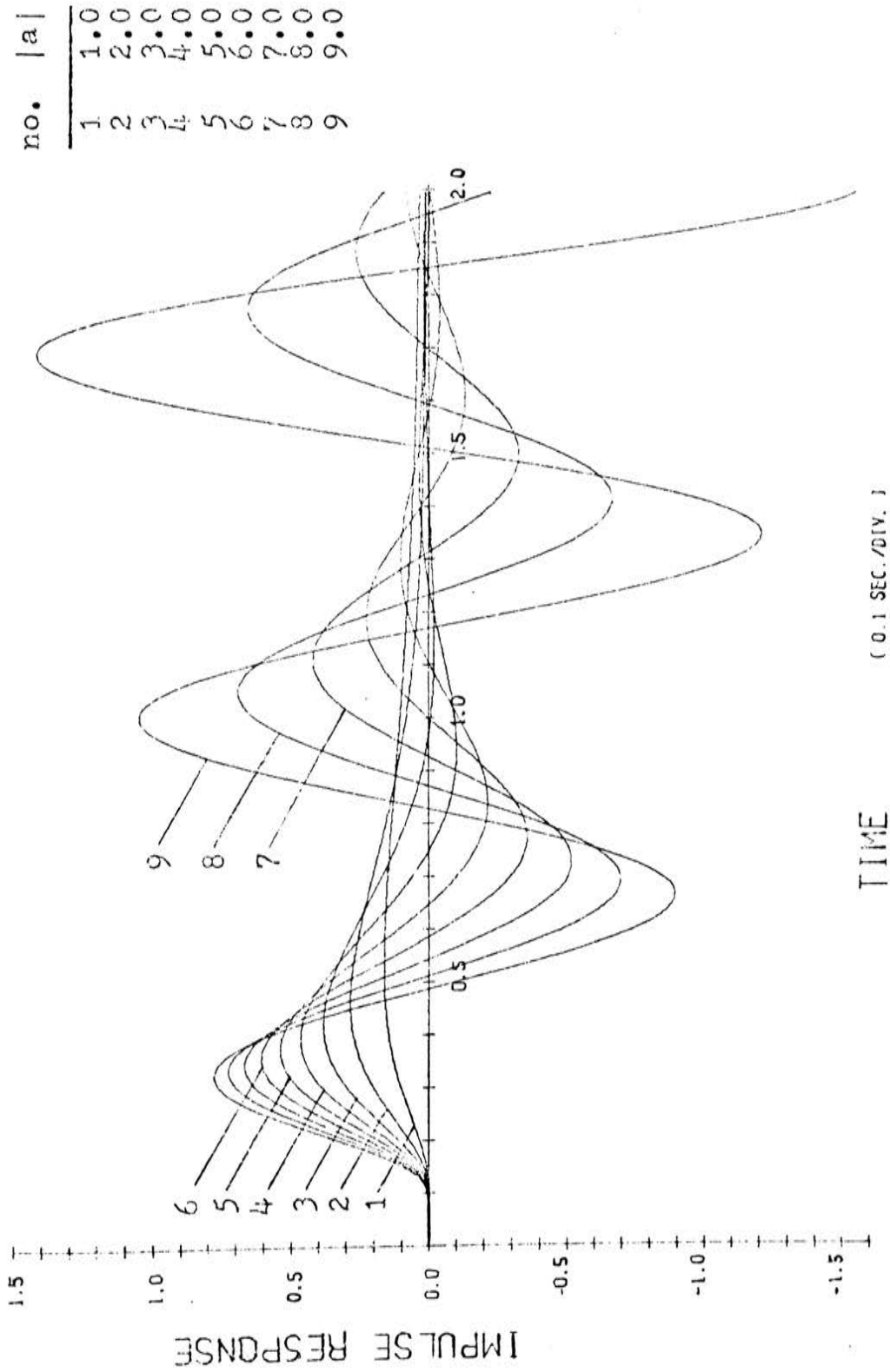


Figure 2-15: Imaginary-part impulse response with pole angle  $\phi=120^\circ$  in the  $w$  plane.

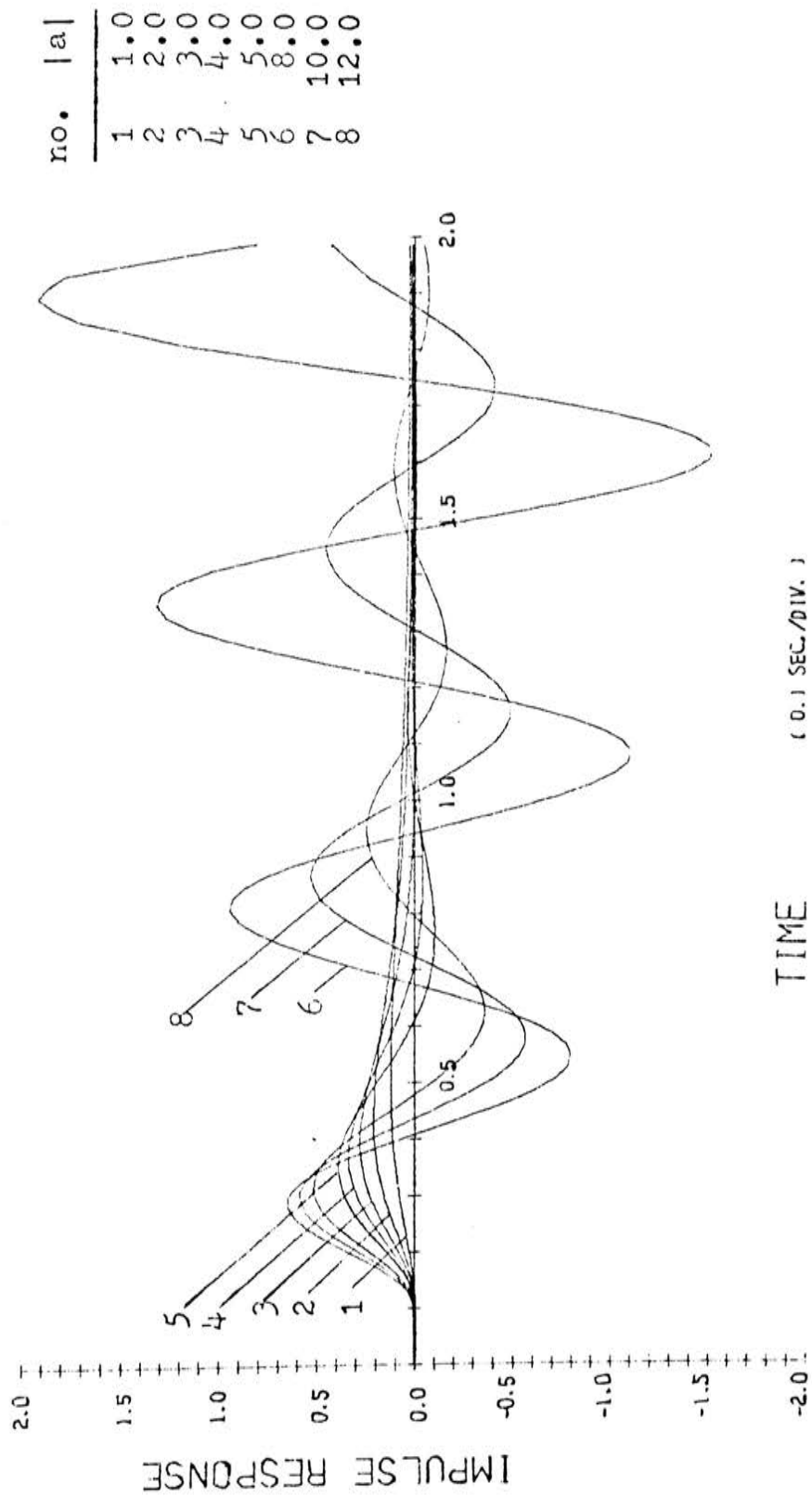


Figure 2-16: Imaginary-part impulse response with pole angle  $\phi=135^\circ$  in the  $w$  plane.

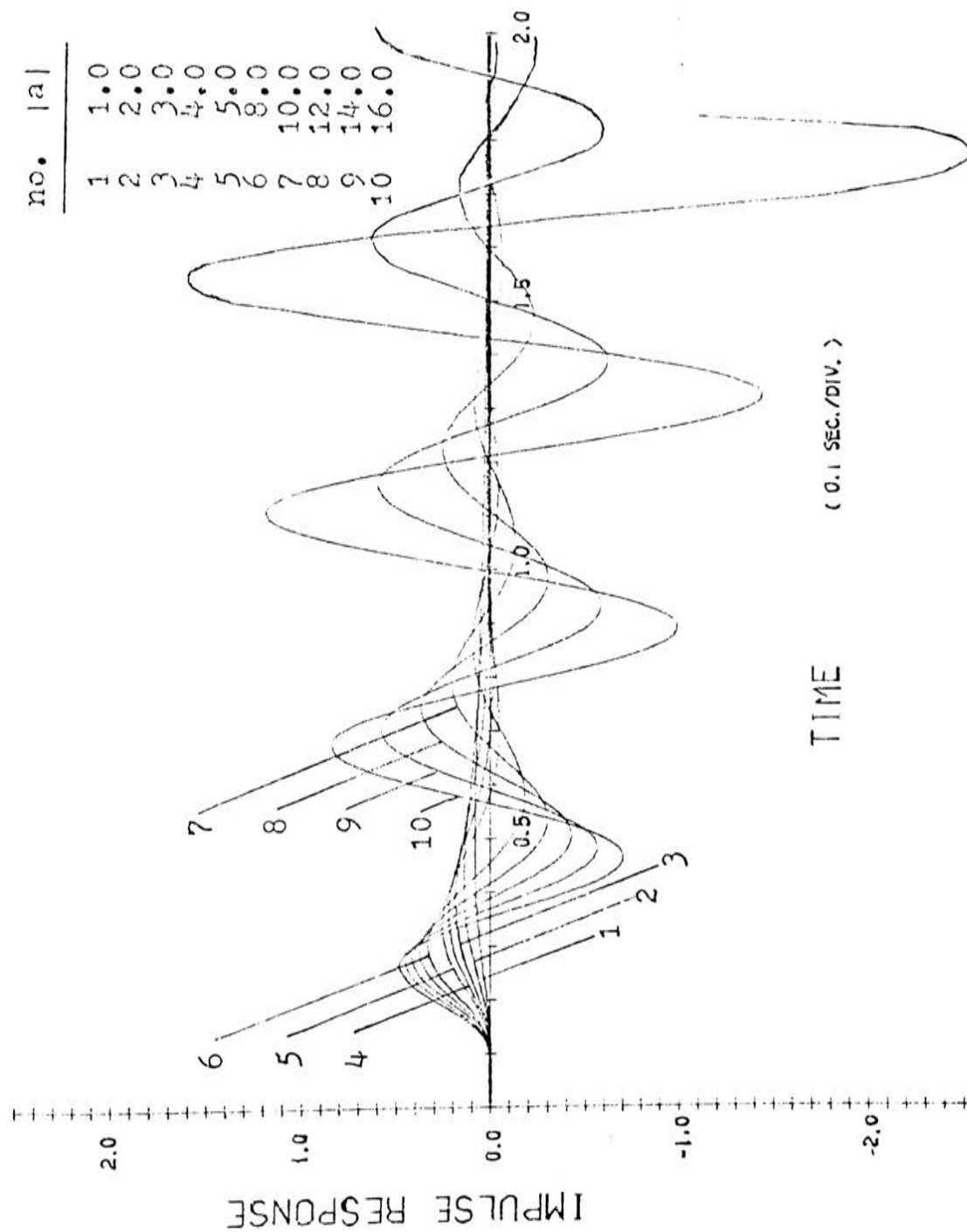


Figure 2-17: Imaginary-part impulse response with pole angle  $\phi=150^\circ$  in the  $w$  plane.

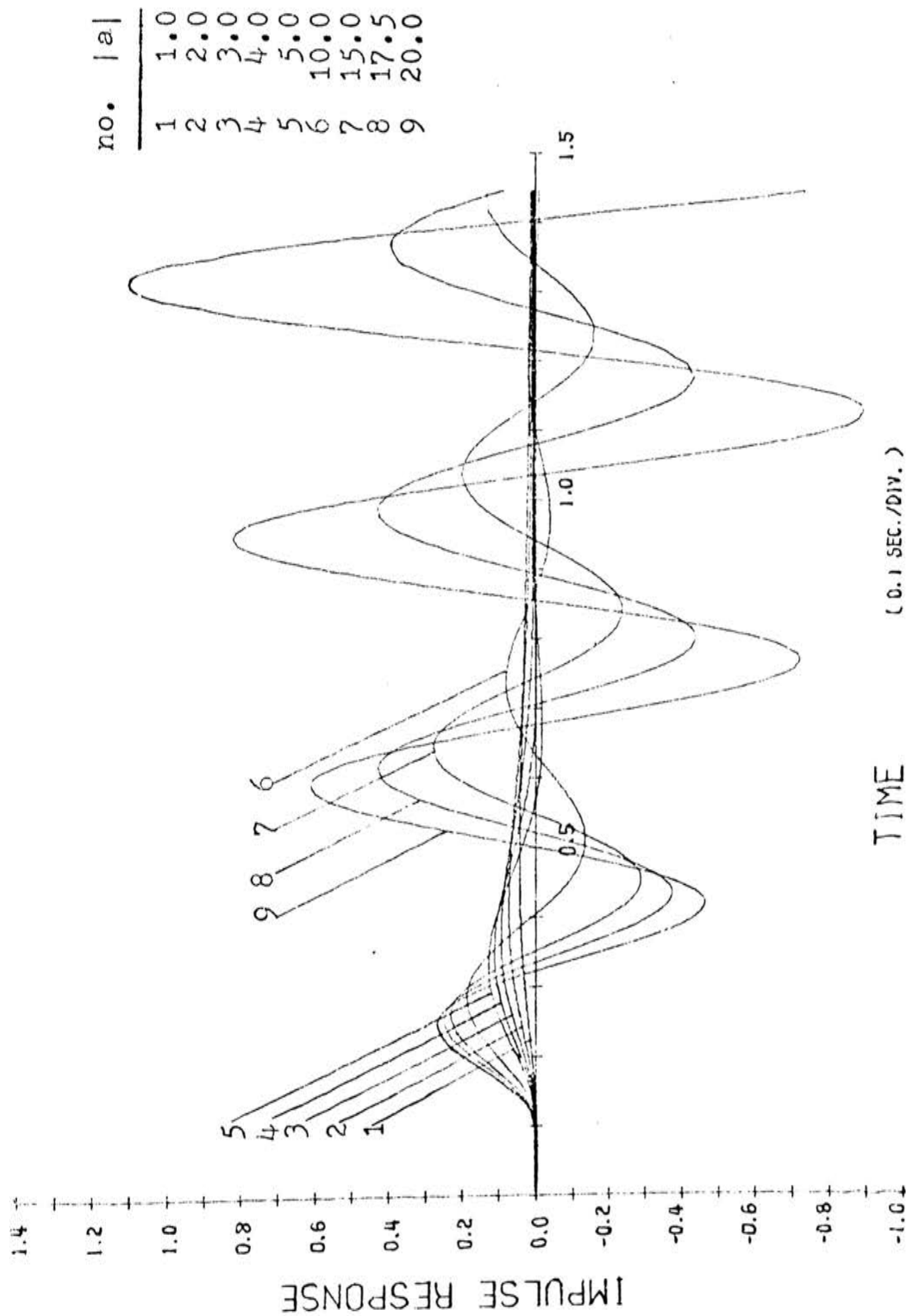


Figure 2-18: Imaginary-part impulse response with pole angle  $\phi=165^\circ$  in the w plane.



Table 2-1: List of pole magnitude being plotted for impulse response \*\*

pole angle	figure number	pole magnitude being plotted (imaginary part)  a	figure number	pole magnitude being plotted (real part)  a
0			2-1	0.0;0.2;0.6;1.0;1.4;1.8;2.2;2.6;3.0;3.4;4.4;5.4;10.4;15.4;
15	2-8	1.1;1.2;1.3;1.4;1.5;1.6;1.7;1.8;	2-24	0.0;1.0;1.1;1.2;1.3;1.4;
30	2-9	1.0;1.2;1.4;1.6;1.65;1.75;1.85;	2-25	0.0;1.0;1.2;1.4;1.6;1.65;1.75;1.85;
45	2-10	1.0;1.2;1.4;1.6;1.8;2.0;2.2;	2-26	0.0;1.0;1.2;1.4;1.6;1.8;2.0;2.2;
60	2-11	0.2;1.0;1.5;2.0;2.8;3.0;3.2;	2-27	0.0;1.0;2.0;2.8;3.0;3.2;
75	2-12	0.2;1.0;2.0;3.0;3.5;3.75;4.0;	2-28	0.0;1.0;2.0;3.0;3.5;3.75;4.0;
90	2-13	0.2;1.0;2.0;3.0;4.0;4.6;4.8;5.0;5.2;	2-29	0.0;1.0;2.0;3.0;4.0;4.6;4.8;5.0;5.2;
105	2-14	0.2;1.0;2.0;3.0;4.0;5.0;6.0;6.25;6.5;	2-30	0.0;1.0;2.0;3.0;4.0;5.0;6.0;6.25;6.5;6.75;
120	2-15	1.0;2.0;3.0;4.0;5.0;6.0;7.0;8.0;9.0;	2-31	0.0;1.0;2.0;3.0;4.0;5.0;6.0;7.0;8.0;9.0;
135	2-16	1.0;2.0;3.0;4.0;5.0;8.0;10.0;12.0;	2-32	0.0;1.0;2.0;3.0;4.0;5.0;8.0;10.0;12.0;
150	2-17	1.0;2.0;3.0;4.0;5.0;8.0;10.0;12.0;14.0;16.0;	2-33	0.0;1.0;2.0;3.0;4.0;5.0;8.0;10.0;12.0;14.0;16.0;18.0;
165	2-18	1.0;2.0;3.0;4.0;5.0;10.0;15.0;17.5;20.0;	2-34	0.0;1.0;2.0;3.0;4.0;5.0;10.0;15.0;17.5;20.0;
180			2-2	0.0;1.0;2.0;3.0;4.0;5.0;10.0;15.0;20.0;23.0;23.5;

\*\* The pole magnitudes for fig. 2-3 through 2-7 and fig. 2-19 through 2-23 are 0.2;

0.4;0.6;0.8;1.0; with pole angle varying 15 step in each graph.

Table 2-2: The period of oscillation of impulse response with pole on the boundary of the region of stability in the w plane

pole angle ( $\phi^\circ$ )	calculated value		measured value		figure number		remark
	pole magnitude	period $t_c(\text{sec.})$	pole magnitude	period $t_m(\text{sec.})$	imaginary part	real part	
15	1.30	45.90	1.30	46.00	2-8	2-24	*For $\phi = 0.0$ , $t_c = \infty$ , it means no oscillation there.
30	1.69	11.48	1.65	11.90	2-9	2-25	
45	2.19	5.10	2.20	5.09	2-10	2-26	
60	2.85	2.86	2.80	2.93	2-11	2-27	
74	3.69	1.83	3.75	1.92	2-12	2-28	
90	4.81	1.272	4.80	1.275	2-13	2-29	
105	6.25	0.938	6.25	0.94	2-14	2-30	
120	8.10	0.715	8.00	0.72	2-15	2-31	
135	10.52	0.567	10.00	0.58	2-16	2-32	
150	13.90	0.458	14.00	0.451	2-17	2-33	
165	17.80	0.379	17.50	0.38	2-18	2-34	
180	23.10	0.318	23.00	0.32	2-19	2-2	

(2) With the transfer function  $\frac{1}{w-a} + \frac{1}{w-a^*}$

$$\text{Let } T_2(w) = \frac{1}{w-a} + \frac{1}{w-a^*} \dots\dots\dots (2-7)$$

The Laplace inverse transformation of  $T_2(w)$  is

$$\begin{aligned} T_2(t) &= \mathcal{L}^{-1}[T_2(w)] = \mathcal{L}^{-1}\left[\frac{1}{w-a}\right] + \mathcal{L}^{-1}\left[\frac{1}{w-a^*}\right] \\ &= 2\text{Re}[h(t)] \dots\dots\dots (2-8) \end{aligned}$$

Thus, the transient response of  $T_2(t)$  can be investigated with double values of the real part of the response  $h(t)$ , which is shown in figures 2-19 through 2-34 according to the list in table 2-1.

The real part of the impulse response  $h(t)$  is plotted with constant pole magnitude and varying pole angle in figures 2-19 through 2-23, and some results are observed as follows:

- (a) The peak values of the response are about 0.9 to 0.95 instead of being unity. It decreases slightly with pole angle increases.
- (b) The separation between curves in each graph becomes more apparent as pole magnitude increases. In other words, the effect of varying pole angle on the response becomes more obvious with increasing pole magnitude.
- (c) The curve for  $a = 0.0$  coincides with the curve for  $\phi = 90^\circ$  during its first 0.3 second, as shown in the enlarged portion of each graph.
- (d) Check the magnitude of the response in figure 2-23: When  $t = 0.3$  second, the magnitude of the response for

$\phi = 180^\circ$  has dampened 24% more than that of  $\phi = 0^\circ$ . The responses in the  $\phi > 90^\circ$  case dampen more rapidly than those do in the  $\phi < 90^\circ$  case with pole magnitude fixed.

(e) Consider the constant pole magnitude within the stable region:

(i) The impulse response has a delay time of about 0.02 to 0.03 second for any pole angle.

(ii) The delay time between the peaks of two extreme curves for  $\phi = 180^\circ$  and  $\phi = 0^\circ$  is within 0.025 second. Hence, the effect of varying pole angle to the first peak time is negligible.

(iii) Note the period of the response with the magnitude above 50% of its peak value; the larger the pole angle, the shorter the period of the response remaining at high value. For example, the period for  $\phi = 180^\circ$  is shorter about 0.82 second than that for  $\phi = 0^\circ$  when  $a = 1$ .

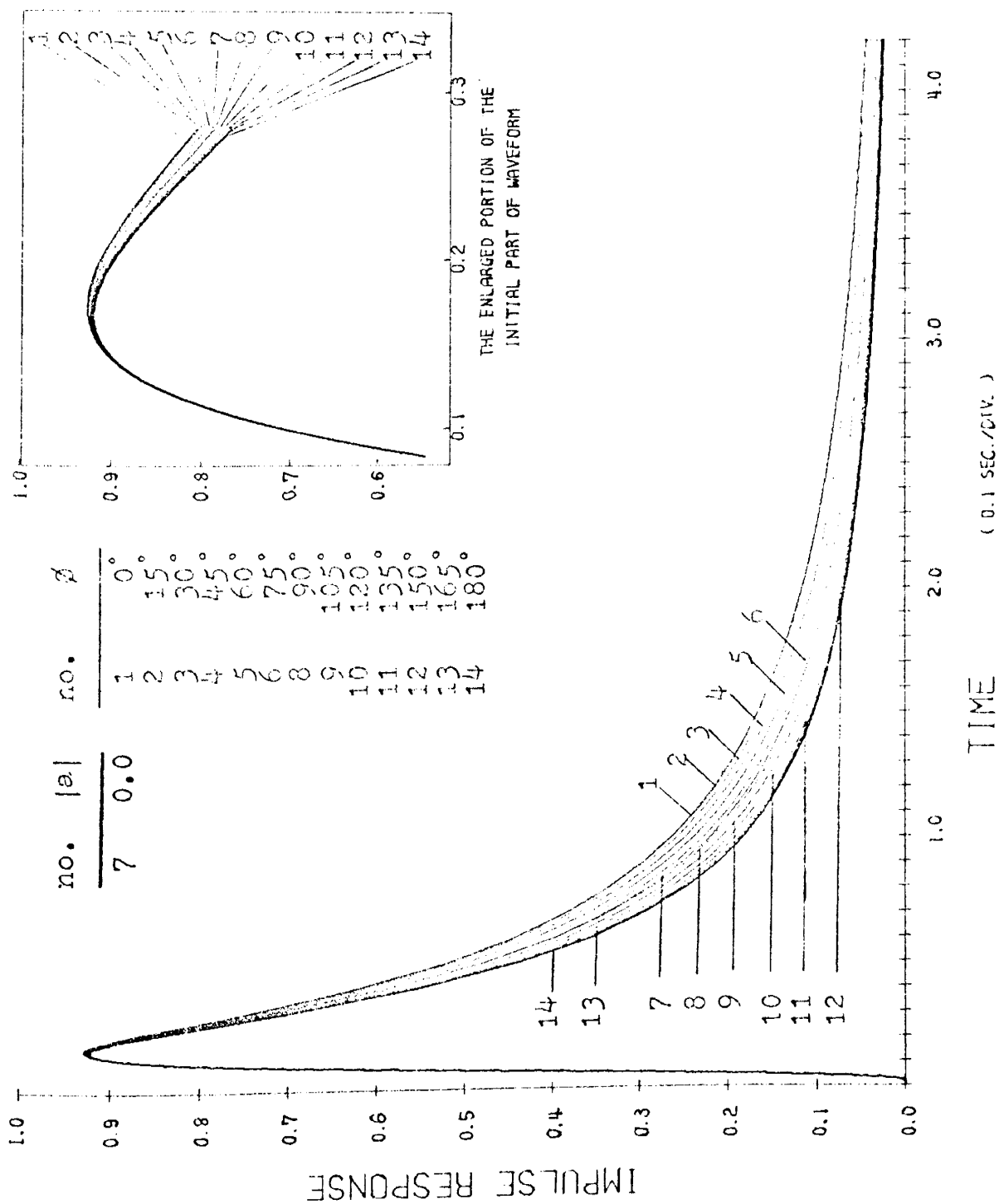


Figure 2-19: Real-part impulse response with pole magnitude  $|a|=0.2$  in the  $w$  plane.

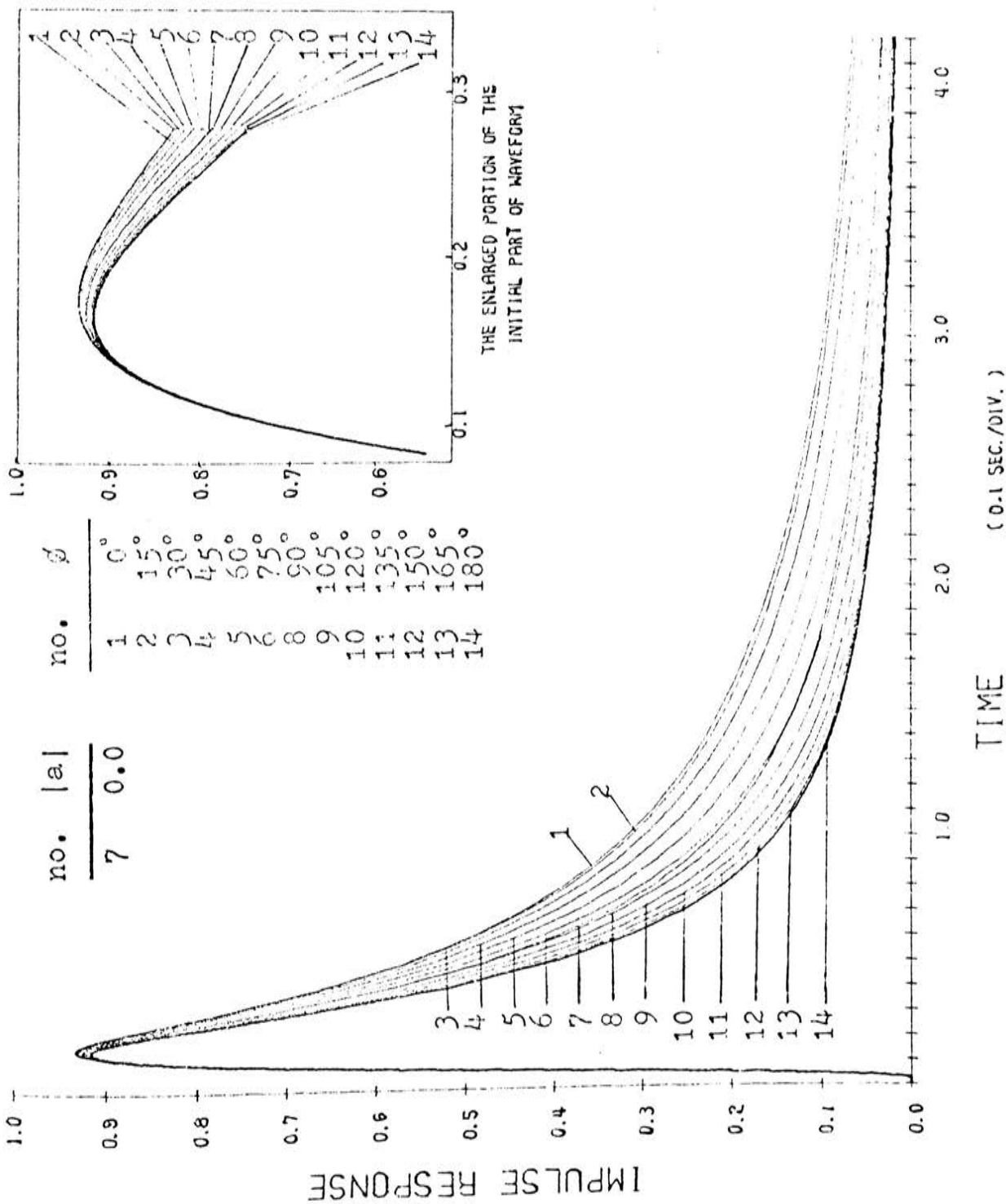


Figure 2-20: Real-part impulse response with pole magnitude  $|a|=0.4$  in the  $w$  plane.

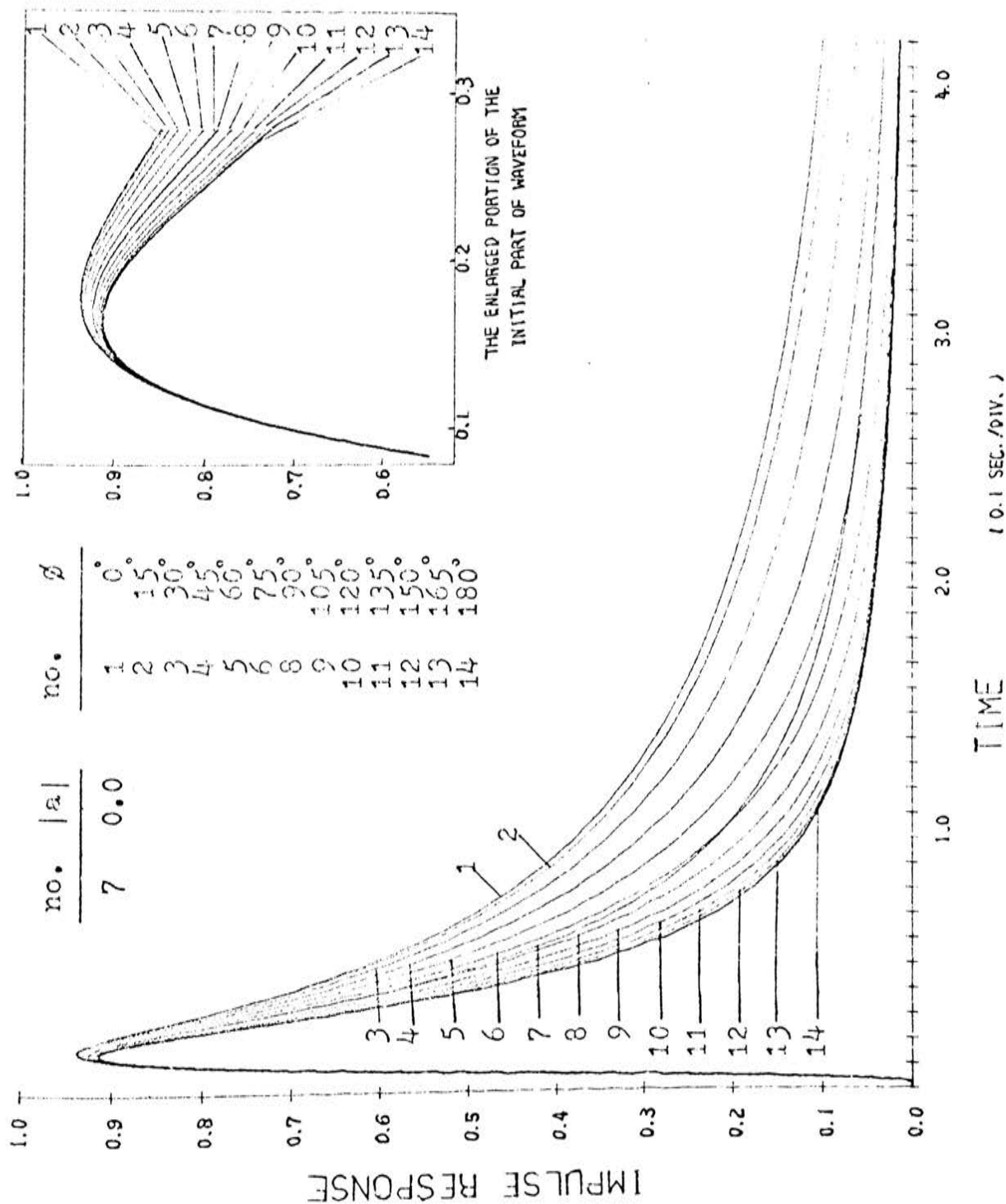


Figure 2-21: Real-part impulse response with pole magnitude  $|a|=0.6$  in the w plane.

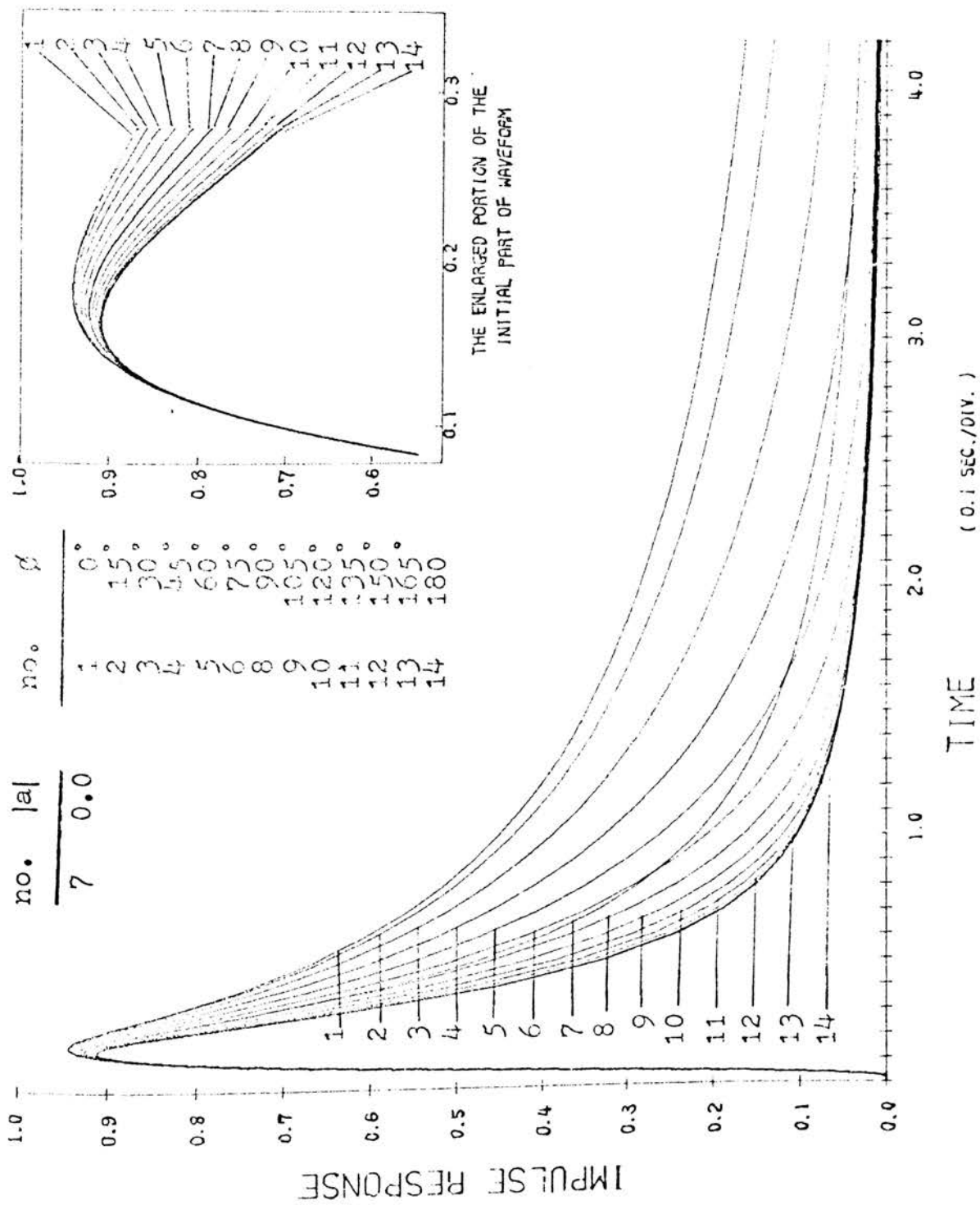


Figure 2-22: Real-part impulse response with pole magnitude  $|a|=0.8$  in the  $w$  plane.



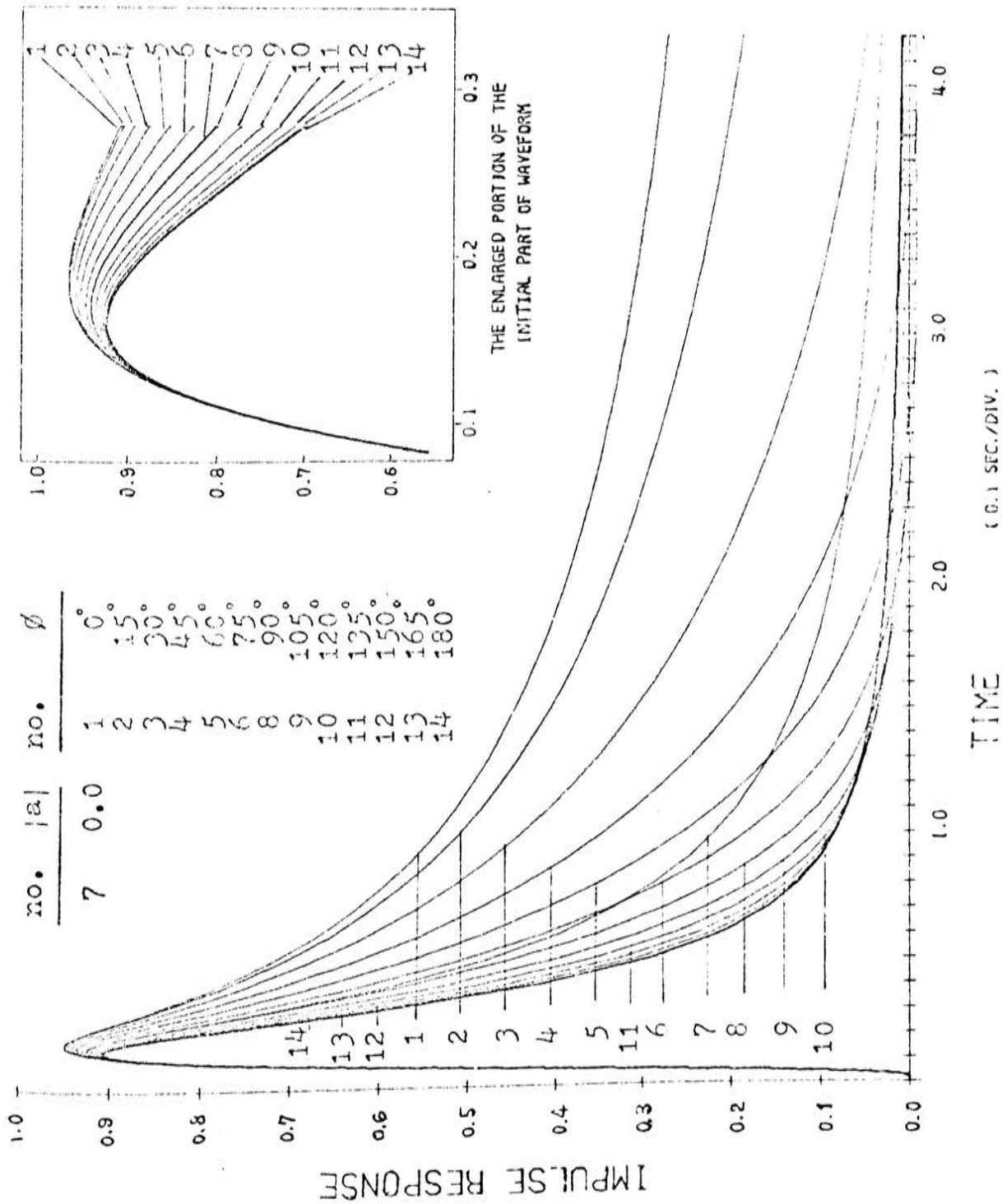


Figure 2-23: Real-part impulse response with pole magnitude  $|a|=1.0$  in the w plane.

With fixed pole angle and varying pole magnitude, the real part of the impulse response, as shown in figures 2-24 through 2-34, behaves similarly to the imaginary part except in the first cycle of the wave.

With these figures, some observations are found as follows:

- (a) Comparing together with figures 2-19 through 2-23, the peak value of the response occurs at  $t \approx 0.16$  to  $0.18$  second, while it remains nearly zero in the imaginary impulse response during this time.
- (b) For the case  $\phi < 90^\circ$ , the peak value is larger and the peak period is longer than those of the curve of  $a = 0$ . But the situation reverses when  $\phi \geq 90^\circ$ .
- (c) The initial slopes of the wave are almost the same before reaching their peaks for any pole magnitude in stable region. However, after passing their peaks, the wave forms, in the  $\phi \geq 90^\circ$  region, decrease with steeper slope, while they decrease more slowly in the right half-w-plane, as the pole magnitude is increased.
- (d) The oscillation period of the real part of the impulse response is the same as that of the imaginary one listed in table 2-2. The larger the pole angle, the shorter the oscillation period; but the oscillating wave of the real part of the impulse response leads the imaginary part by one quarter cycle.

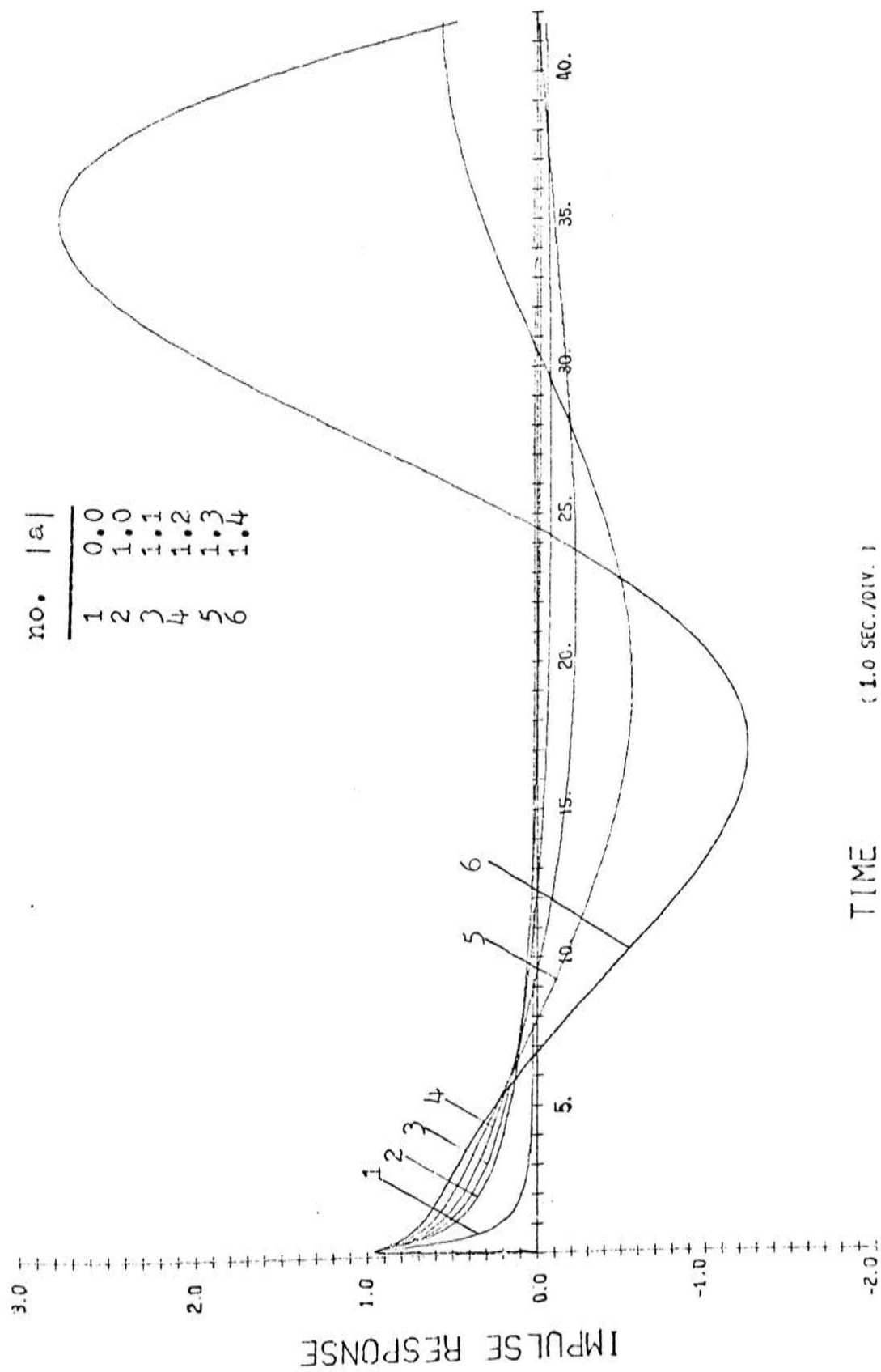


Figure 2-24: Real-part impulse response with pole angle  $\phi=15^\circ$  in the  $w$  plane.

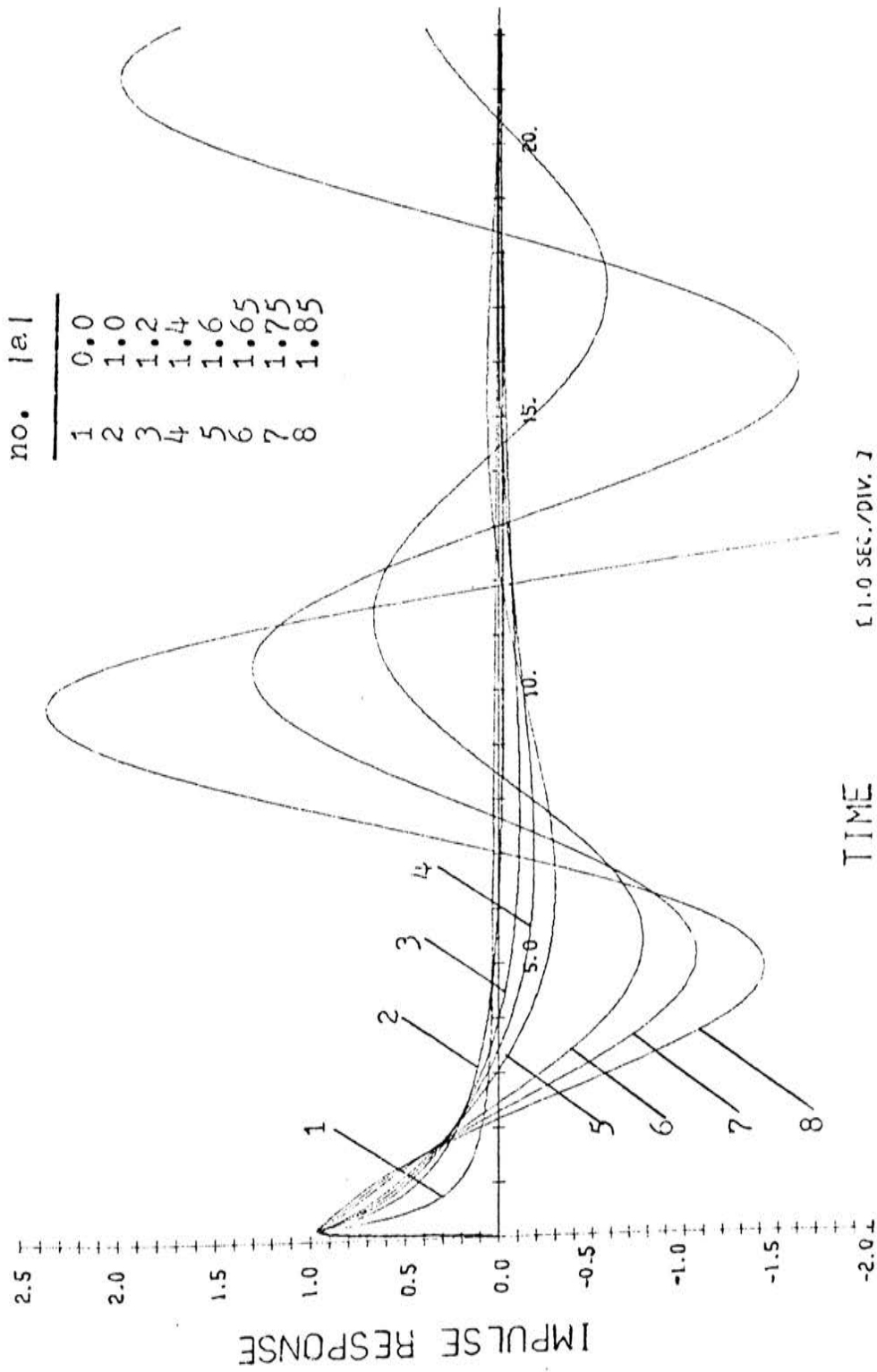


Figure 2-25: Real-part impulse response with pole angle  $\phi=30^\circ$  in the  $w$  plane.

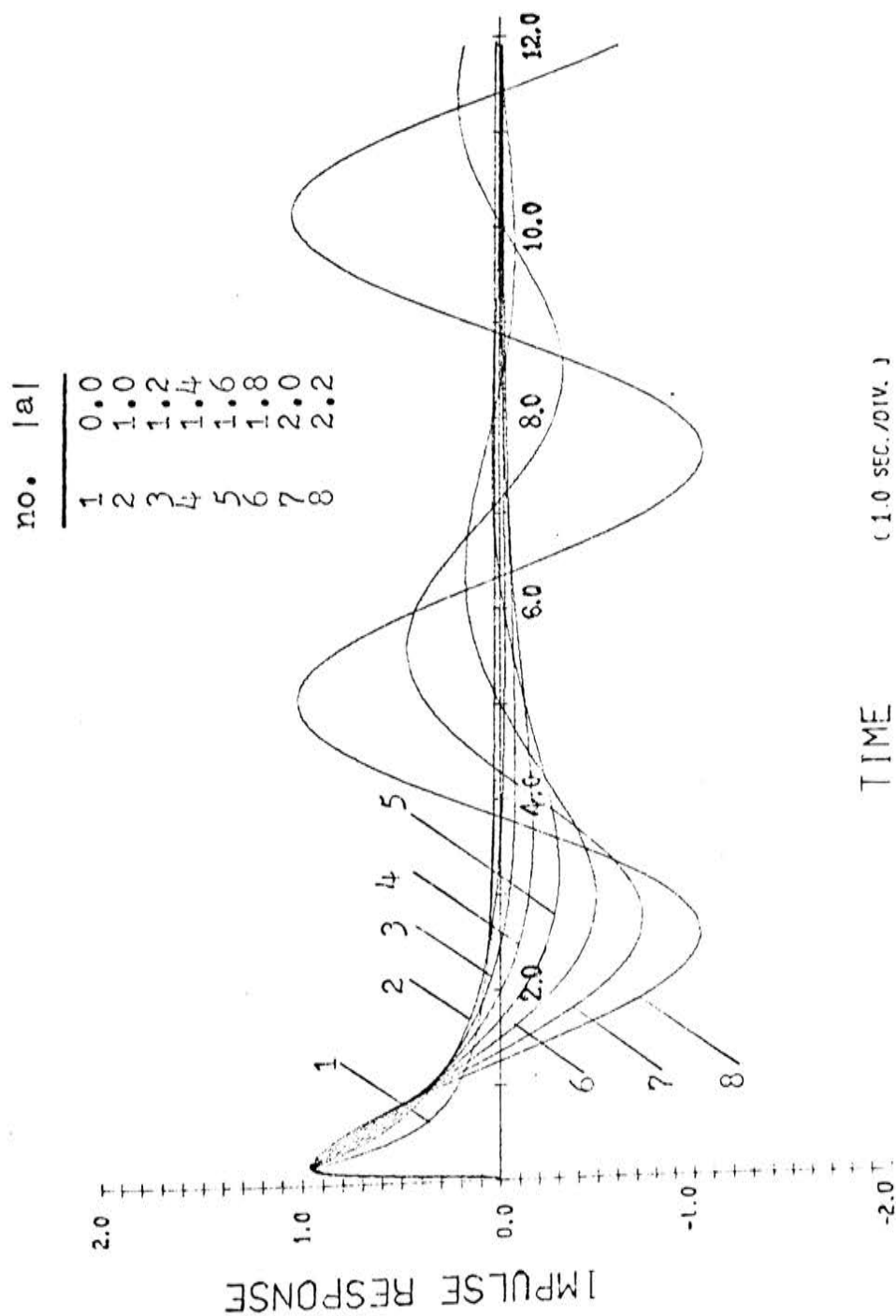


Figure 2-26: Real-part impulse response with pole angle  $\phi=45^\circ$  in the w plane.

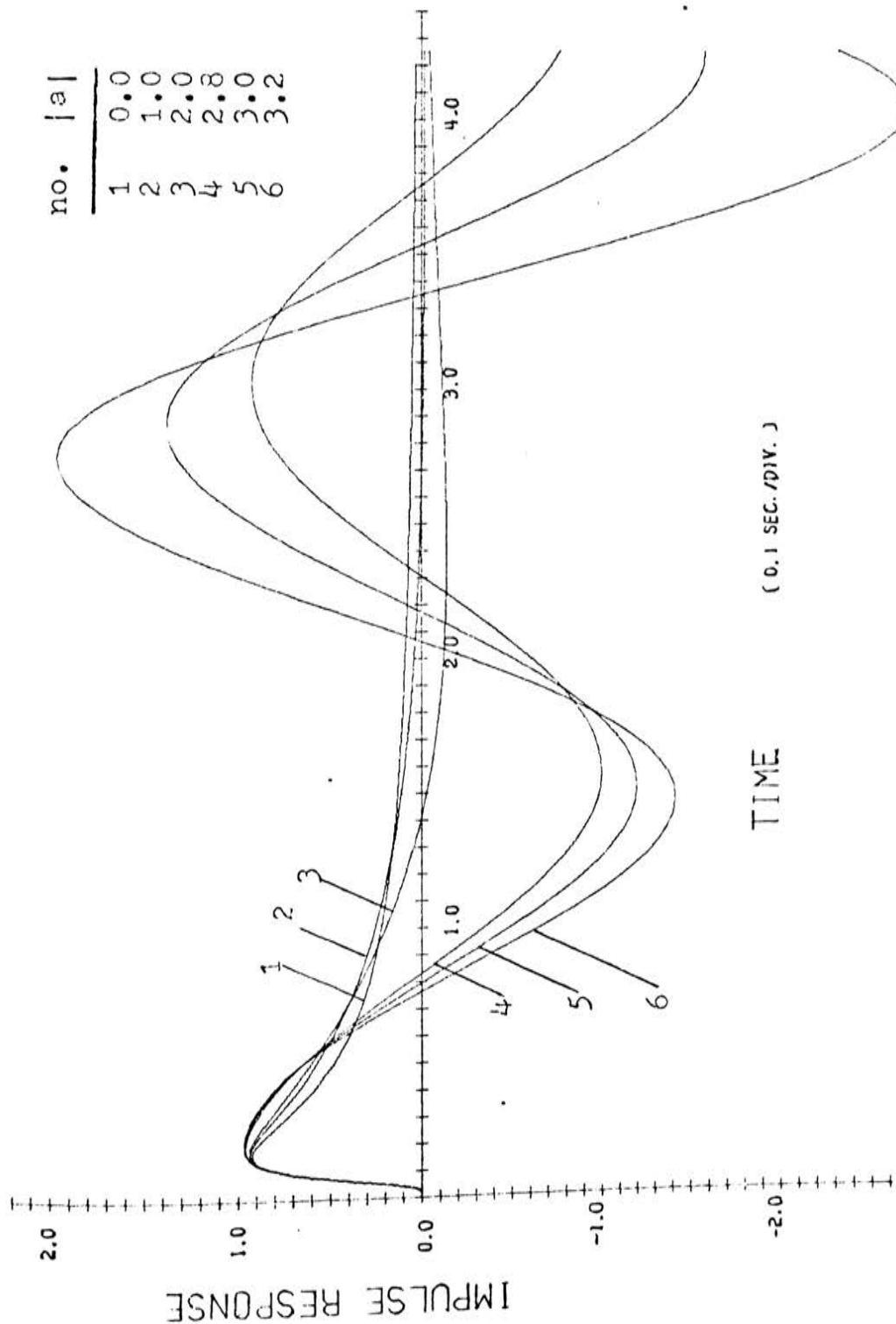


Figure 2-27: Real-part impulse response with pole angle  $\phi=60^\circ$  in the  $w$  plane.

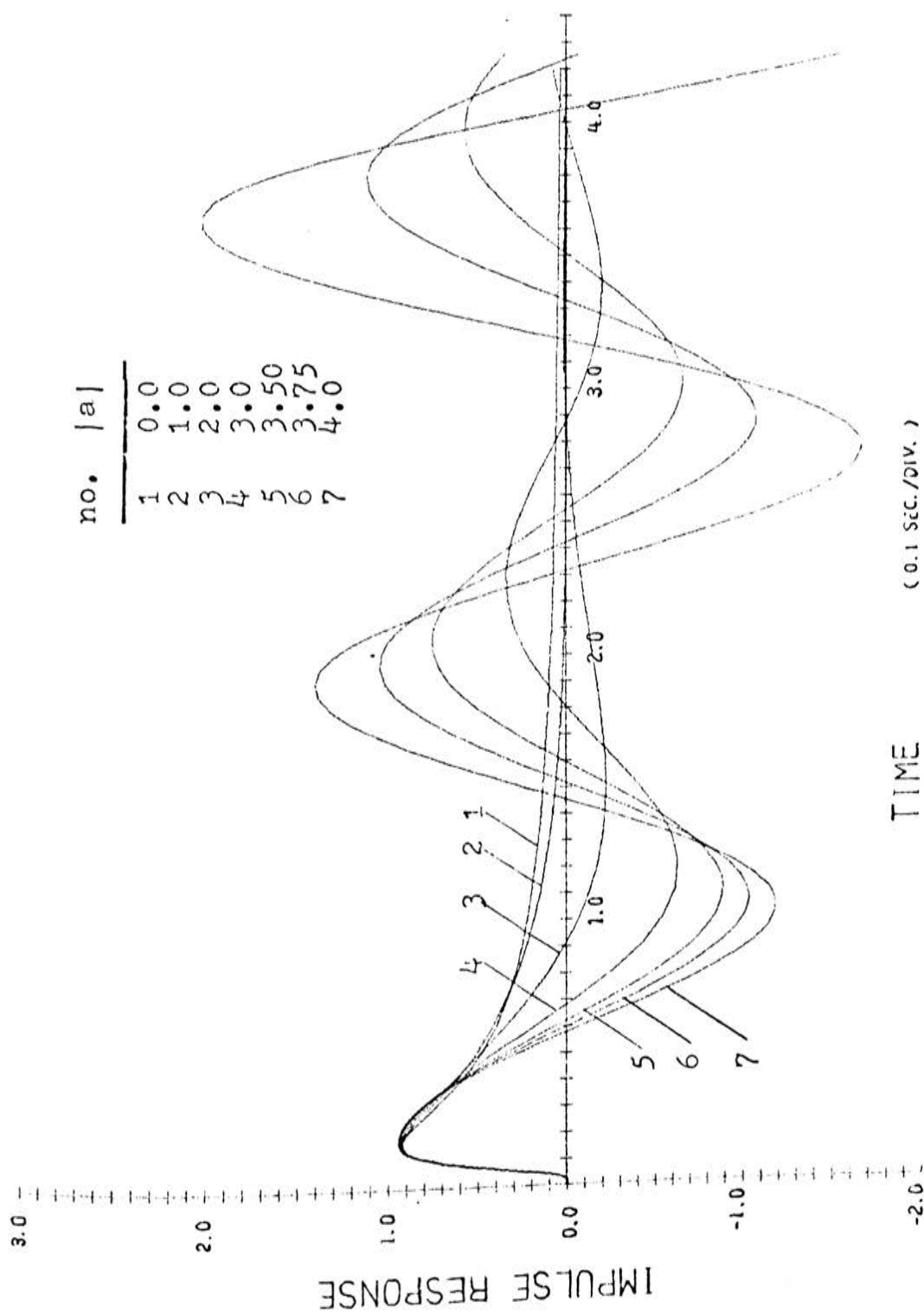


Figure 2-28: Real-part impulse response with pole angle  $\phi=75^\circ$  in the  $w$  plane.

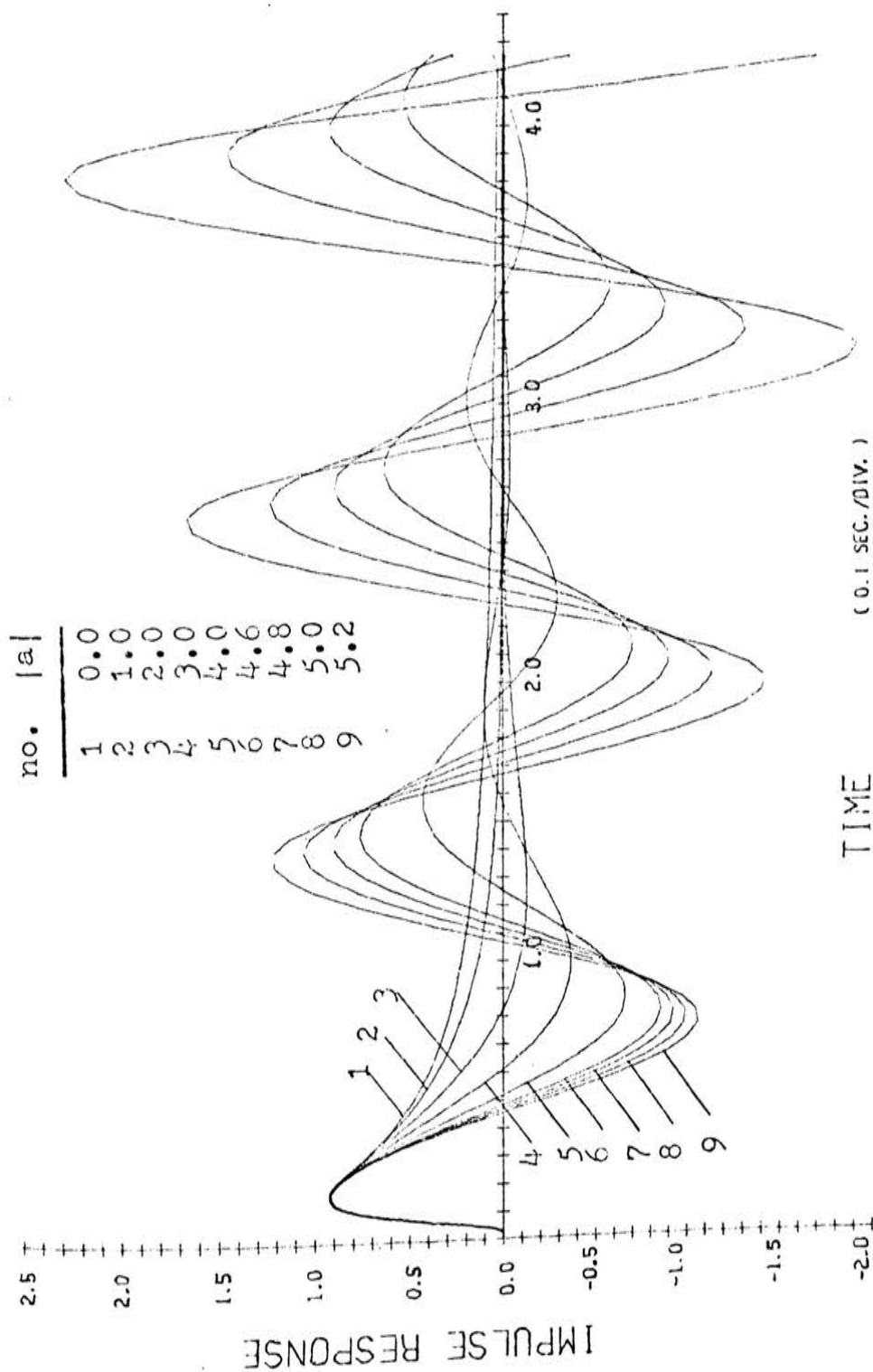


Figure 2-29: Real-part impulse response with pole angle  $\phi=90^\circ$  in the  $w$  plane.



no.	a
1	0.0
2	1.0
3	2.0
4	3.0
5	4.0
6	5.0
7	6.0
8	6.25
9	6.50
10	6.75

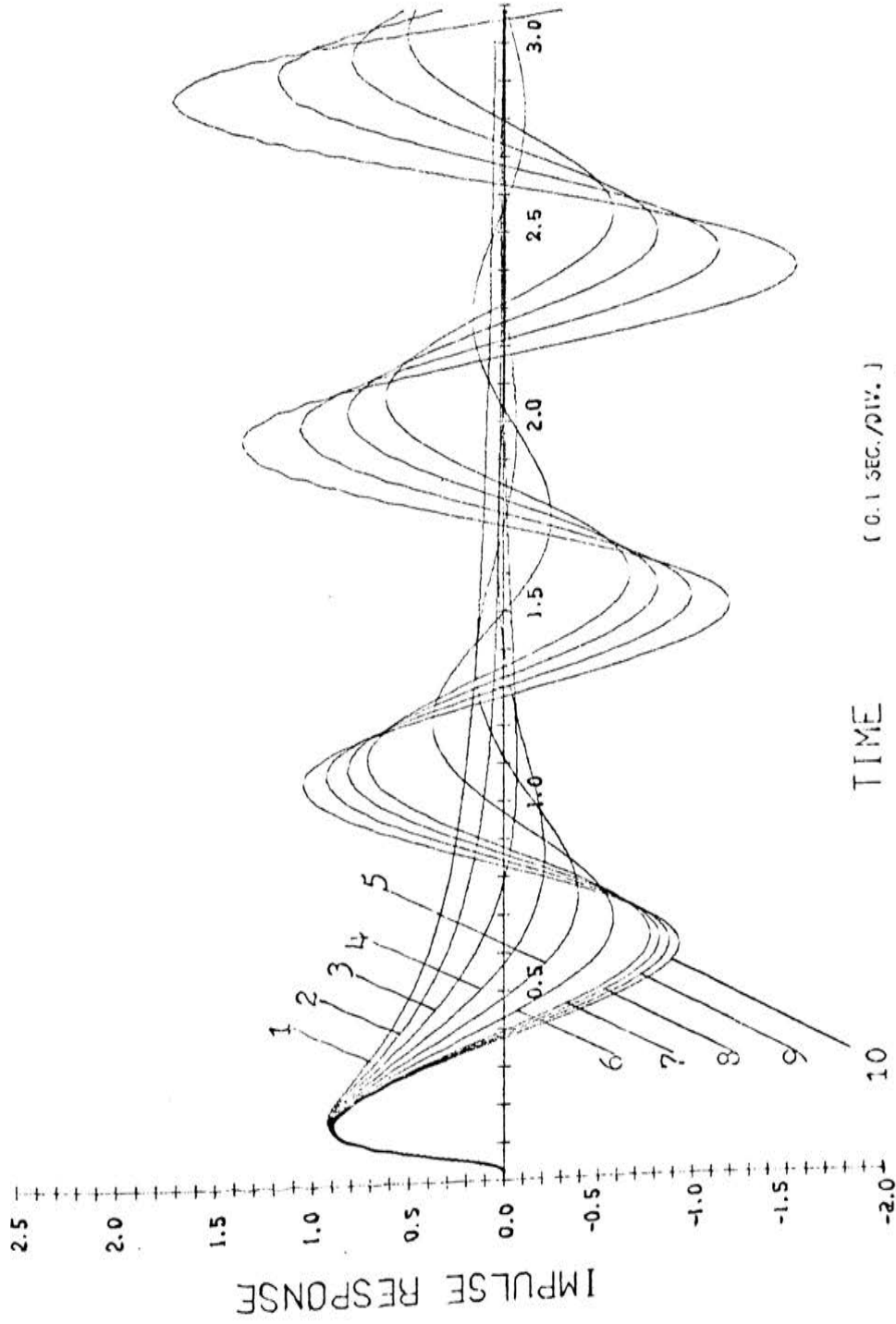


Figure 2-30: Real-part impulse response with pole angle  $\phi=105^\circ$  in the  $w$  plane.

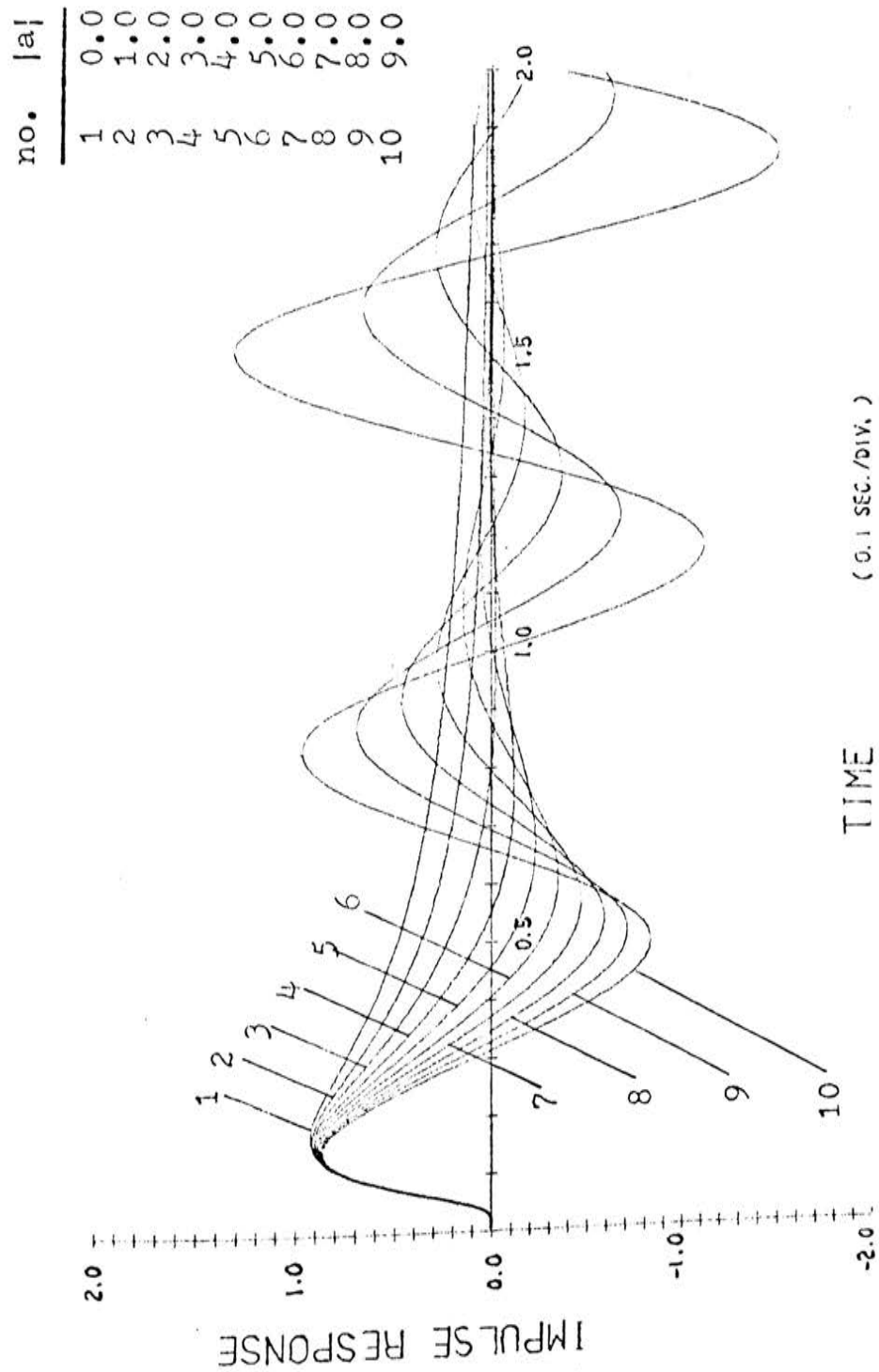


Figure 2-31: Real-part impulse response with pole angle  $\phi=120^\circ$  in the w plane.

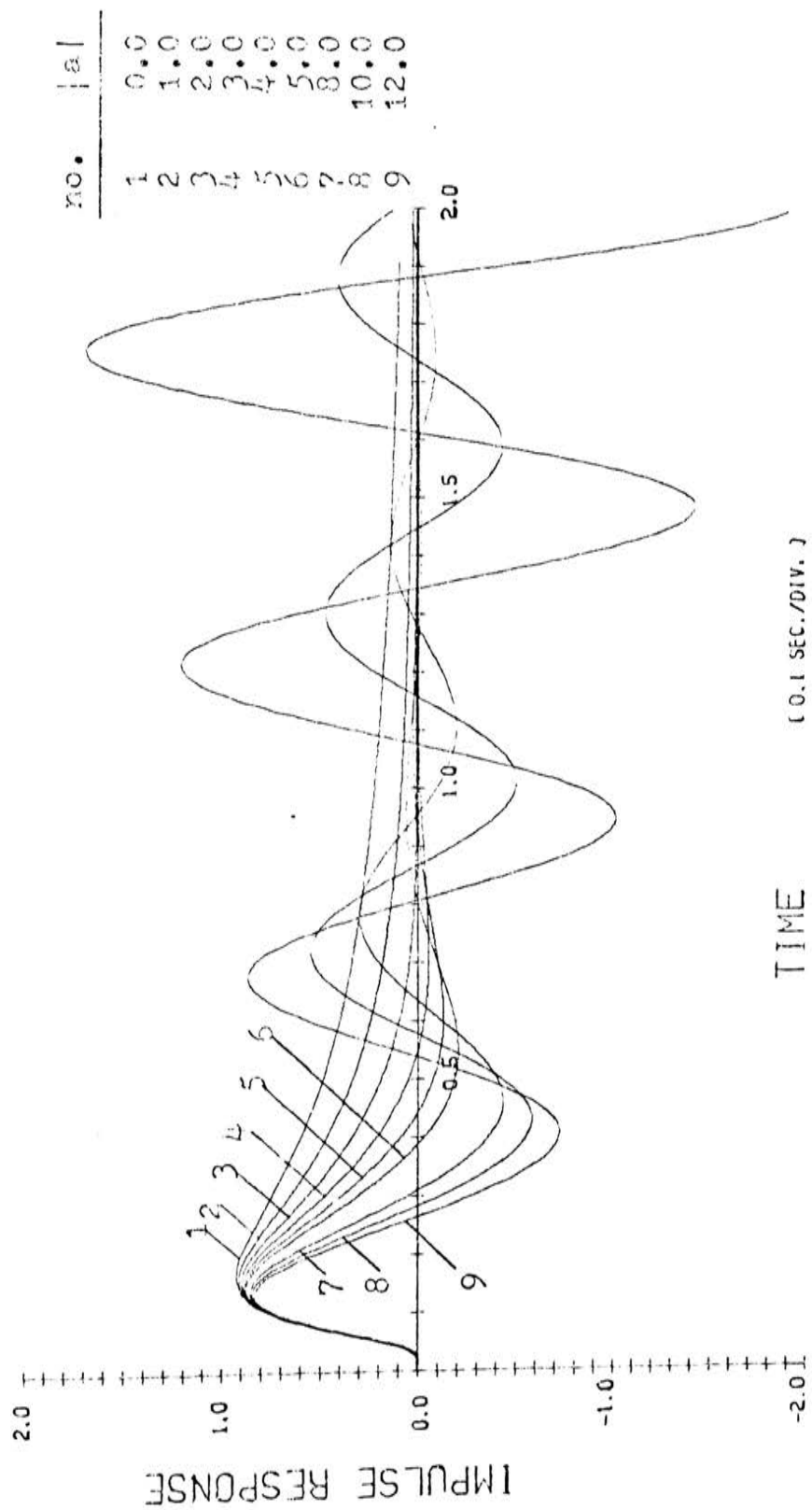


Figure 2-32: Real-part impulse response with pole angle  $\phi=135^\circ$  in the  $w$  plane.

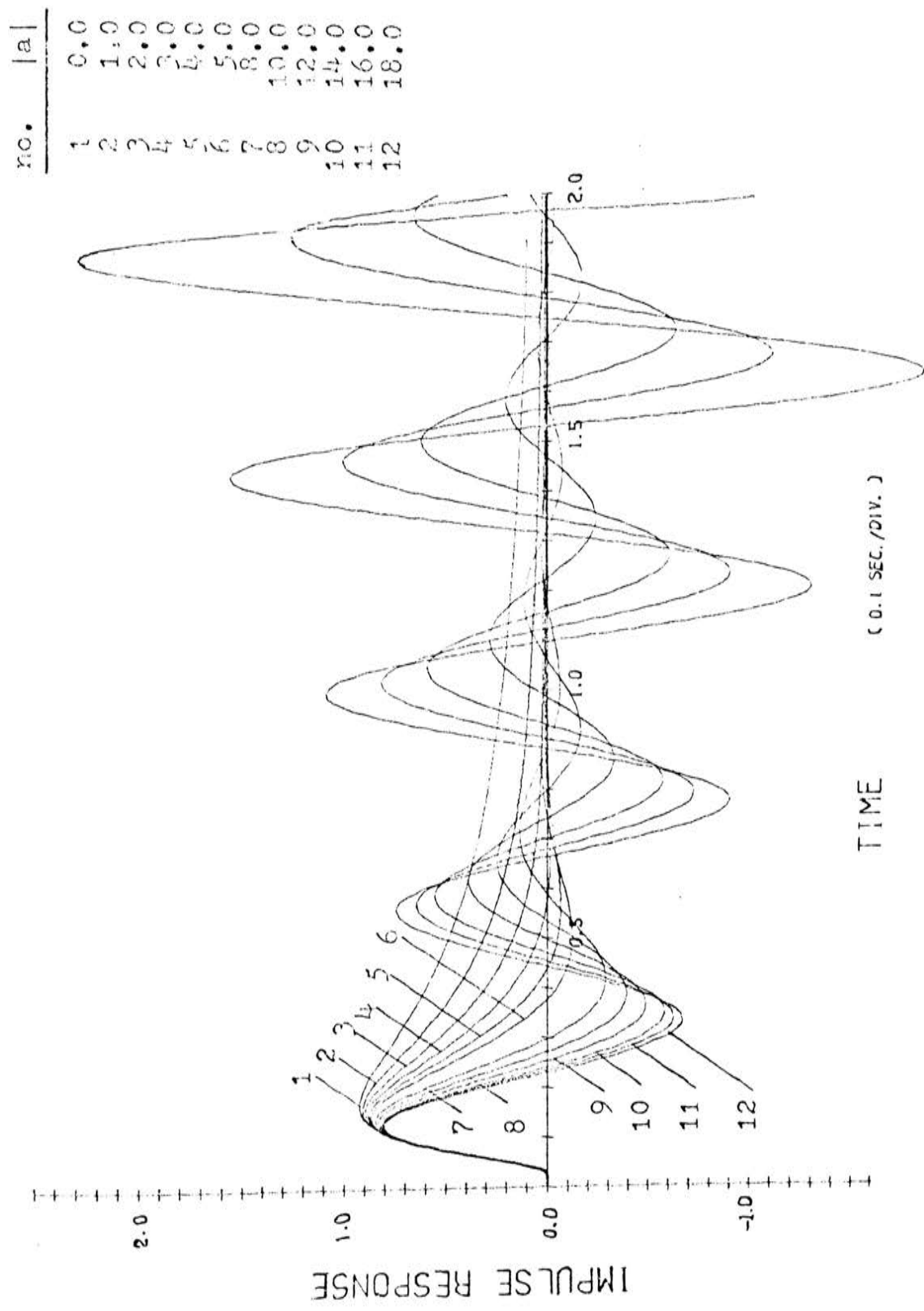


Figure 2-33: Real-part impulse response with pole angle  $\phi=150^\circ$  in the w plane.

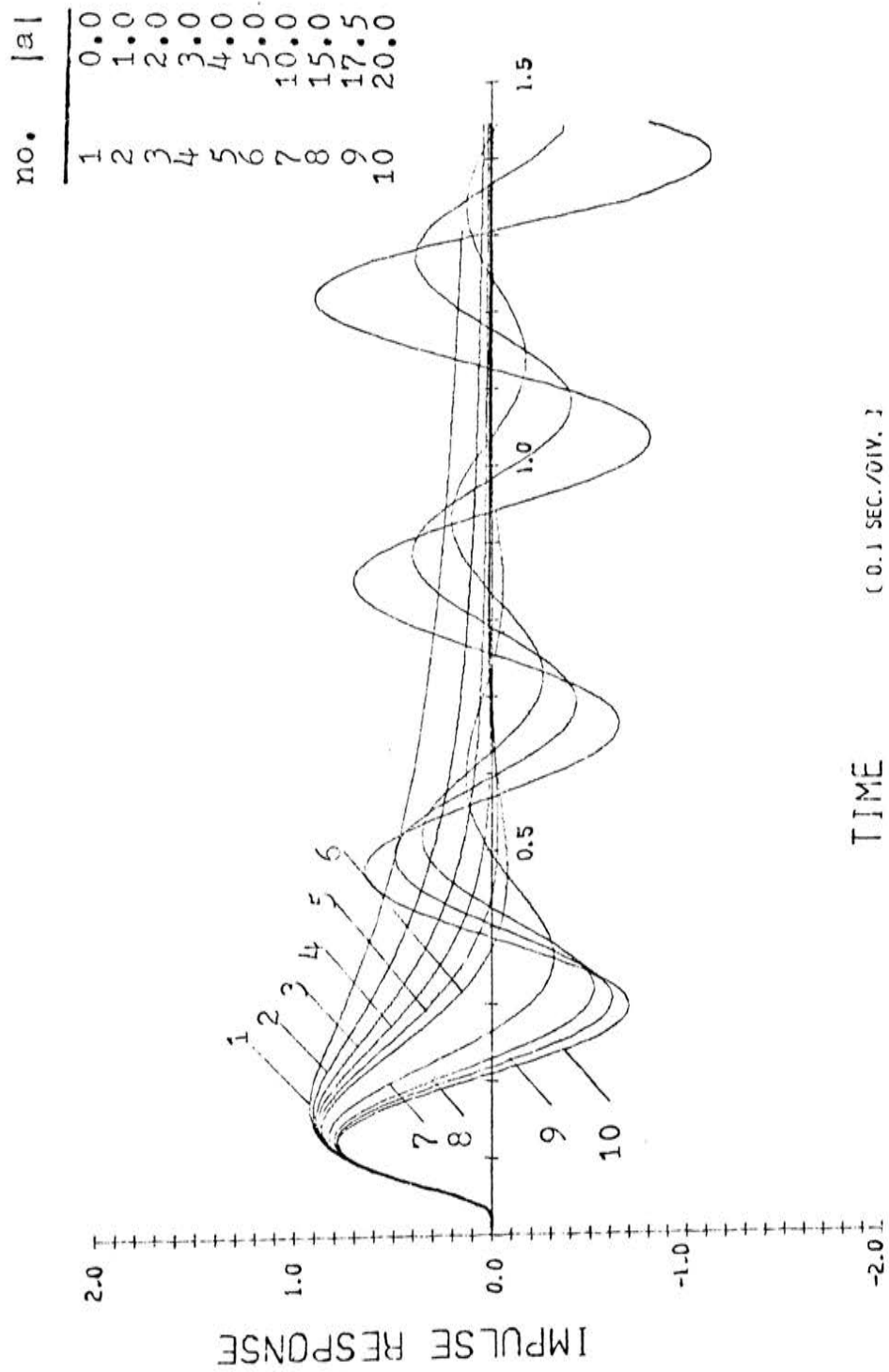


Figure 2-34: Real-part impulse response with pole angle  $\phi=165^\circ$  in the  $w$  plane.

It is possible that the numerator of the transfer function is of the first order in  $w$ , instead of being a constant, such as:

$$F_2(w) = \frac{w}{(w-a)(w-a^*)} \dots\dots\dots(2-9)$$

To realize eq.(2-9), it can be done with eq.(2-3) and eq.(2-7), i.e.

$$\begin{aligned} F_2(w) &= \frac{1}{2} \left\{ T_2(w) + \frac{2\operatorname{Re}[a]}{(w-a)(w-a^*)} \right\} \\ &= \frac{\frac{1}{2}}{w-a} + \frac{\frac{1}{2}}{w-a^*} + \operatorname{Re}[a] F_1(w) \dots\dots\dots(2-10) \end{aligned}$$

The time function of  $F_2(w)$  can be found by taking the inverse Laplace transformation of eq.(2-10),

$$\begin{aligned} f_2(t) &= \mathcal{L}^{-1}[F_2(w)] = \frac{1}{2} [h(t) + h^*(t)] + \operatorname{Re}[a] \left\{ \frac{\operatorname{Im}[h(t)]}{\operatorname{Im}[a]} \right\} \\ &= \operatorname{Re}[h(t)] + \frac{\operatorname{Re}[a]}{\operatorname{Im}[a]} \operatorname{Im}[h(t)] \\ &= \operatorname{Re}[h(t)] + \cot(\phi) \operatorname{Im}[h(t)] \dots\dots\dots(2-11) \end{aligned}$$

Thus,  $f_2(t)$  can be analyzed by both the real and imaginary parts of the response of  $h(t)$ , as in eq.(2-11).

Though it seems more complicated for predicting the transient response precisely by the curves given above, it can be found that the real part of the response  $h(t)$  will dominate the response of  $f_2(t)$  when  $\phi$  is close to  $\frac{\pi}{2}$ , since  $|\operatorname{Re}[a]| < |\operatorname{Im}[a]|$ . And the imaginary part of the response of  $h(t)$  becomes important when the poles lie close to the real axis in the  $w$  plane since the factor  $|\cot(\phi)|$  for the second

term in eq.(2-11) becomes larger. Therefore, both parts of the response of  $h(t)$  are still useful for analyzing the transient response of  $f_2(t)$ , as in eq.(2-11).

The calculation of the response with transfer function  $F_2(w)$  in eq.(2-9) is illustrated as an example of the manipulation of these two parts as follows:

Example:

The system, shown in figure 2-35, consists of the amplifiers and uniform distributed elements:

Amplifier A : a lumped amplifier with constant gain  $K_2$ .

Element B : a matched uniform distributed RC network.

Element C : a matched uniform distributed RC network cascaded with a constant gain ( $K_1$ ) amplifier such that it has one-fourth of the time constant of element B.

The transient impulse response of the whole system is to be evaluated for a  $w$ -plane pole  $a = 3e^{j2\pi/3}$ , by suitably choosing the values of  $K_1$  and  $K_2$ .

Since the overall transfer function of the system is

$$T_O(w) = \frac{\frac{K_1 K_2 w}{w^2 + K_2}}{1 + \frac{K_1 K_2 w}{w^2 + K_2}} = \frac{K_1 K_2 w}{w^2 + K_1 K_2 w + K_2}$$

$$= \frac{K_1 K_2 w}{(w-a)(w-a^*)},$$

where  $|a|^2 = K_2$  and  $K_1 = -\frac{2\text{Re}[a]}{|a|^2}$

If  $|a| = 3$  and  $\phi = 120^\circ$ , then  $K_2 = 9$  and  $K_1 = \frac{1}{3}$

$$T_O(w) = \frac{3w}{(w-a)(w-a^*)} \dots\dots\dots(2-12)$$

Hence, the time function of  $T_O(w)$  is three times the one in eq.(2-11). Thus, the response in this example can be calculated directly from figures 2-15 and 2-31, or evaluated by the same computer program as presented in appendix (I).

The data of the calculation for  $|a|=3$  and  $\phi=120^\circ$  are given in table 2-3, and the results of the transient response can be found in the figure 2-36; the peak of the response is high but it dies out very fast. Hence, the system with the transfer function  $T_O(w)$  as in eq.(2-12) is stable.



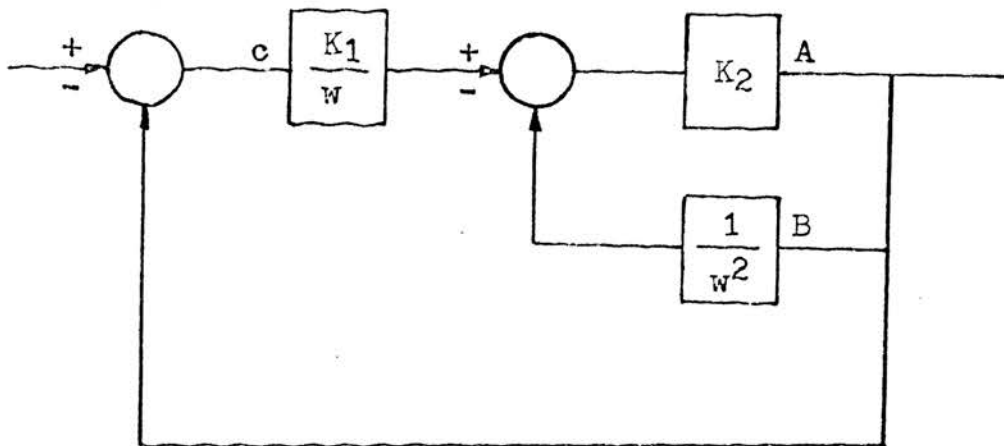


Figure 2-35: The system with the lumped and distributed amplifiers.

Table 2-3: Calculation of the impulse  
response in eq.(2-12)

time (sec.)	Re[h(t)] in fig.2-31	Im[h(t)] in fig.2-15	$f_2(t)$ in eq.(2-12)
0.05	0.17	0.0	0.51
0.10	0.72	0.0	2.25
0.15	0.89	0.03	2.76
0.20	0.84	0.11	2.79
0.25	0.70	0.20	2.67
0.30	0.54	0.29	2.43
0.35	0.40	0.35	2.13
0.40	0.27	0.38	1.83
0.45	0.16	0.37	1.47
0.50	0.07	0.35	1.14
0.60	-0.05	0.26	0.54
0.70	-0.11	0.16	0.108
0.80	-0.12	0.08	-0.132
0.90	-0.09	0.02	-0.21
1.00	-0.06	-0.01	-0.213
1.50	0.01	0.01	0.048
2.00	0.0	0.01	0.021
2.50	0.0	0.01	0.021
3.00	0.0	0.01	0.021

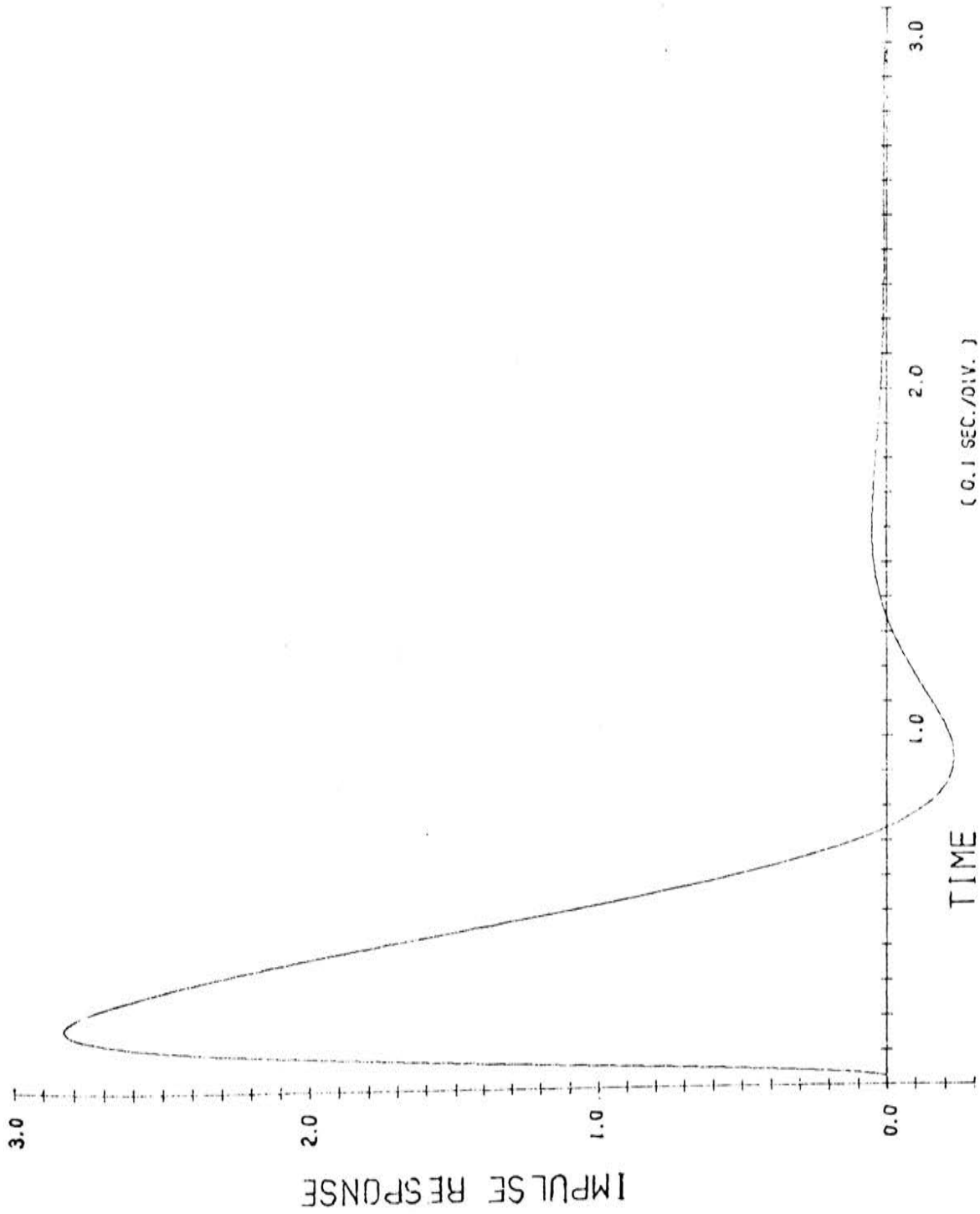


Figure 2-36: The response of the system with transfer function in eq. (2-12).

### III. STEP RESPONSE

For a step function excitation in this class of systems, the response may be investigated by observing the system response to a unit step applied at the input of the system.

(A) A System having a Single Pole on the Real Axis in the  $w$  Plane

By eq.(1-12) with  $\phi = 0^\circ$  and  $a = |a|$ , the step responses for pole magnitudes changing along the positive real axis are plotted in figure 3-1. With pole magnitude  $a < 1.0$ , the transient response increases in magnitude as the value of the pole is increased, but the system is still stable. This is illustrated in figure 3-2, which is plotted by multiplying a factor  $(1-a)$  to eq.(1-12). By the final value theorem, the limit of the response is

$$\lim_{t \rightarrow \infty} [v(t)] = \lim_{s \rightarrow 0} \left[ \frac{1-a}{s-a} \right] = \frac{1-a}{1-a} = 1.$$

In other words, these normalized responses approach unity in steady state, and are useful for comparison.

When  $a = 0$ , by eq.(1-12),  $v(t) = \text{erfc}\left(\frac{1}{2} \sqrt{\frac{T}{t}}\right)$  .....(3-1)

This curve is also plotted on both figures 3-1 and 3-2. All curves lie below the curve for  $a = 0.0$ ; thus, as shown in figure 3-2, the smaller the pole magnitude, the faster the system response for poles on the positive real axis. In other words, the transient period of the step response for larger values of  $|a|$  is longer than that for smaller pole magnitudes. The responses for  $a \geq 1.0$  are unstable and increase without limit, as shown in figure 3-1. As compared to the curve for  $a = 0$ , the transient step response for  $a$

single pole on the positive real axis reaches steady more slowly as pole magnitude approaches to the value  $a=1.0$ .

The increasing slope of the curve for a single pole  $a=0.0$  is shown in figure 3-3. In the first 3 seconds the wave increases to 69% of its final value, after which it changes very slowly and reaches 90% at  $t=30$  seconds, at which time the transient is almost over. The transient period of the response for  $a=0$ , based on the definition of the time constant, is about 3 seconds, and those of the responses for pole  $a<1.0$  must then be longer than 3 seconds.

If  $\phi=180^\circ$  and  $a=-|a|$ , the response in eq.(1-12) is the one for the pole on the negative real axis in the  $w$  plane. These responses are plotted in figure 3-4 for the transfer function  $\frac{1-a}{w-a}$ , for which the response, with  $|a|<23.1$ , approaches unity as time increases to infinity.

Now note the way in which these curves approach unity in figure 3-4. The curves for  $|a|<4$  act as overdamped waves and the degree of damping of the wave is increased with smaller pole magnitude; i.e. the larger the pole magnitude, the faster the response approaches unity. For  $|a|=5.0$ , the curve oscillates slightly. Its peak value during the first cycle is still less than unity; then it increases toward unity with slow oscillation. With pole magnitude  $|a|=10.0$ , the response overshoots during its first cycle, then returns to the value less than unity and oscillates toward unity without overshooting again. The transient responses for  $|a|>10.0$  behave as the underdamped wave; their magnitudes

dampen toward unity as time increases to infinity. To the value of  $|a|=23.0$ , the curve becomes nearly an oscillating wave without damping, the period of which checks quite closely with the value listed in table 3-2.

If these curves are compared with the curve for  $a=0.0$ , the responses are faster for pole on the negative real axis than for those on the positive real axis within the stable region. Hence, the transient period of the response for poles on the negative real axis is shorter but the wave magnitude is larger than that for poles on the positive real axis.

The delay time of the initial response is about 0.05 second for poles both on the positive and negative real axes in the  $w$  plane.

no.	a
1	0.0
2	0.2
3	0.4
4	0.6
5	0.8
6	0.9
7	0.95
8	1.05
9	1.1
10	1.3
11	1.5
12	2.0
13	2.5
14	3.0
15	5.0
16	7.0

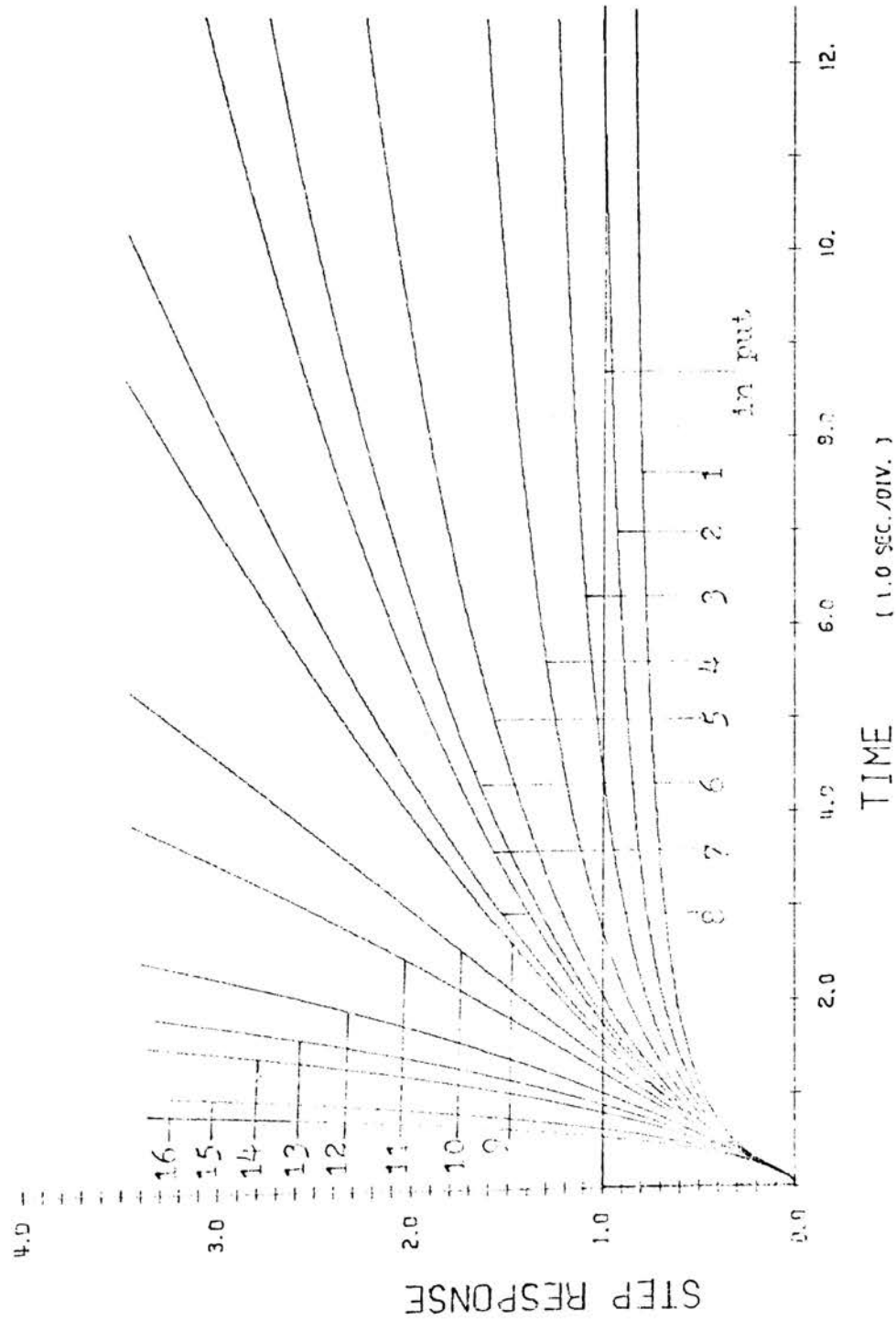


Figure 3-1: Un-normalized unit step response with a single pole on the positive real axis in the  $s$  plane.

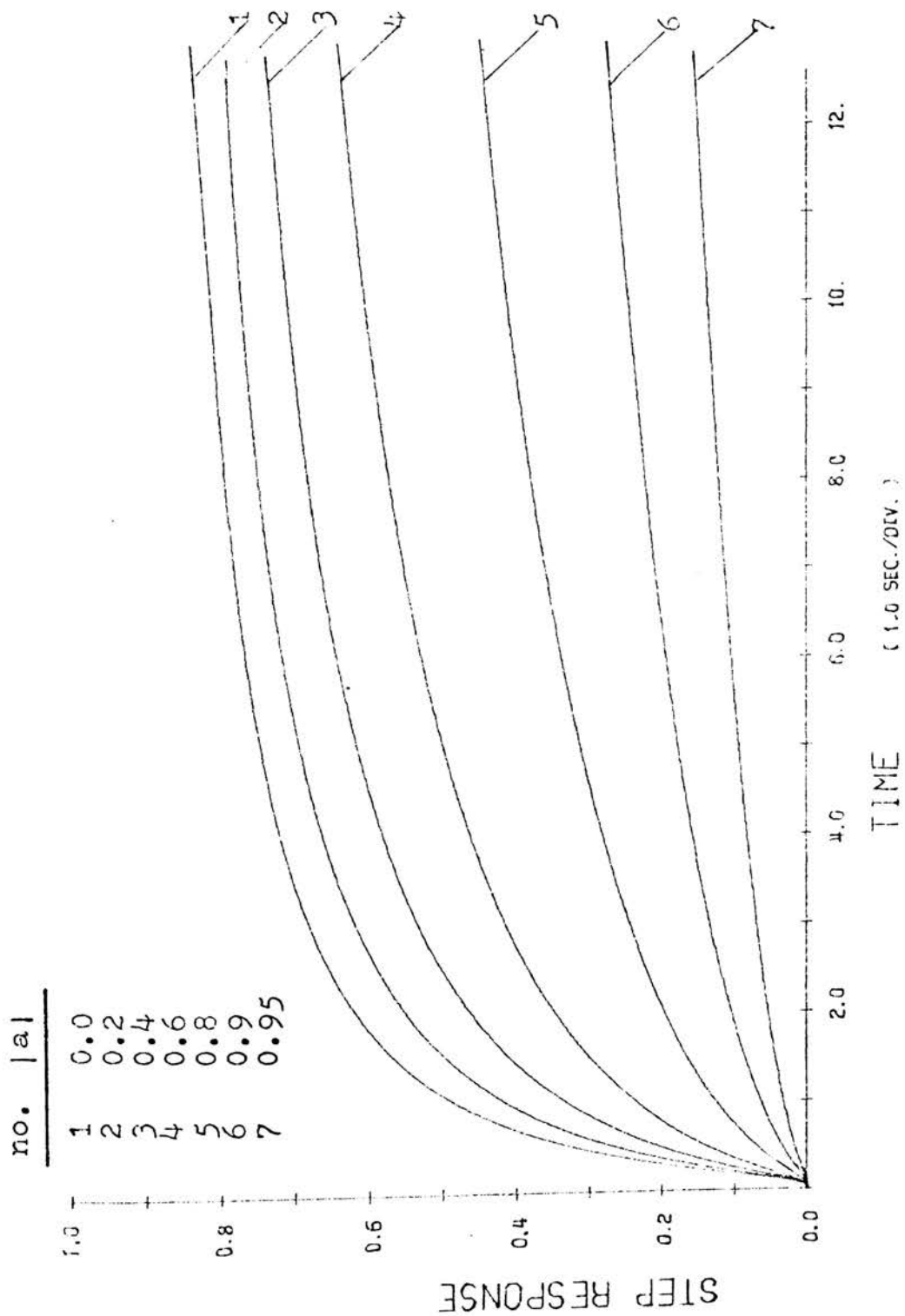
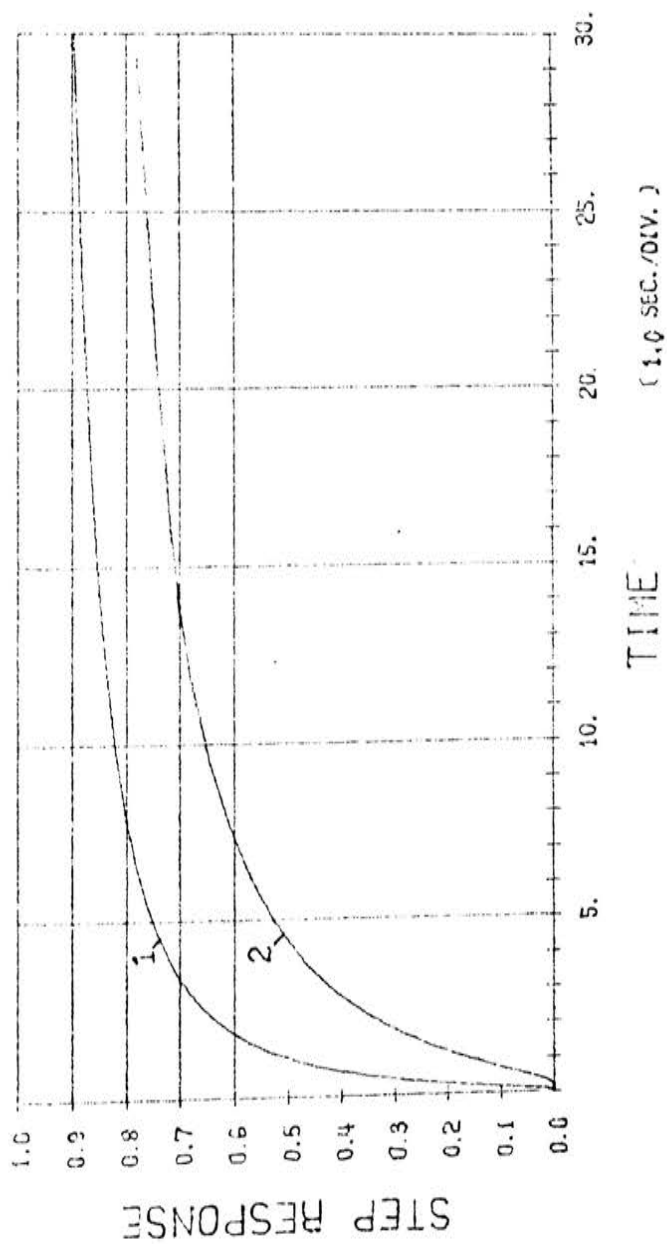


Figure 3-2: Normalized unit step response with a single pole on the positive real axis in the  $w$  plane.





1 : With a single pole  $|a|=0.0$

2 : With a double pole  $|a|=0.0$

Figure 3-3: Step response with a single pole and a double pole of magnitude  $a=0$ .

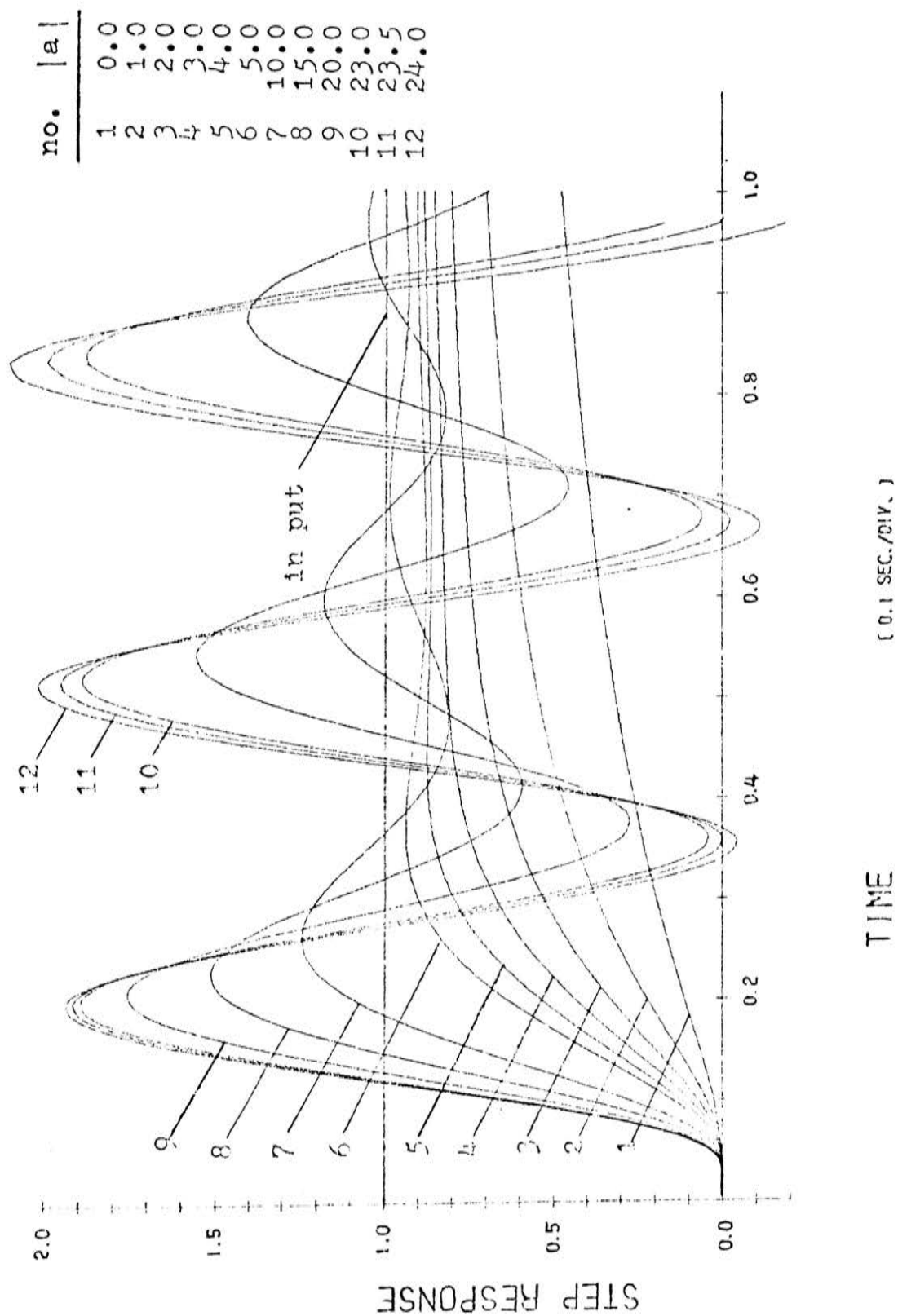


Figure 3-4: Unit step response with a single pole on the negative real axis in the w plane.

## (B) A System having Conjugated Poles in the w Plane

The transfer function considered here is of the form  $V_2(w) = \frac{(1-a)(1-a^*)}{(w-a)(w-a^*)}$  which, as the system is stable, approaches unity when time approaches infinity. By partial fraction expansion,

$$V_2(w) = (1-a)(1-a^*) \left\{ \frac{1/2\text{Im}[a]}{w-a} - \frac{1/2\text{Im}[a]}{w-a^*} \right\}$$

$$= \frac{1 + |a|^2 - 2\text{Re}[a]}{2\text{Im}[a]} \left\{ \frac{1}{w-a} - \frac{1}{w-a^*} \right\}$$

After taking the inverse Laplace transformation,

$$v_2(t) = \mathcal{L}^{-1}[V_2(w)] = \frac{1 + |a|^2 - 2\text{Re}[a]}{2\text{Im}[a]} \left\{ v_1(t) - v_1^*(t) \right\}$$

$$= \frac{1 + |a|^2 - 2\text{Re}[a]}{\text{Im}[a]} \left\{ \text{Im}[v_1(t)] \right\}, \dots\dots\dots (3-2)$$

where  $v_1(t)$  is the time function of the step response in eq.(1-12),  $v_1^*(t)$  is its conjugated function.

The result of eq.(3-2) shows that the unit step response of this system with conjugated poles in the w plane is determined by the imaginary part of the response in eq.(1-12). The resulting curves are plotted in figures 3-5 through 3-20 with the curve for a double pole  $a=0.0$  added in each graph for comparison.

The step function for a double pole at  $a=0.0$  can be derived as follows:

$$V_0(s) = \frac{1}{sw^2} = \frac{1}{se^{2\sqrt{s}}} = \frac{1}{se^{\sqrt{4s}}} = \frac{4}{4se^{\sqrt{4s}}} \dots\dots\dots (3-3)$$

$$\text{By the relation: } \mathcal{L}^{-1}[F(bs)] = \frac{1}{b} f(t/b),$$

where  $f(t) = \mathcal{L}^{-1}[F(s)]$ .

Then eq.(3-3) becomes

$$v_0(t) = \frac{4}{4} \text{erfc}\left(\frac{1}{2}\sqrt{4T/t}\right) = \text{erfc}(\sqrt{T/t}). \dots\dots\dots (3-4)$$

The slope of the curve in eq.(3-4) is different from the one in eq.(3-1). By observing figure 3-3, it can be found that the curve for a double pole  $a=0.0$  increases to 63.8% of its final value at  $t=9$  seconds, which is 6 seconds delayed to the response for a single pole  $a=0$ . This means that the transient period of the response with a double pole is longer than that for a single pole on the real axis in the  $w$  plane.

The transient step responses with constant pole magnitude and varying pole angle are plotted from figures 3-5 through 3-9. Observing these graphs, some conclusions can be drawn:

- (1) The responses for pole angle  $\phi \geq 90^\circ$  lie above the curve of  $a=0.0$ . Hence, the speed of the response is faster and the magnitude is greater for left-half- $w$ -plane poles when the pole magnitude is fixed.
- (2) Note the case  $\phi < 75^\circ$ , the slope initially decreases with increasing pole magnitude during  $t < 0.8$  seconds, then increases with increasing pole magnitude as  $t \geq 0.8$  seconds except the one for  $\phi=15^\circ$ .
- (3) For pole angle  $\phi=15^\circ$  and  $|a| < 1.0$ , the response magnitude decreases as the pole magnitude increases. With slower changing in slope, it behaves similarly to the response with a single pole on the positive real axis, as shown in figure 3-2.

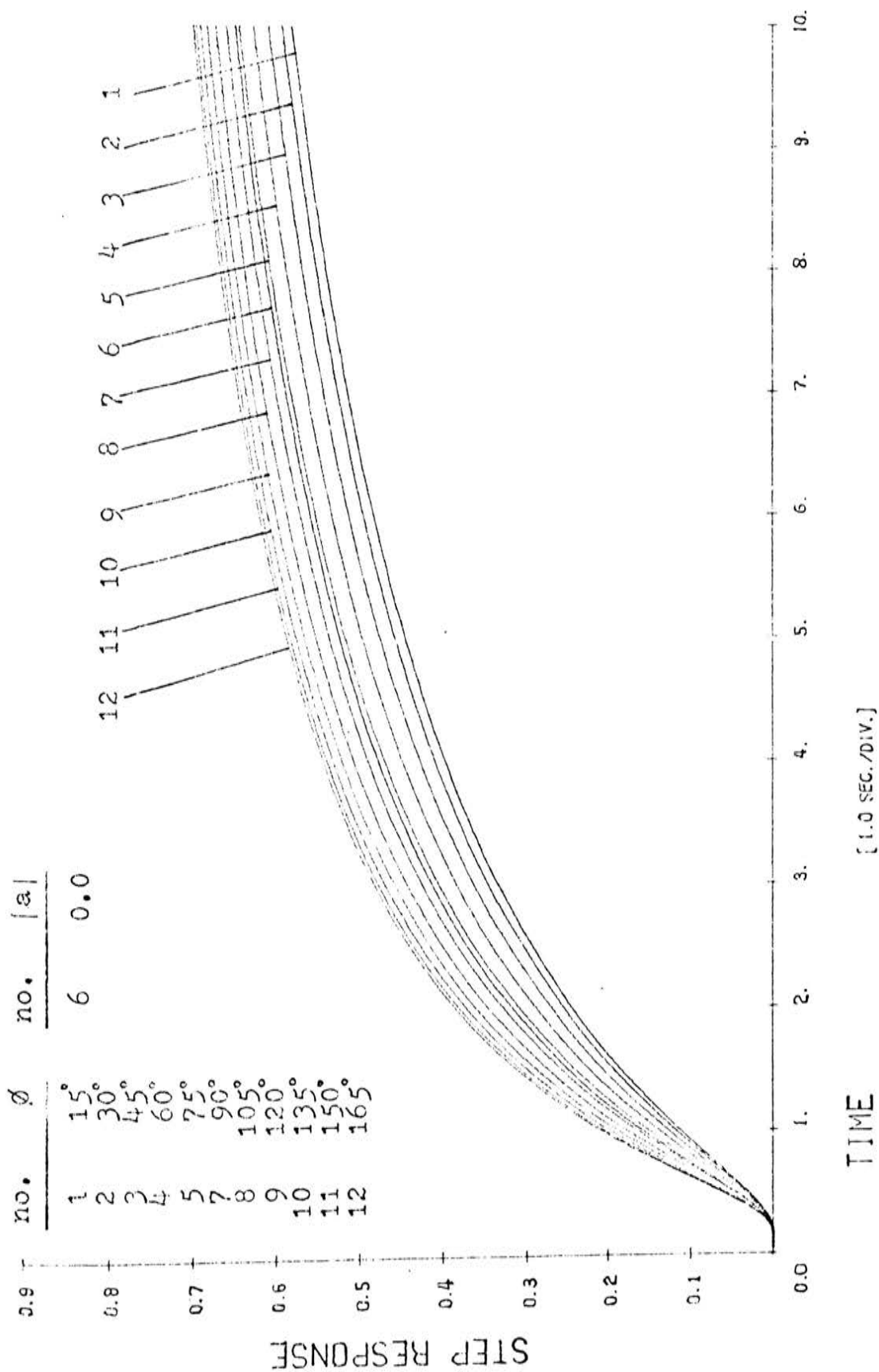


Figure 3-5: Unit step response with pole magnitude  $|a| = 0.2$  in the  $w$  plane.

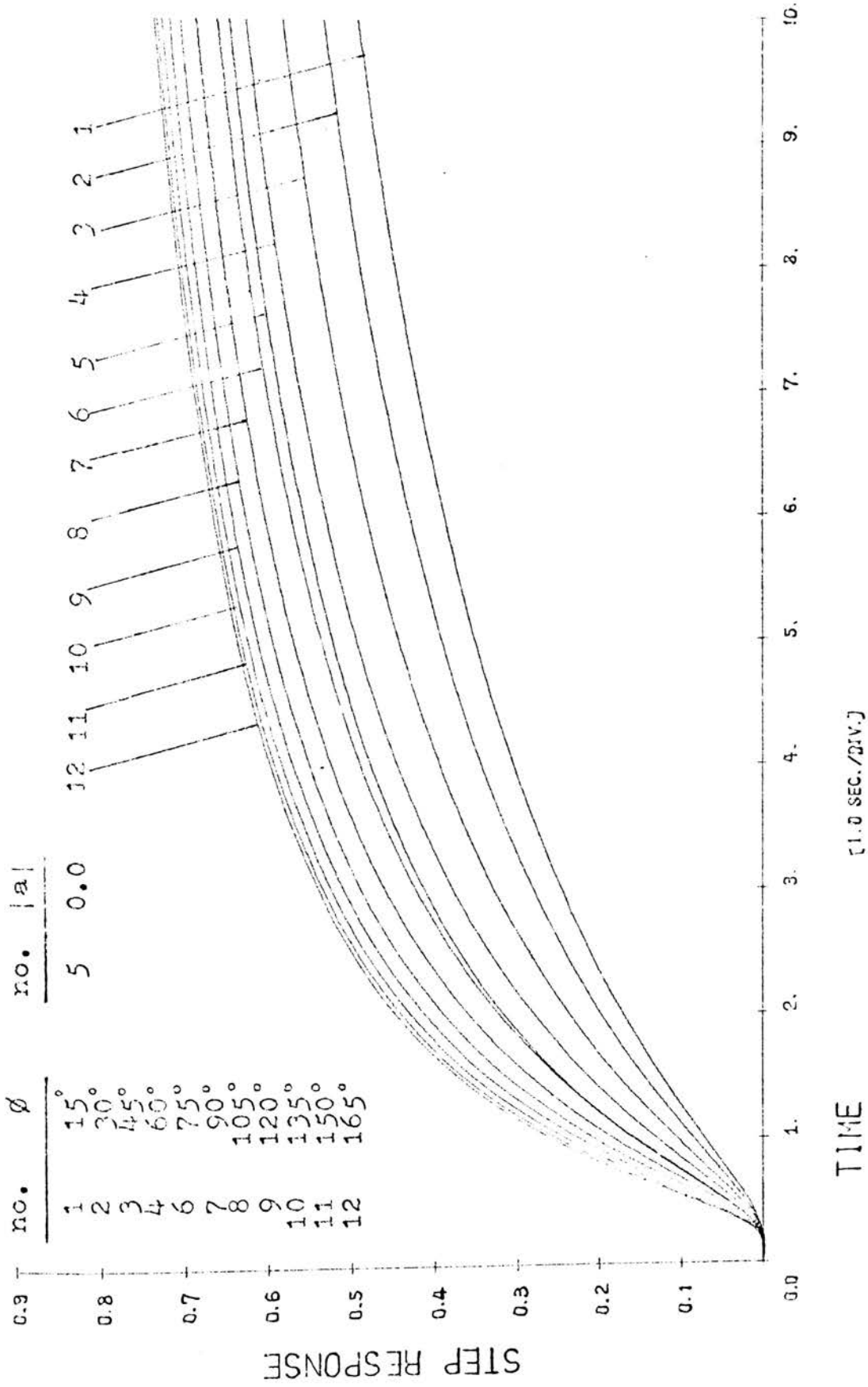


Figure 3-6: Unit step response with pole magnitude  $|a|=0.4$  in the  $w$  plane.

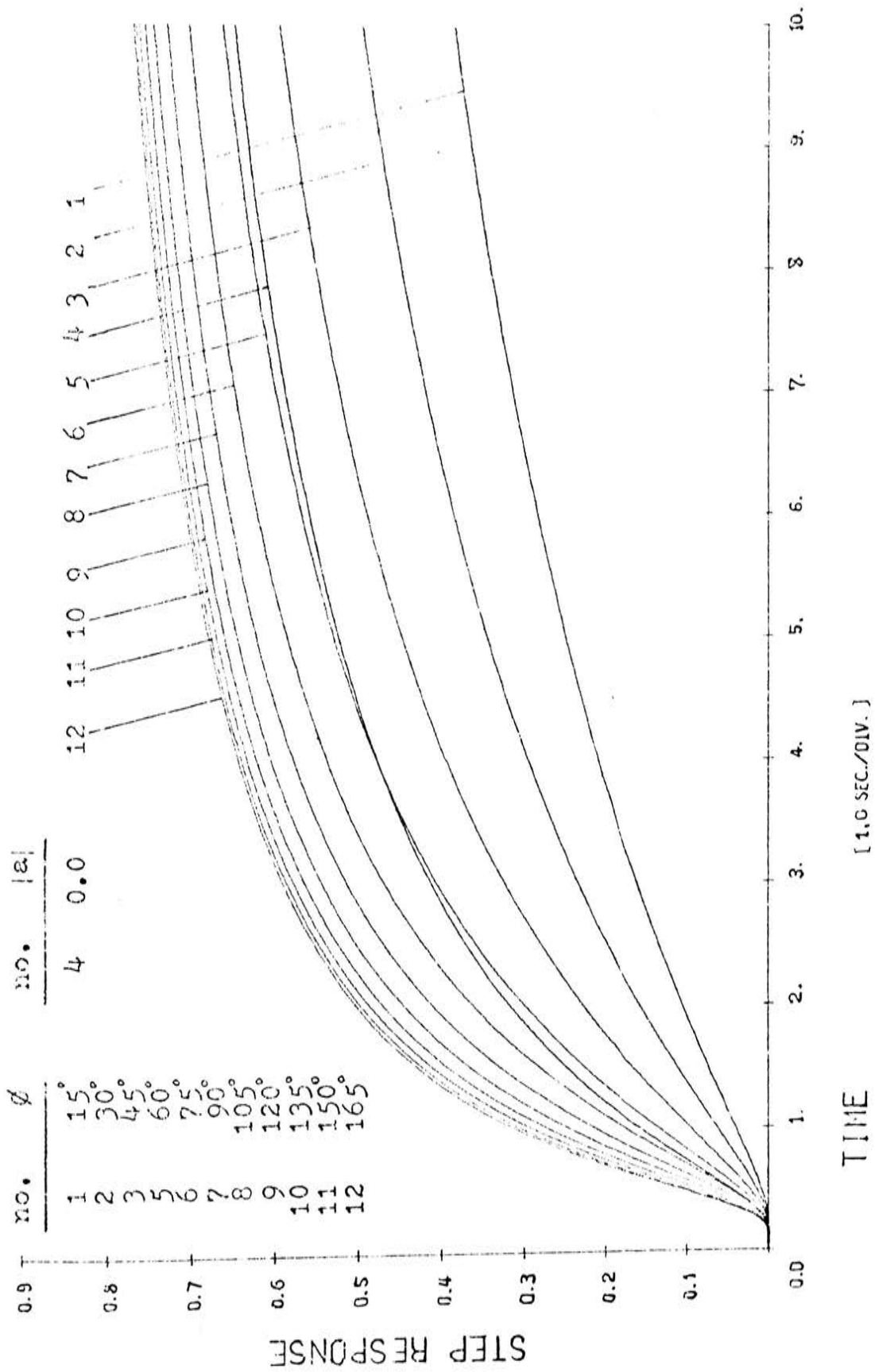


Figure 3-7: Unit step response with pole magnitude  $|a|=0.6$  in the  $w$  plane.

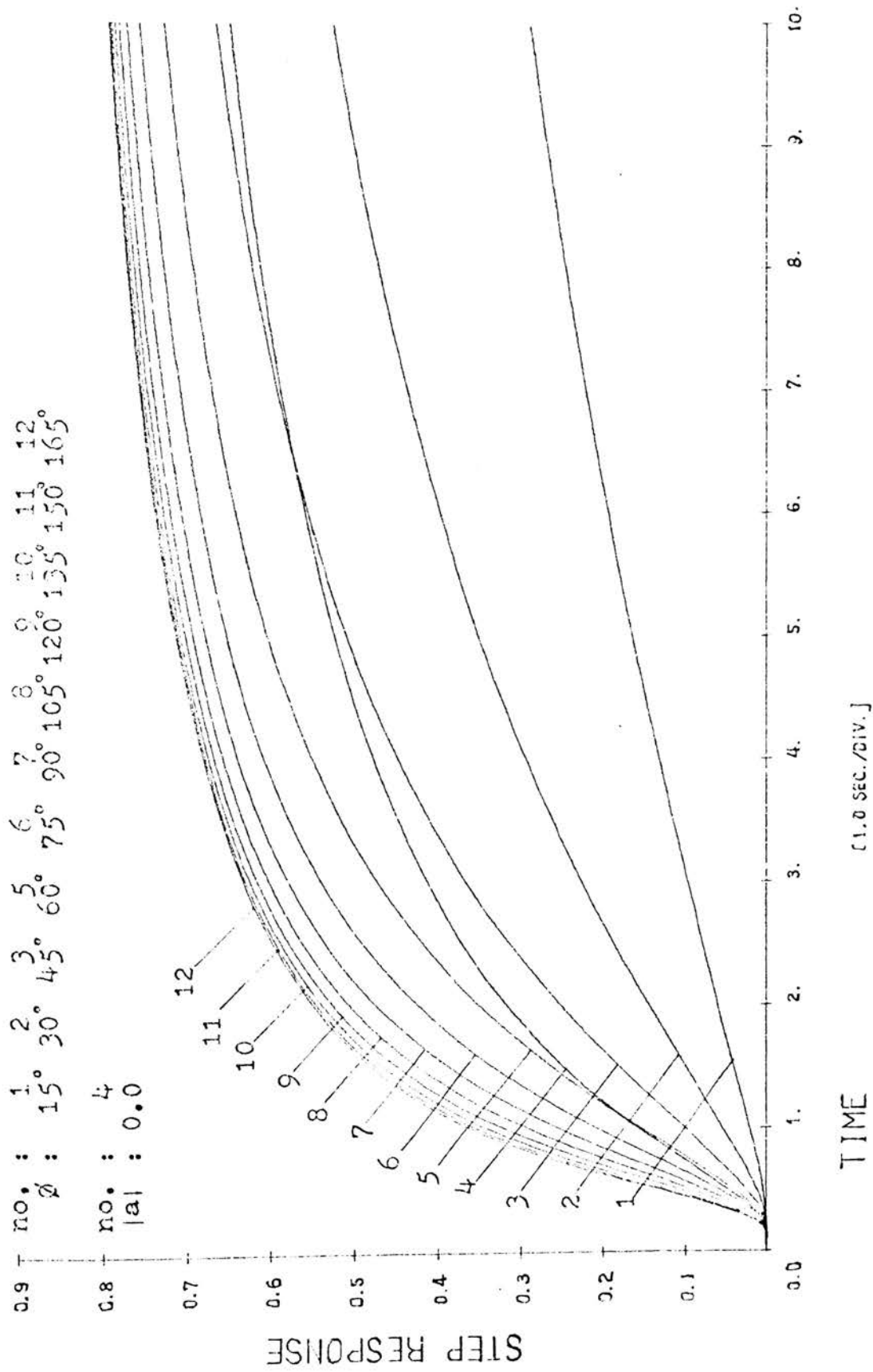


Figure 3-8: Unit step response with pole magnitude  $|a|=0.8$  in the  $w$  plane.



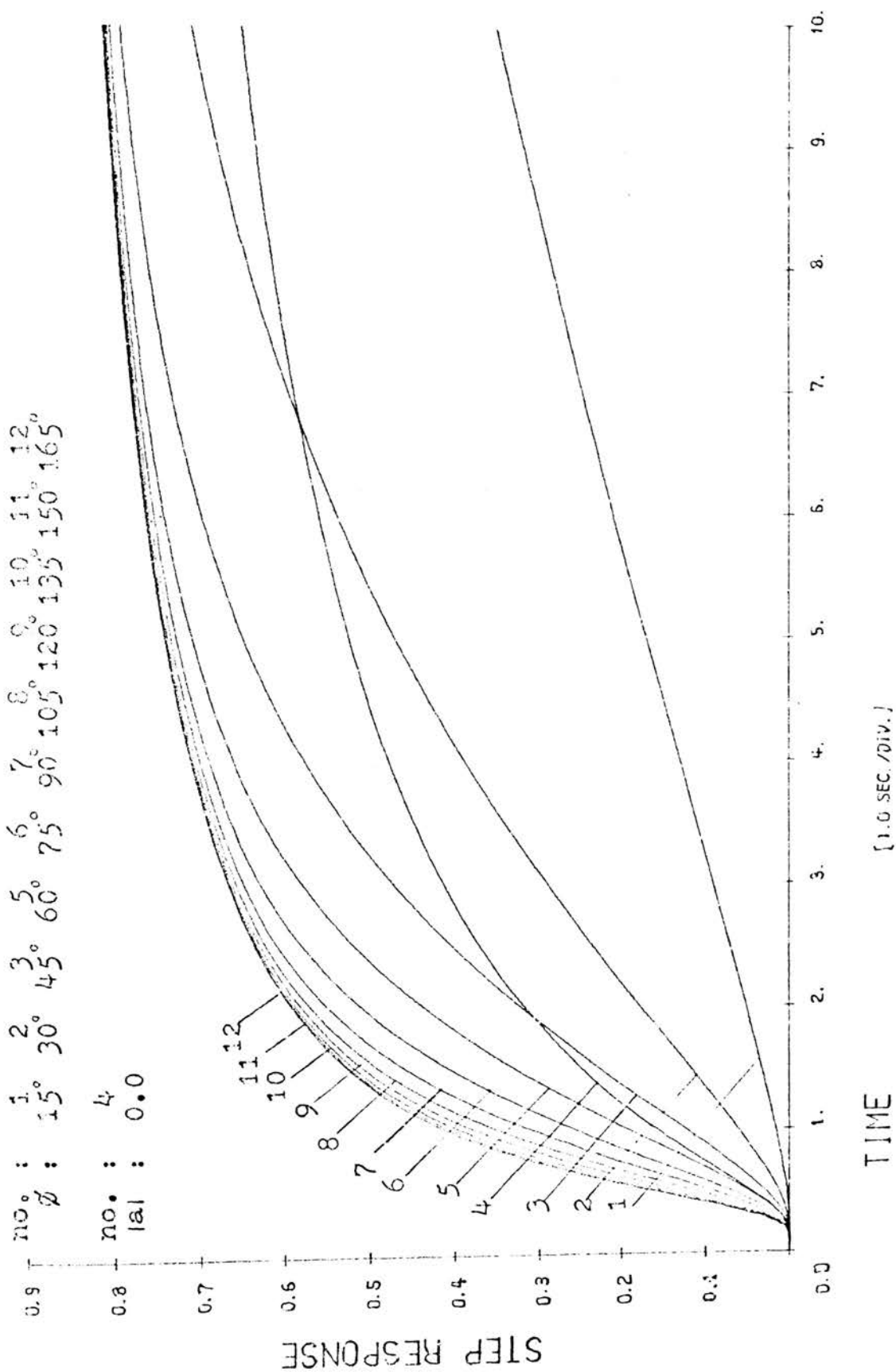


Figure 3-9: Unit step response with pole magnitude  $|a|=1.0$  in the w plane.

Now observe the response curves from figures 3-10 through 3-20, which are plotted for fixed pole angle and varying magnitude of conjugated poles in the  $w$  plane. Some data are summarized in table 3-1 and 3-2. And the results have been found as below:

- (1) The larger the pole angle, the faster the step response for conjugated poles, as compared by the first peak time in table 3-2.
- (2) With a pole on the boundary of the region of stability, the magnitude of the first peak of the response increases as the pole angle approaches either real axis. But it becomes smaller when the pole angle is close to  $\phi = 120^\circ$ .
- (3) With the pole inside the region of stability, the response dampens to unity as time approaches infinity. However, as compared to the magnitude of the input wave, the average magnitude of the oscillating wave is greater for the case  $\phi < 60^\circ$ , but is smaller for the case  $\phi > 60^\circ$ . For  $\phi = 60^\circ$ , the underdamped wave oscillates about unity with decreasing amplitude.
- (4) The period of oscillation of the response for poles near the boundary of stability region checks quite closely with the calculated value in table 3-2.
- (5) The delay time of the initial response is about 0.12 to 0.15 second.
- (6) In table 3-1, the values of pole magnitude for plotting these curves in each graph are listed. Note

the underlined pole magnitude below which the response, with listed pole magnitude, behaves without any overshooting. This value increases with the pole angle.

As indicated by the results cited above, the step response for conjugated poles tends to be more unstable for smaller pole angles. The first peak magnitude of the transient response is higher for poles near either real axis in the  $w$  plane. It is possible to find out the best pole location for which the system with any pole angle approaches the steady state in most rapid but least oscillatory way.

Table 3-1: List of pole magnitude being plotted for unit step response\*\*

pole angle ( $\phi^\circ$ )	figure number	pole magnitude being plotted	$ a $	Remark
0	3-1	0.0;0.2;0.4;0.6;0.8;0.9;0.95;1.05;1.1;1.3;1.5; 2.0;2.5;3.0;5.0;7.0;		The underlined pole magnitude is the value below which the response, with pole magnitude listed, behaves without any overshooting.
15	3-10	0.0;1.0;1.1;1.2;1.3;1.4;1.5;1.6;1.7;1.8;		
30	3-11	0.0;1.0;1.2;1.4;1.6;1.65;1.7;1.8;		
45	3-12	0.0;1.0;1.2;1.4;1.6;1.8;2.0;2.2;		
60	3-13	0.0;1.0;1.5;2.0;2.3;2.5;2.7;2.9;		
75	3-14	0.0;1.0;2.0;3.0;3.5;3.65;3.8;		
90	3-15	0.0;1.0;2.0;3.0;4.0;4.8;5.0;		
105	3-16	0.0;1.0;2.0;3.0;4.0;5.0;5.25;5.5;5.75;6.0;6.25;6.5;		
120	3-17	0.0;1.0;2.0;3.0;4.0;5.0;6.0;7.0;8.0;9.0;		
135	3-18	0.0;1.0;2.0;3.0;4.0;5.0;6.0;8.0;9.0;10.0;11.0;12.0;		
150	3-19	0.0;1.0;2.0;3.0;4.0;5.0;8.0;10.0;12.0;14.0;16.0;		
165	3-20	0.0;1.0;2.0;3.0;4.0;5.0;10.0;15.0;17.0;17.5;20.0;		
180	3-4	0.0;1.0;2.0;3.0;4.0;5.0;10.0;15.0;20.0;23.0;23.5; 24.0;		

\*\* The pole magnitudes for figures 3-5 through 3-9 are 0.2;0.4;0.6;0.8;1.0; with pole angle varying  $15^\circ$  step in each graph.

Table 3-2: Some data of the characteristics of the unit step response

pole angle ( $\phi$ )	calculated value		measured value		first * peak value (%)	first * peak time (sec.)	time at * its first overshoot (sec.)
	pole magnitude $a_c$	period $t_c$ (sec.)	pole magnitude	period * $t_m$ (sec.)			
15	1.3	45.90	1.3	46.80	357	18.70	5.7
30	1.69	11.48	1.65	11.8	280	5.8	2.2
45	2.19	5.10	2.2	5.10	261	2.5	1.2
60	2.85	2.86	2.9	2.4	234	1.6	0.75
75	3.69	1.83	3.65	1.85	201	1.07	0.61
90	4.81	1.272	4.8	1.28	190	0.8	0.48
105	6.25	0.938	6.25	0.93	182	0.78	0.44
120	8.1	0.715	8.0	0.72	178	0.52	0.34
135	10.52	0.567	11.0	0.53	210	0.41	0.27
150	13.9	0.458	14.0	0.45	211	0.37	0.25
165	17.8	0.379	17.5	0.38	240	0.34	0.23
180	23.1	0.318	23.0	0.32	192	0.19	0.12

\* All data are measured directly from the curves with the pole magnitude ( $a_m$ )

listed in this table.

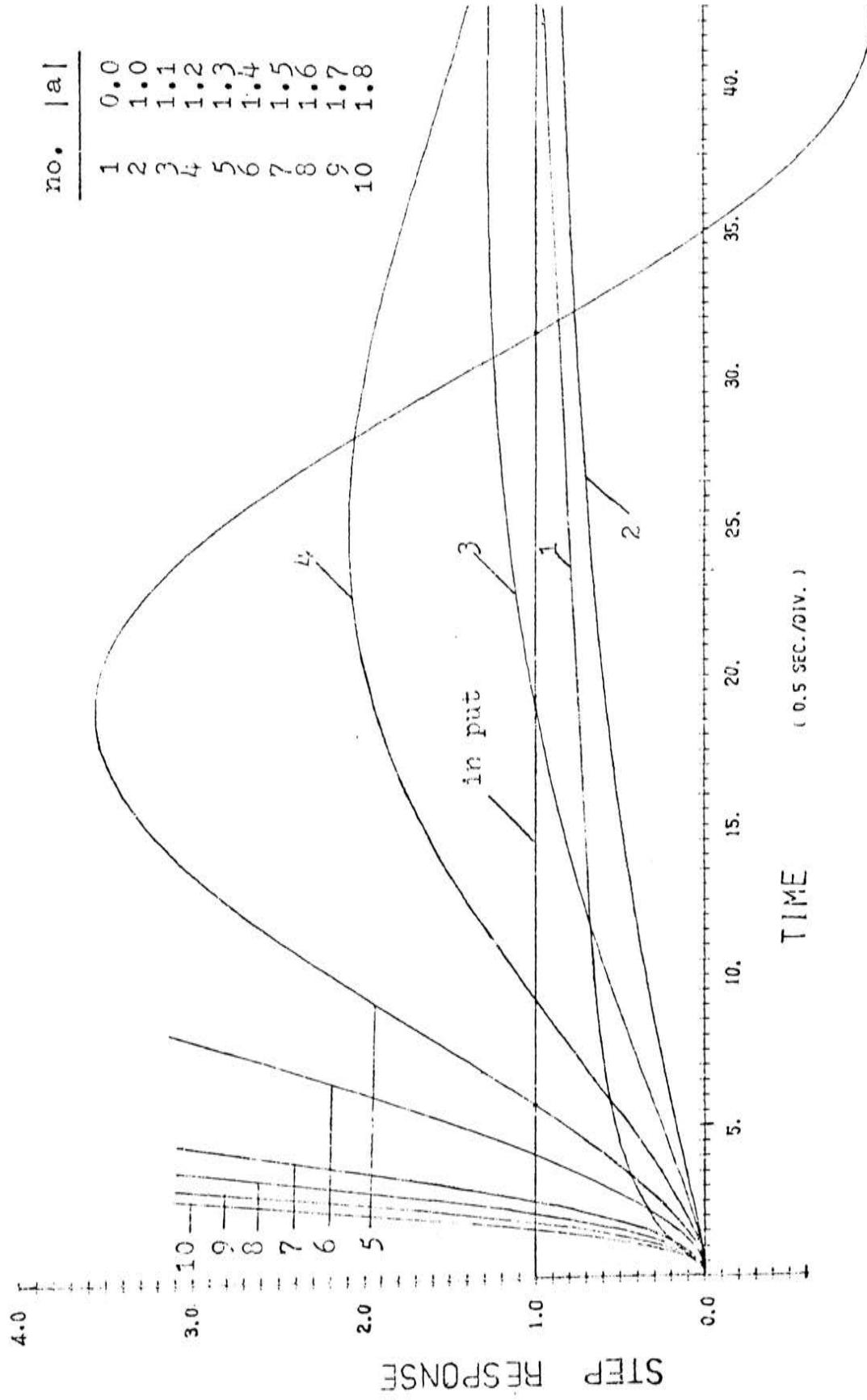


Figure 3-10: Unit step response with pole angle  $\phi=15^\circ$  in the  $w$  plane.

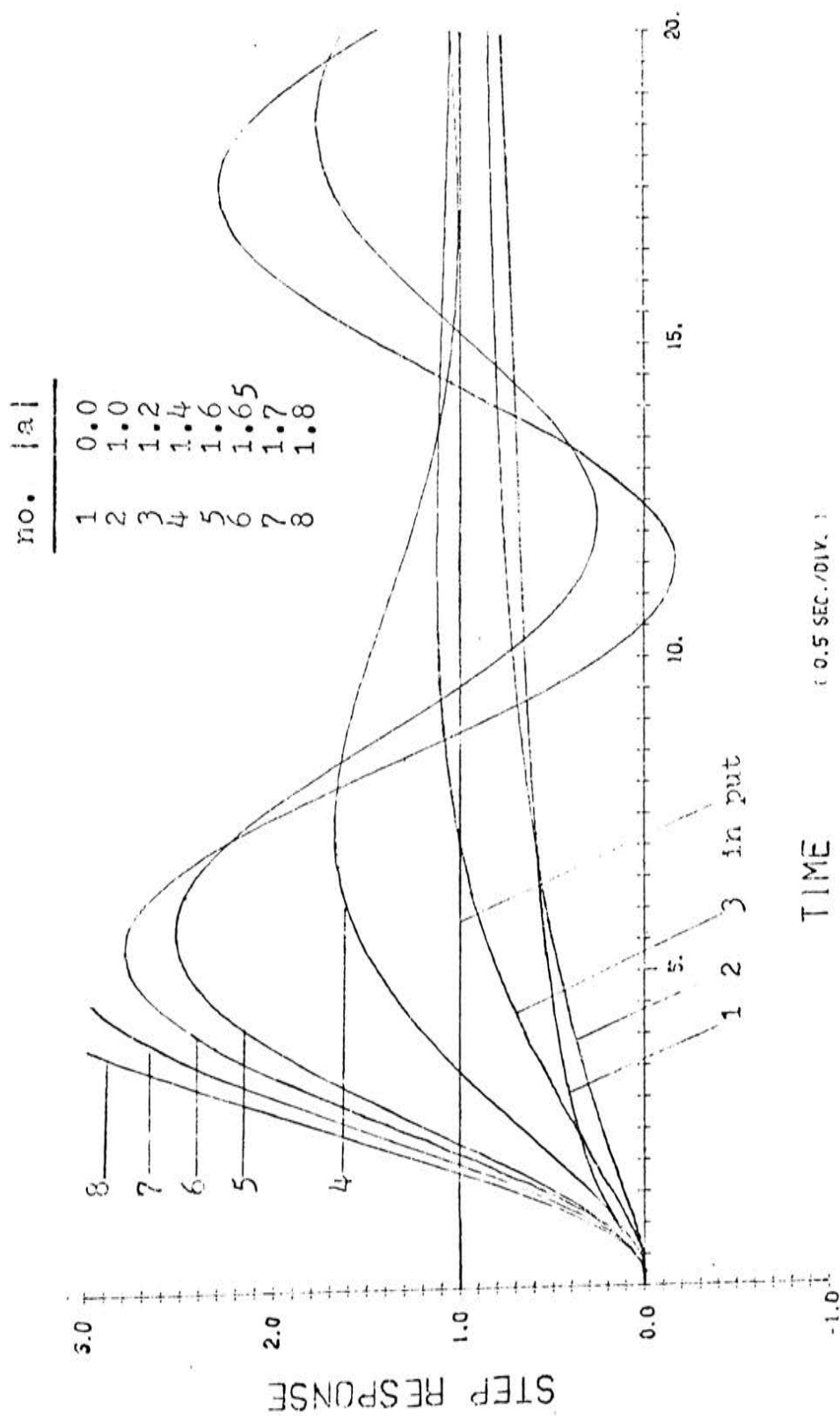


Figure 3-11: Unit step response with pole angle  $\phi=30^\circ$  in the w plane.

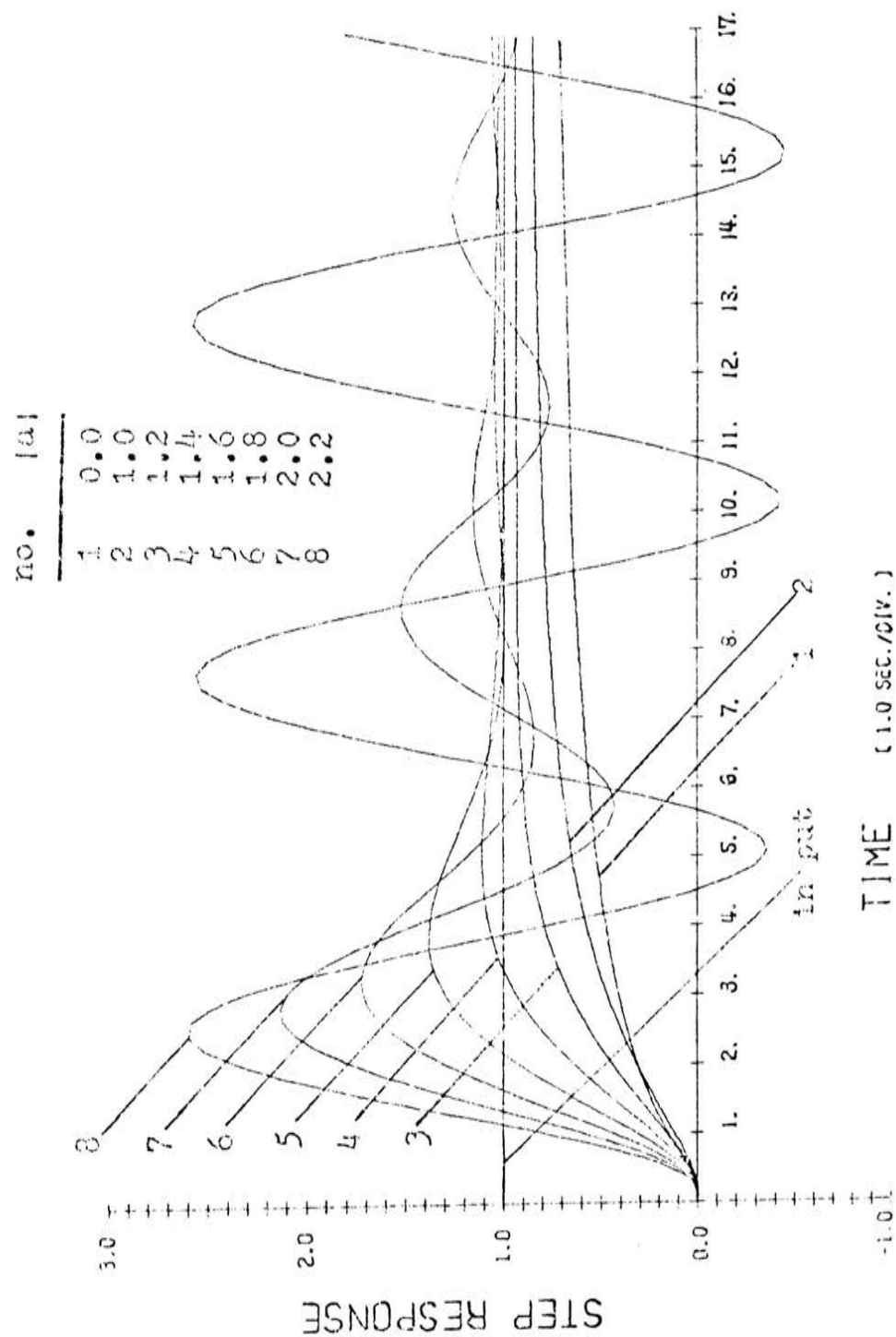


Figure 3-12: Unit step response with pole angle  $\phi=45^\circ$  in the  $w$  plane.



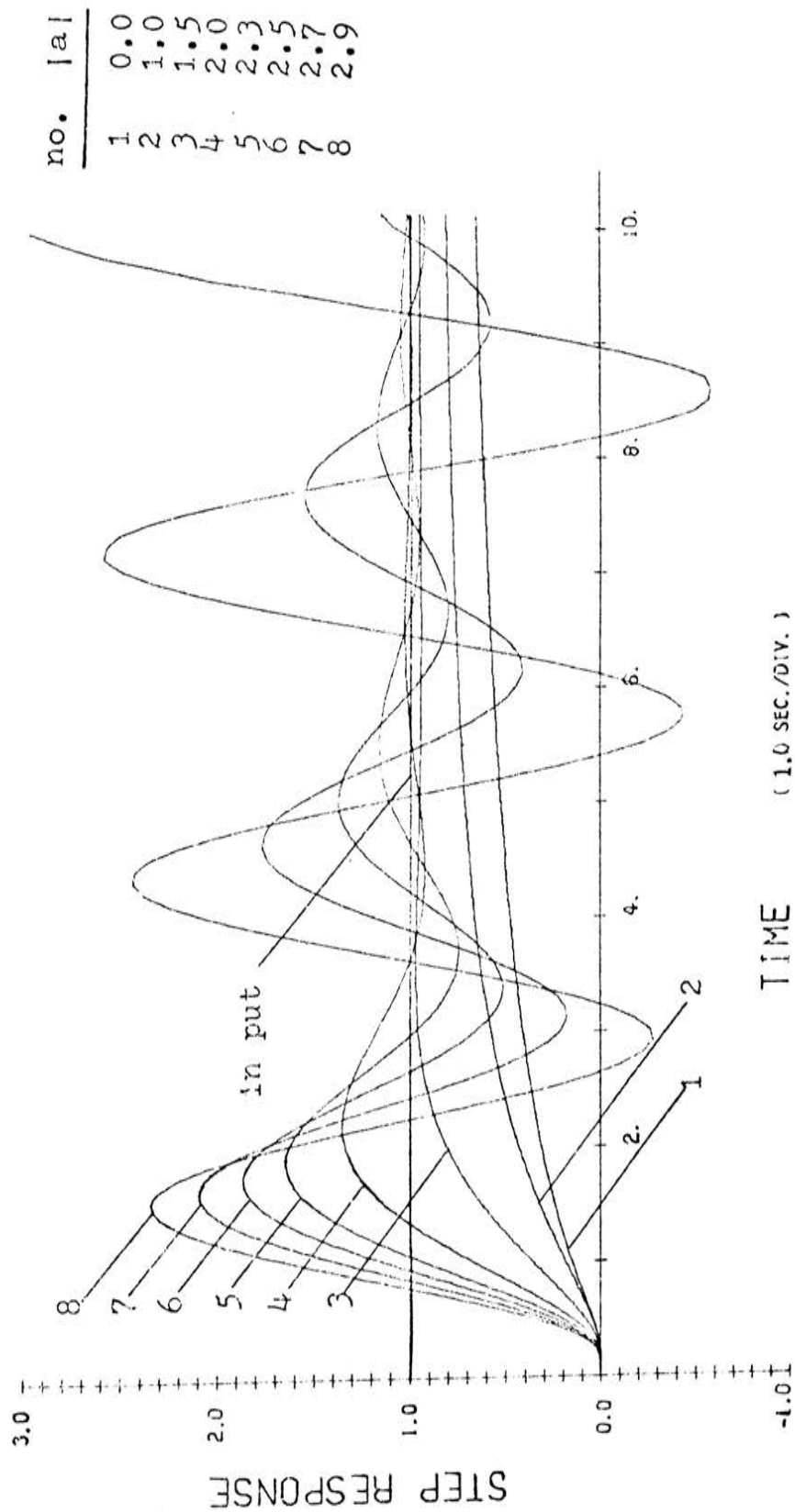


Figure 3-13: Unit step response with pole angle  $\phi=60^\circ$  in the  $w$  plane.

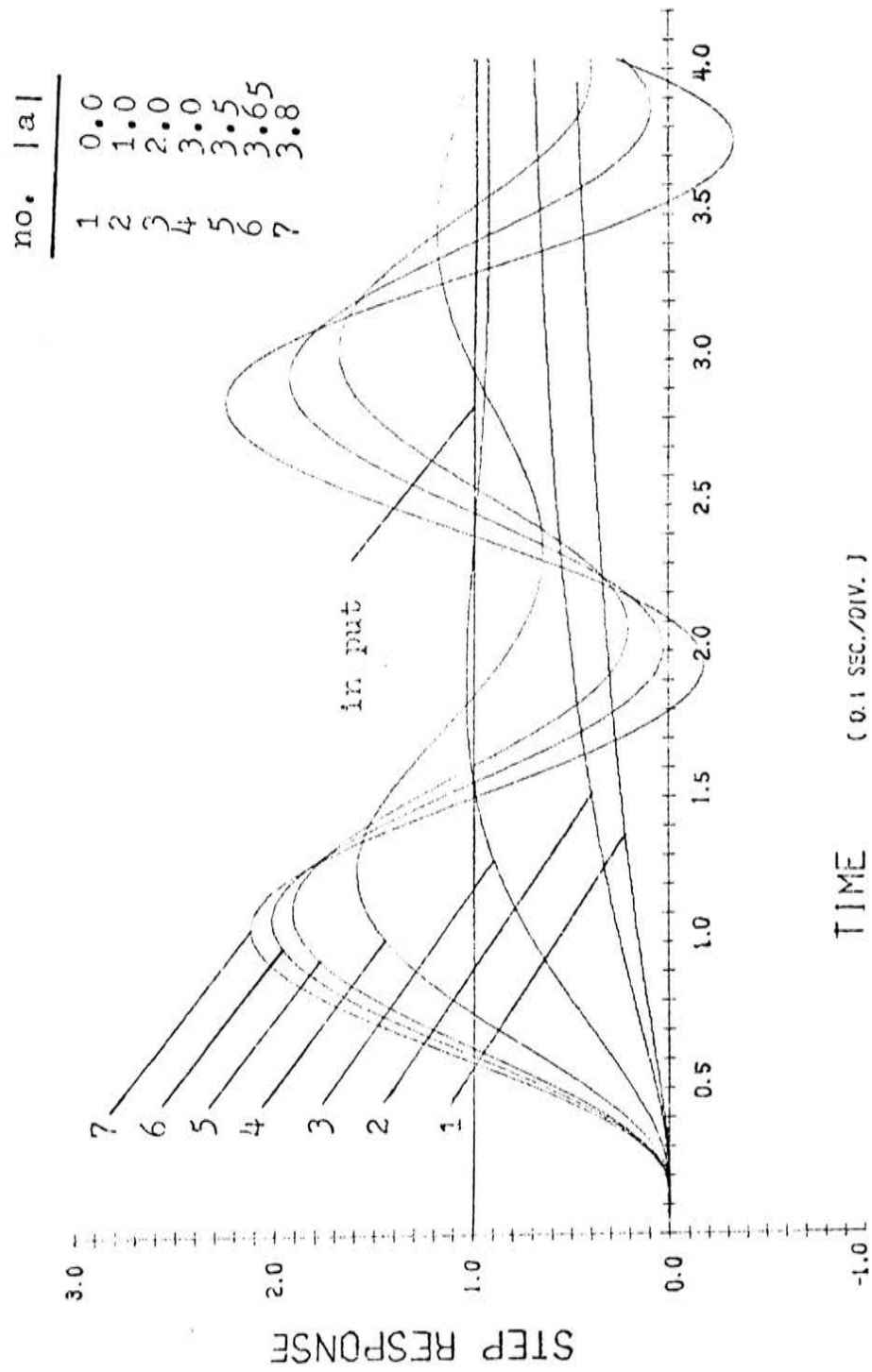


Figure 3-14: Unit step response with pole angle  $\phi=75^\circ$  in the w plane.

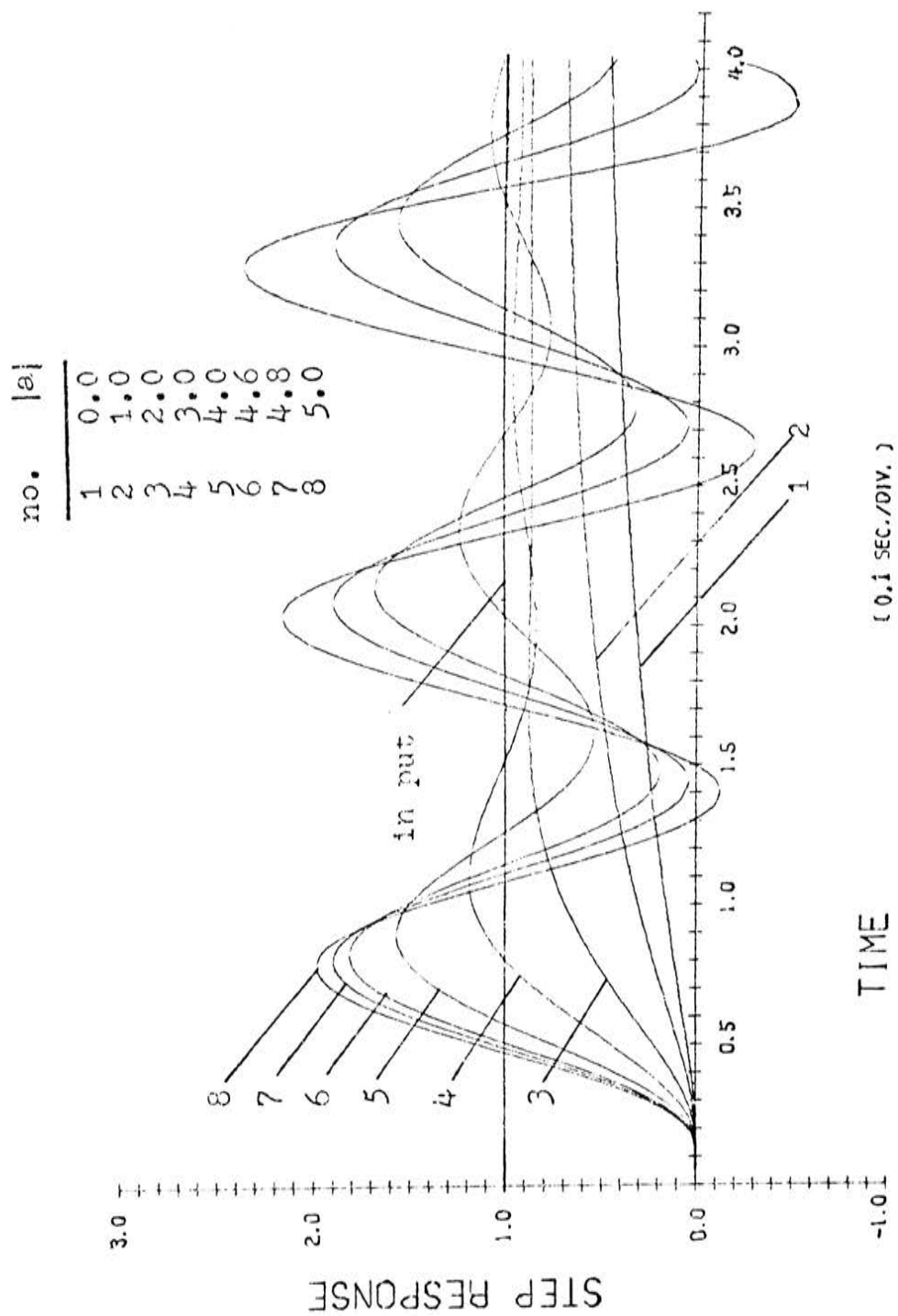


Figure 3-15: Unit step response with pole angle  $\phi=90^\circ$  in the  $w$  plane.

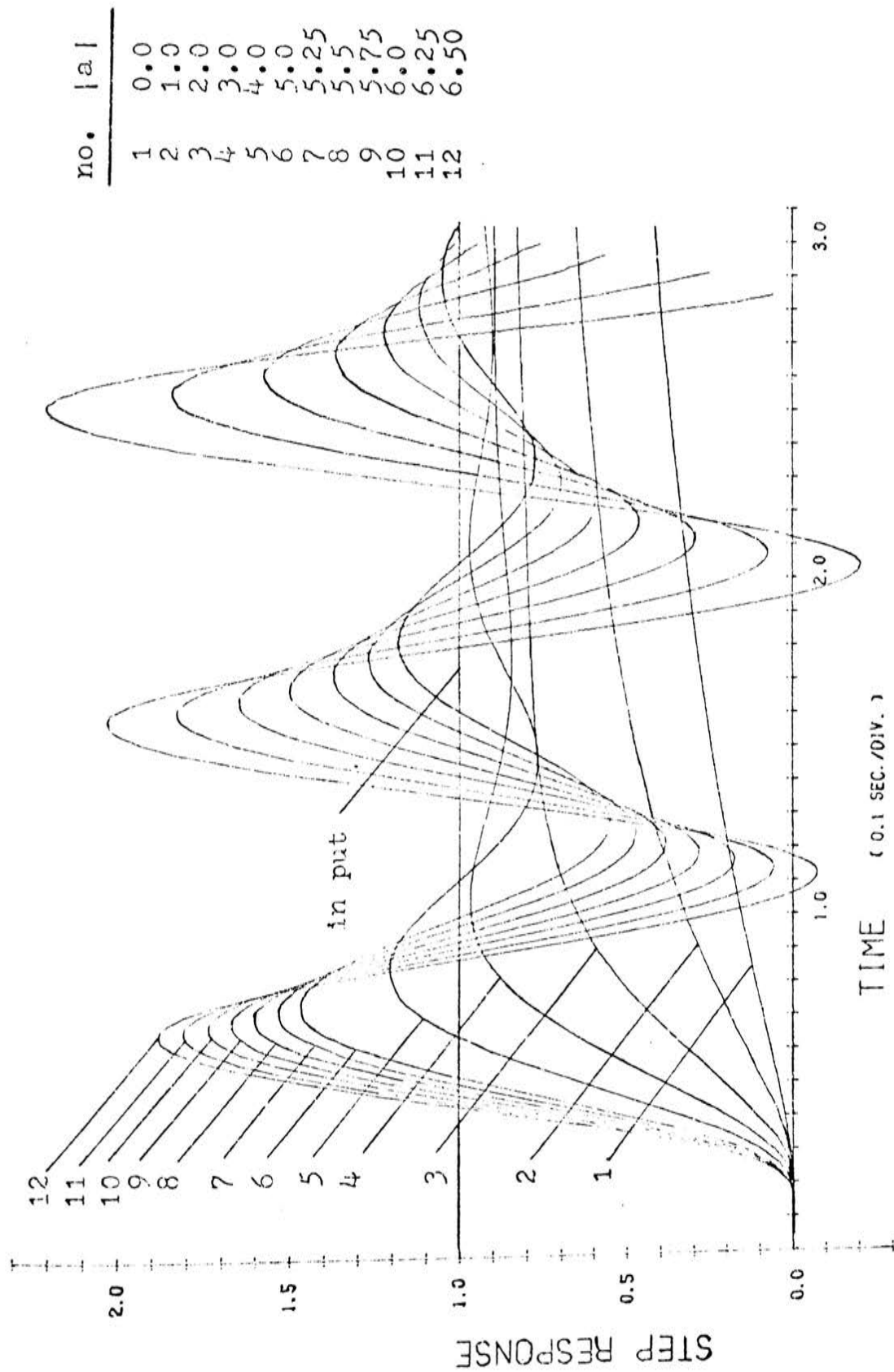


Figure 3-16: Unit step response with pole angle  $\phi=105^\circ$  in the  $w$  plane.

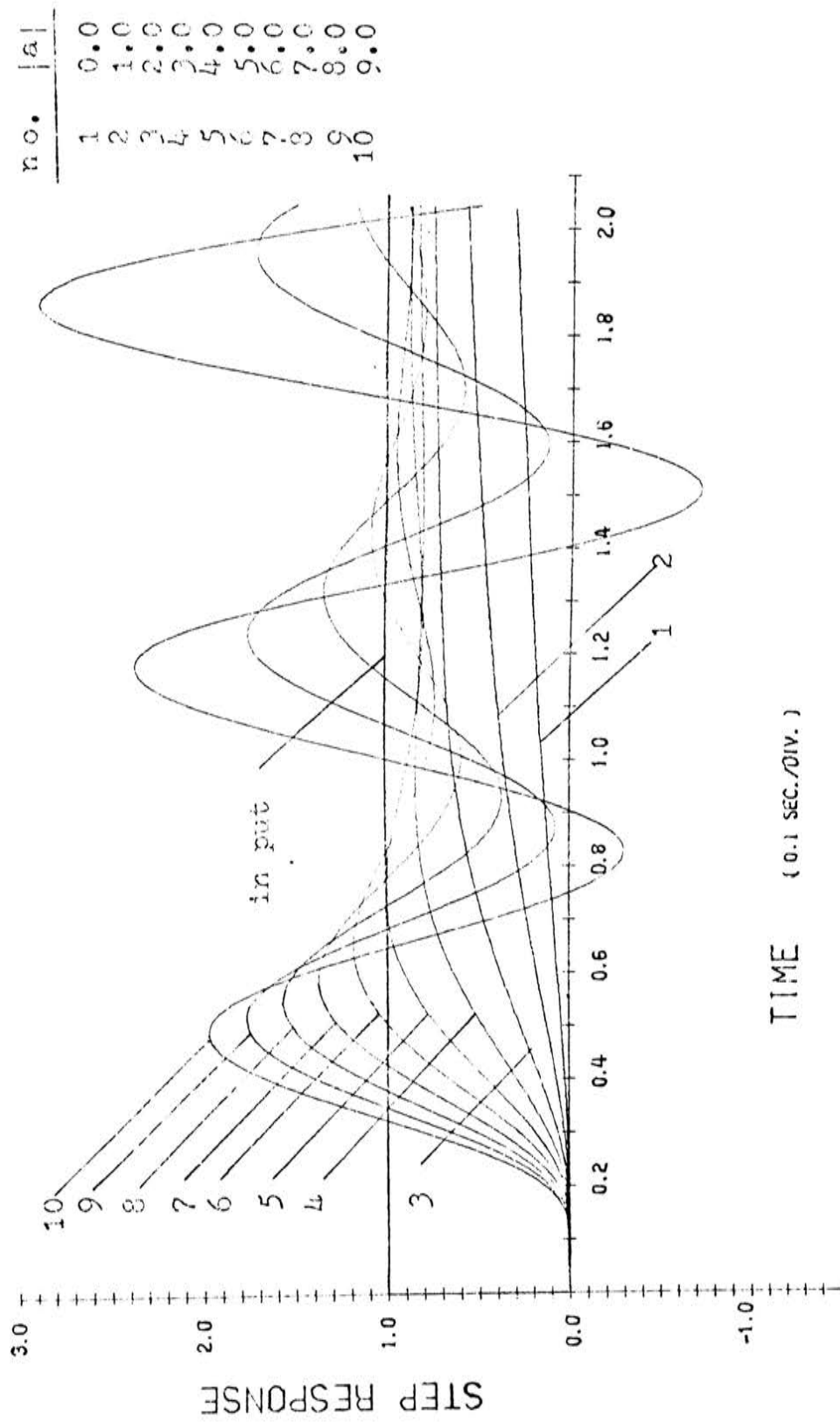


Figure 3-17: Unit step response with pole angle  $\phi=120^\circ$  in the  $w$  plane.

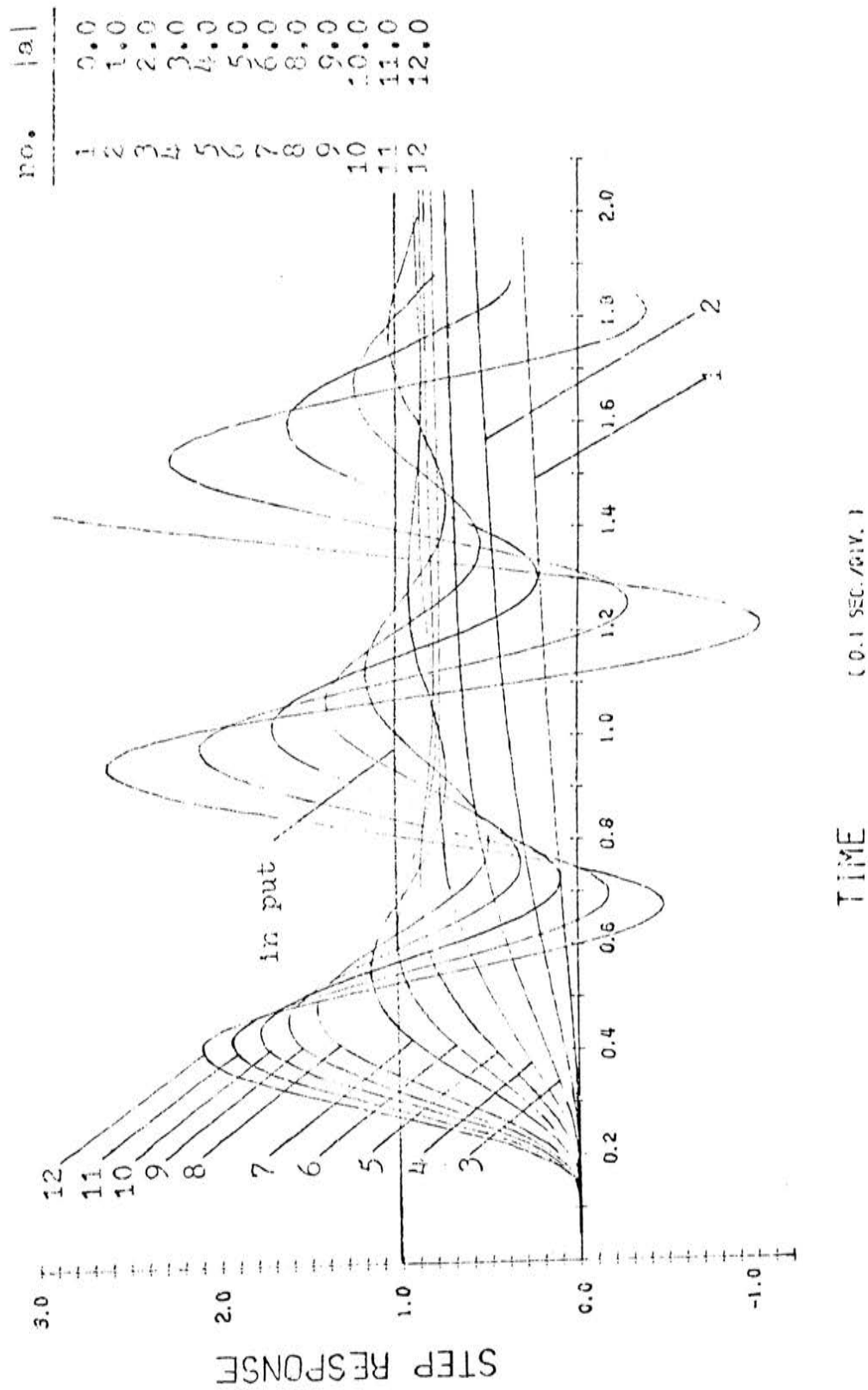


Figure 3-18: Unit step response with pole angle  $\phi = 135^\circ$  in the  $w$  plane.

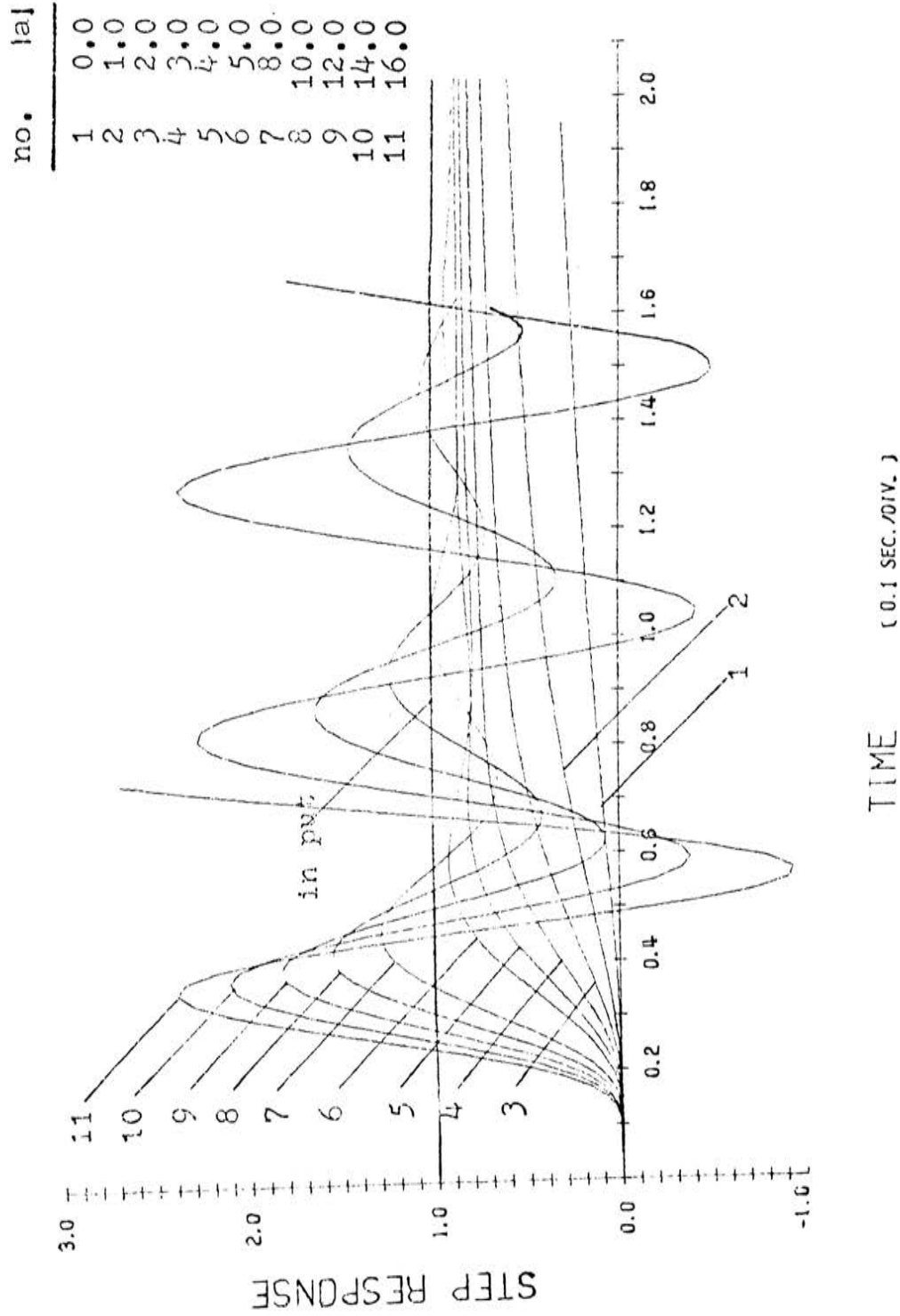


Figure 3-19: Unit step response with pole angle  $\phi=150^\circ$  in the  $w$  plane.

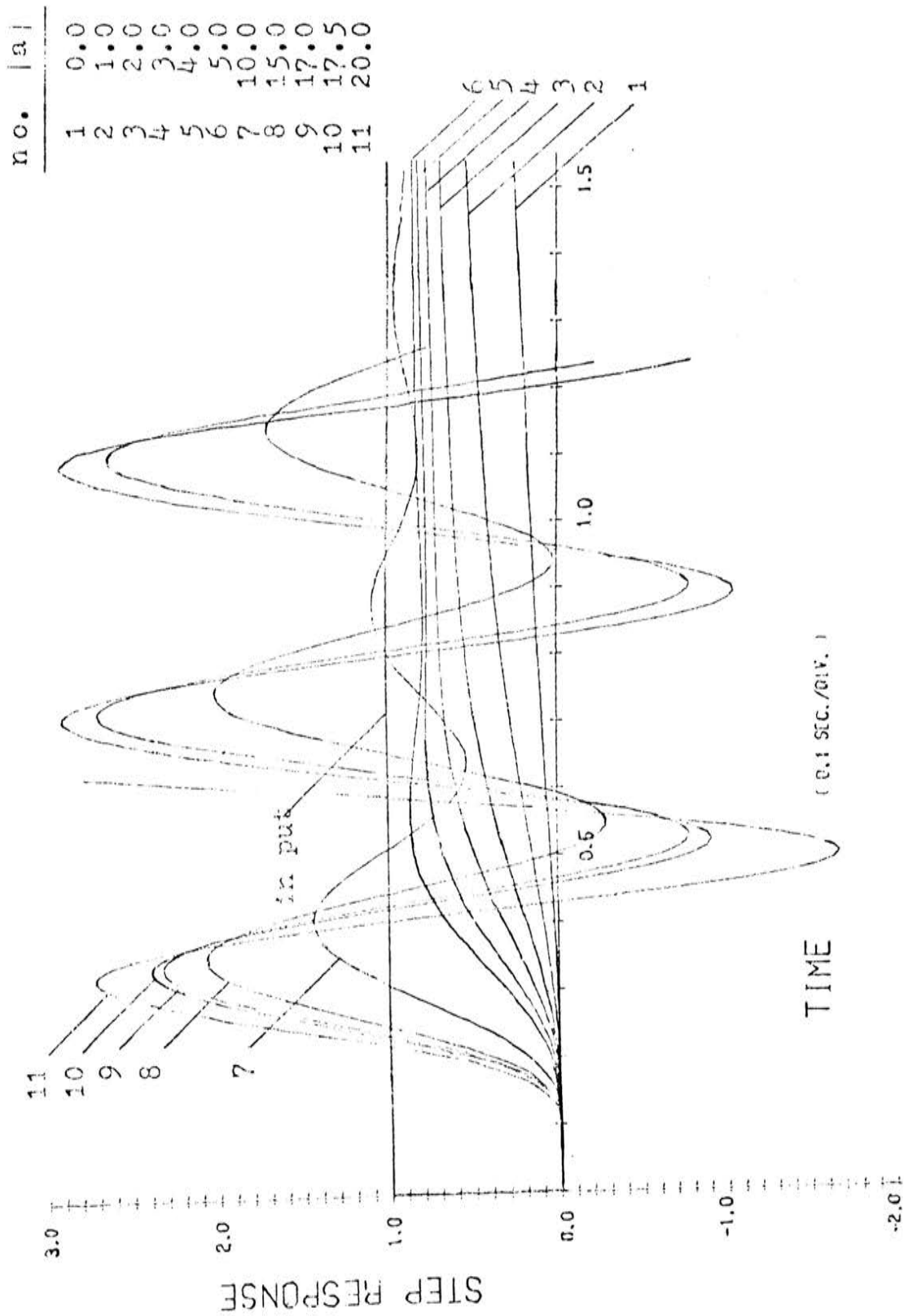


Figure 3-20: Unit step response with pole angle  $\phi=165^\circ$  in the  $w$  plane.



#### IV. CONCLUSION

##### (A) Results

The transient response of a uniform distributed systems with any transfer function that is rational in  $w$  can be analyzed with the basic form of the transfer function  $\frac{1}{w-a}$  by partial fraction expansion.

With complex poles within the stable region in the  $w$  plane, there are only two possible combinations of the basic transfer function,  $T_1(w)$  in eq.(2-2) and  $T_2(w)$  in eq.(2-7).

The transient response with transfer function  $T_1(w)$  can be observed from the imaginary part of the response with transfer function  $\frac{1}{w-a}$ ; while the real part of the response of  $\frac{1}{w-a}$  can describe the one with  $T_2(w)$ .

General results of the transient response of  $\frac{1}{w-a}$  and its relationship to stability are concluded briefly as follows:

- (1) The system with poles in the left- $w$ -plane is more stable than with those in the right half plane, as compared with the same pole magnitude.
- (2) With fixed pole angle in the  $w$  plane, when the pole magnitude becomes larger and approaches its unstable value, the response wave oscillates with less dampened amplitude but larger magnitude, and with increased oscillating frequency. Hence, the system is less stable.
- (3) The transient period, or the settling time of the response is a function of the pole locations. For poles in the right half  $w$ -plane, the transient response has longer settling time.

(4) The overshoot of the unit step response is varied with the pole location. By suitably choosing the pole magnitude, it is possible to make the system react with minimum error for a particular pole angle.

(B) Suggestions for further investigation

All results cited above are obtained from the figures in this thesis. The accuracy of these figures depends upon the increment of the plotting machine, (IBM calcomp 556) 0.05 inch in this case, and the limit of the error criterion used in the computer program. The five decimal point accuracy evaluated in these computer programs is sufficient for plotting these curves; but the round off error of the computer becomes very obvious, if the steady state response is to be observed. Hence, the time function of step response for large time must then be changed to another one as presented in eq.(5-15) in Bourquin's paper [2]. Meanwhile, the subprogram of the error function with complex argument should be carefully developed before evaluating the program for this function.

Observe the similarity among the curves of impulse or step response, for instance between figures 3-4 and 3-16, it seems that there exists a relationship between the time scale of the curve and the pole locations to obtain a single  $w$ -plane curve. The relation held for the  $\sqrt{s}$ -plane curve can no longer be applied here. It might exist in the exponential function relationship which needs to be verified. If a  $w$ -plane curve can be established, it is more convenient to investigate the response of this class of systems in the  $w$

plane just by modifying the time scale of the  $w$ - plane curve, instead of observing the phenomena by a number of the curves as presented in this paper.

As stated in the last section, the overshoot of the unit step response is a function of the pole location. Since a step response with a slow response time or excess overshoot and oscillation about the steady state value is undesirable. There is an interesting problem to find the best pole location for minimum error of the unit step response by the computer program. It can be started in the computer program with the pole magnitude underlined in table 3-1, and decreasing the pole magnitude until the output checks the first maximum value to be unity within certain desired accuracy. Then, the optimum condition of pole location for certain systems can be achieved; it could be of value in the area of designing this class of systems in the  $w$  plane, especially to the servo control systems.

## APPENDIX

\*\*\*\*\*

THE FORTRAN PROGRAM (I)

\*\*\*\*\*

THE TRANSIENT RESPONSE OF THE IMPULSE FUNCTION OF  
EQ.(1-8)

SYMBOLS USED IN THIS PROGRAM

ANG : THE POLE ANGLE IN THE W PLANE  
A(I) : THE VARYING POLE MAGNITUDE IN THE W PLANE  
TX(J): THE EVALUATING TIME  
R : THE ERROR CRITERION  
SRP : THE REAL PART OF THE IMPULSE RESPONSE  
SIP : THE IMAGINARY PART OF THE IMPULSE RESPONSE  
T : THE PRODUCT OF THE TOTAL RESISTANCE AND TOTAL  
CAPACITANCE OF THE UNIFORM DISTRIBUTED NETWORK

```
DIMENSION A(20),TX(500),V(900),SRP(900),SIP(900),ANG(20),U(900)
COMPLEX AA,B1,B3,V,AS,S
T=1.0
M=2
A(1)=1.0
ANG(1)=165.*3.14159/180.0
DO 1 I=1,9
K=1
Q=ALOG(ABS(A(I)))
AR=A(I)*COS(ANG(M-1))
AI=A(I)*SIN(ANG(M-1))
AA=CMPLX(AR,AI)
TX(1)=5.0E-3
DO 2 J=1,300
B=TX(J)*TX(J)*TX(J)
C=4.0*TX(J)
F1=T/(3.14159*B)
F2=SQRT(F1)/2.0
V(1)=1.0/EXP(T/C)
DO 3 N=2,900
B2=-T*N*N/C
5 NN=N-1
AS=AA**NN
F3=N*EXP(B2)
AS=AS*F3
7 V(N)=V(N-1)+AS
```

THE ERROR CRITERION IN EQ.(1-9) IS LIMITED TO THE  
ACCURACY OF FIVE DECIMAL POINT PLACE

```
W1=1.0+1.0/N
W2=(2.0*N+1.0)*T/C
W=ALOG(W1)+Q-W2
R=EXP(W)
```

```

      IF(R-1.0E-5)4,3,3
3  CONTINUE
4  S=F2*V(N)
   SRP(K)=REAL(S)
   SIP(K)=AIMAG(S)

```

```

C
C   TO PUNCH THE OUTPUT WITH THE MAGNITUDE SMALLER THAN 3.
C

```

```

      KK=K
50 IF(ABS(SRP(K))-3.0)30,60,60
30 K=K+1
   TX(J+1)=TX(J)+0.005
2  CONTINUE

```

```

C
C   IF THE IMAGINARY OUTPUT IS TO BE PUNCHED,"SRP" IN
C   STATE NO. 50,60 AND 70 MUST BE CHANGED TO BE "SIP"
C

```

```

60 WRITE (2,20)(SRP(K),K=1,KK)
70 WRITE (3,20)(SRP(K),K=1,KK)
20 FORMAT(5E16.8)
   IF(I-5)74,23,23
74 A(I+1)=A(I)+1.0
   GO TO 1
23 IF(I-7)24,25,25
24 A(I+1)=A(I)+5.0
   GO TO 1
25 A(I+1)=A(I)+2.5
1  CONTINUE
   STOP

```

```

C
C   NOTES:
C

```

```

C   (1):
C   POLE MAGNITUDES EVALUATED WITH PARTICULAR POLE ANGLE
C   ARE LISTED IN TABLE 2-1 FOR THIS PROGRAM
C

```

```

C   (2):
C   THE PROGRAM FOR EVALUATING THE CASE WITH FIXED POLE
C   MAGNITUDE AND VARYING POLE ANGLE CAN BE ACHIEVED BY
C   DIMENSIONING "ANG" WITH "A" FIXED
C

```

```

C   END

```

```

C *****
C
C THE FORTRAN PROGRAM (II)
C
C *****
C
C THE TRANSIENT RESPONSE OF THE UNIT STEP FUNCTION
C OF EQ. (1-12)
C
C SYMBOLS USED IN THIS PROGRAM
C
C ANG : THE POLE ANGLE IN THE W PLANE
C A(I) : THE VARYING POLE MAGNITUDE IN THE W PLANE
C TX(J): THE EVALUATING TIME
C R : THE ERROR CRITERION
C SRP : THE REAL PART OF THE STEP RESPONSE
C SIP : THE IMAGINARY PART OF THE STEP RESPONSE
C U(K) : THE NORMALIZED OUTPUT OF THE UNIT STEP RESPONSE
C T : THE PRODUCT OF THE TOTAL RESISTANCE AND TOTAL
C CAPACITANCE OF THE UNIFORM DISTRIBUTED NETWORK
C
C DIMENSION A(20),TX(500),V(900),SRP(900),SIP(900),U(500)
C COMPLEX AA,B1,B3,V,AS
C T=1.0
C ANG=165.0*3.14159/180.
C A(1)=1.0
C DO 1 I=1,9
C K=1
C Q=A*LOG(ABS(A(I)))
C AR=A(I)*COS(ANG)
C AI=A(I)*SIN(ANG)
C AA=CMPLX(AR,AI)
C TX(1)=5.0E-3
C DO 2 J=1,300
C B=SQRT(T/TX(J))/2.0
C C=ERFC(B)
C V(1)=C
C DO 3 N=2,900
C H=ERFC(N*B)
C B1=CLDG(AA)*(N-1.0)
C AS=H*CEXP(B1)
C V(N)=V(N-1)+AS
C
C THE ERROR CRITERION IN EQ.(1-13) IS LIMITED TO THE
C ACCURACY OF FIVE DECIMAL POINT PLACE
C
C W=Q-(2.0*N+1.0)*1/(4.0*TX(J))
C R=EXP(W)
C IF(R-1.0E-5)4,3,3
3 CONTINUE
4 SRP(K)=REAL(V(N))
SIP(K)=AIMAG(V(N))
V3=2.0*A(I)*COS(ANG)
V4=A(I)*SIN(ANG)

```

```

C      V5=A(I)*A(I)
C
C      THE NORMALIZING FACTOR FACT
C
      FACT=(1.0-V3+V5)/V4
      U(K)=FACT*SIP(K)
      KK=K
C
C      TO PUNCH THE VALUE OF U(K) SMALLER THAN 3.0
C
      TX(J+1)=TX(J)+0.005
      IF(ABS(U(K))-3.0)30,21,21
30  K=K+1
      2 CONTINUE
21  WRITE (2,20)(U(K),K=1,KK)
      WRITE (3,20)(U(K),K=1,KK)
20  FORMAT(5E16.8)
      IF(I-5)74,23,23
74  A(I+1)=A(I)+1.0
      GO TO 1
23  IF(I-7)24,25,25
24  A(I+1)=A(I)+5.0
      GO TO 1
25  A(I+1)=A(I)+2.5
      1 CONTINUE
      STOP
C
C      NOTES:
C
C      (1):
C      POLE MAGNITUDES EVALUATED WITH PARTICULAR POLE ANGLE
C      ARE LISTED IN TABLE 3-1 FOR THIS PROGRAM
C
C      (2):
C      THE PROGRAM FOR EVALUATING THE CASE WITH FIXED POLE
C      MAGNITUDE AND VARYING POLE ANGLE CAN BE ACHIEVED BY
C      DIMENSIONING "ANG" WITH "A" FIXED
C
      END

```



## BIBLIOGRAPHY

- 1 : Mohammed S. Ghausi and John J. Kelly, Introduction to Distributed-Parameter Networks with Application to Integrated Circuits, Holt, Rinehart and Winston INC. New York, 1968.
- 2 : Jack J. Bourquin, "Stability of A Class of Lumped-Distributed System", Report R-373, Coordinated Science Laboratory, Jan. 1968.
- 3 : Jack J. Bourquin and J. S. Tzeng, "Transient Response of A Class of Active Lumped-Distributed Systems", Proceedings of the Sixth Allerton Conference on Circuit and System Theory, October 2-4, 1968.
- 4 : Eateman Manuscript Project, Tables of Integral Transforms, Vol. I, McGraw-Hill Book Company, New York 1954.

## VITA

Tzeng, Jaw Shyong was born on Dec. 9, 1937 at Tainan, Taiwan, China. He received his elementary education at Tainan Cheng-Kung Primary School at Tainan, Taiwan. His high school education was obtained at Taiwan Provincial Kaohsiung High School, Kaohsiung, Taiwan. He attended Taiwan provincial Cheng-Kung University in Sep. 1956 and received with honors the degree of B.S.E.E. in June 1960.

Two weeks after his graduation from his university, he was employed as a design engineer in Ta-tung Engineering Company at Taipei. He served his military program as an ordnance reserve officer in Army Vehical Base from Oct. 1960 to Oct. 1961. In May 1964, Mr. Tzeng was sponored by Tatung Engineering Company to enhance his design technique of "Kilo-Watt-Hour" meters at Toshiba Electrical Company in Japan for six months. One year after his return from Japan, he presented a new type of single phase "KWH" meter; and was promoted as the supervisor of Meter Assembly Shop in Tatung Eng. Company. A year before his coming aboard, he was appointed as an instructor at Electrucal Engineering Department of Ta-tung Institute of Technology, while as an advisor in designing "KWH" meters. At the spring semester of 1967, he was also a part-time instructor of Shih Chien Home Economics School.

In July 1967, Mr. Tzeng came to the United States for his advance study, and since Sep. of 1967, he has been enrolled in Graduate School of University of Missouri at

Rolla, Rolla, Missouri.

He is married to Miss Mei-Ying Hsueh and is the father of a child, Gary F.C., Tzeng.

He was an honor member of China Radio Association, from which he received the scholarship to support his college studying in Taiwan, and now he is a member of the Institute of Electrical and Electronics Engineers.

**147522**